Injector Systems 5

5.1 Injection System Overview

The SSRL injector system (Figure 2.1) [1], which provides high-energy electron beam lines to fill the SPEAR storage ring, is composed of a 2.5 MeV microwave cavity gun, a 112 MeV S-band linear accelerator, and a 10 Hz booster synchrotron that currently accelerates the beam to 2.3 GeV. The linac beam is injected into a single booster bucket to provide single-bucket SPEAR filling at a routine filling rate of 20 mA per minute.

Although the booster is designed to accelerate beams to 3 GeV, ratings of the SPEAR septum magnet and other magnets in the booster-to-SPEAR (BTS) transport line now limit the injection energy to 2.3 GeV. The booster has operated at this energy since its commissioning in 1991. During the early stages of commissioning, several components of the booster and extraction systems were identified as requiring minor upgrades before they could operate routinely at 3 GeV. These components will be upgraded along with the septum and BTS magnets to facilitate 3 GeV injection into SPEAR 3.

5.1.1 Linac System

The injector electron beam is created in a thermionic, 1.5-cell RF gun [2]. About 3000 S-band (2856 MHz) bunches are accelerated out of the gun at 2.5 MeV during the approximately 1 μs RF power pulse from the linac klystrons. Each bunch is compressed in time as it passes through an alpha magnet. A high-voltage electromagnetic pulse in the linac chopper then allows three to five of these bunches (approximately 5×10^8 electrons) to pass into the linac section. Three standard SLAC linac sections accelerate these bunches to an energy of 112 MeV for injection into the booster. The gun and linac are powered by one SLAC 5045 klystron with pulsed power from a modulator.

5.1.2 LTB Transport Line

The 112 MeV beam travels down a transport line into the booster injection septum magnet. The injection kicker magnet makes the final orbit correction before the injected beam is captured in a single booster RF bucket. The beam is injected at the end of the kicker pulse; the kicker field decays in 100 ns, well before the bunch returns 447 ns later.

5.1.3 Booster Synchrotron

The injector beam is accelerated to the SPEAR-ring injection energy by the booster synchrotron. This booster has a 20-cell FODO lattice, with magnet strengths that oscillate at 10 Hz (Table 5.2.1), ramping in energy from zero to the ejection value.

The booster RF system operates at 358.533 MHz and is phase-locked to the 476.337 MHz SPEAR RF system (Section 4.8.4). Since the booster circumference is 4/7 that of SPEAR, the time-of-flight for four SPEAR revolution periods exactly equals that for seven booster periods, bringing a specific SPEAR target beam bucket into alignment with the injector-beam bunch every 3.1 μs. The injection timing system takes advantage of this recurring synchronism in developing ejection triggers as described in Table 4.8.4.

The SPEAR operator selects the specific SPEAR bucket to be filled and, when the booster energy approaches the linac energy, the injection timing system triggers the linac system so that the chopper sends the S-band bunches into the correct booster bucket. During the ramp, the 358.533 MHz RF frequency, slightly greater than one-eighth of the linac frequency, compresses the injected S-band bunches into a single booster bunch. When, after approximately 36 ms, the booster beam reaches the ejection energy (as detected by the booster magnet current monitor), the next recurring ejection trigger fires the ejection kicker. The only timing constraints on this kicker are: 1) the rise time must be less than the 447 ns revolution period of the booster, and 2) the firing timing jitter must be less than a few tens of nanoseconds.

5.1.4 BTS Transport Line

The kicked electron bunch from the booster travels through a vertical Lambertson septum magnet and into the booster-to-SPEAR (BTS) transport line. The BTS has an isochronous lattice and is equipped with steering magnets and beam monitors to guide the beam to the SPEAR injection septum.

5.2 Booster Synchrotron Upgrade

When the booster operating energy is raised from 2.3 GeV to 3 GeV, the power and stored energy in the synchrotron will almost double, placing added thermal and mechanical stresses on its components. During booster commissioning in 1991, the magnet system was run at 3 GeV power levels in order to evaluate upgrade requirements for routine 3 GeV operation. These requirements are summarized below.

5.2.1 10 Hz Power Supply System (White Circuit)

The booster magnets are driven by a biased 10 Hz resonant power supply system, called a White circuit [3]. The magnetic fields range from slightly negative before injection to a field corresponding to slightly more than 3 GeV after ejection from SPEAR 3.

The ring is divided into sixteen resonant cells, each of which is a tuned 10 Hz circuit. Connected in series, these individual cells form a single, large resonant circuit. Each cell consists of two dipole magnets, two quadrupole magnets (one focusing and one defocusing), a choke, and a capacitor (Figure 5.1). The lattice is designed to produce the correct field strengths when all magnets are driven with the same current.

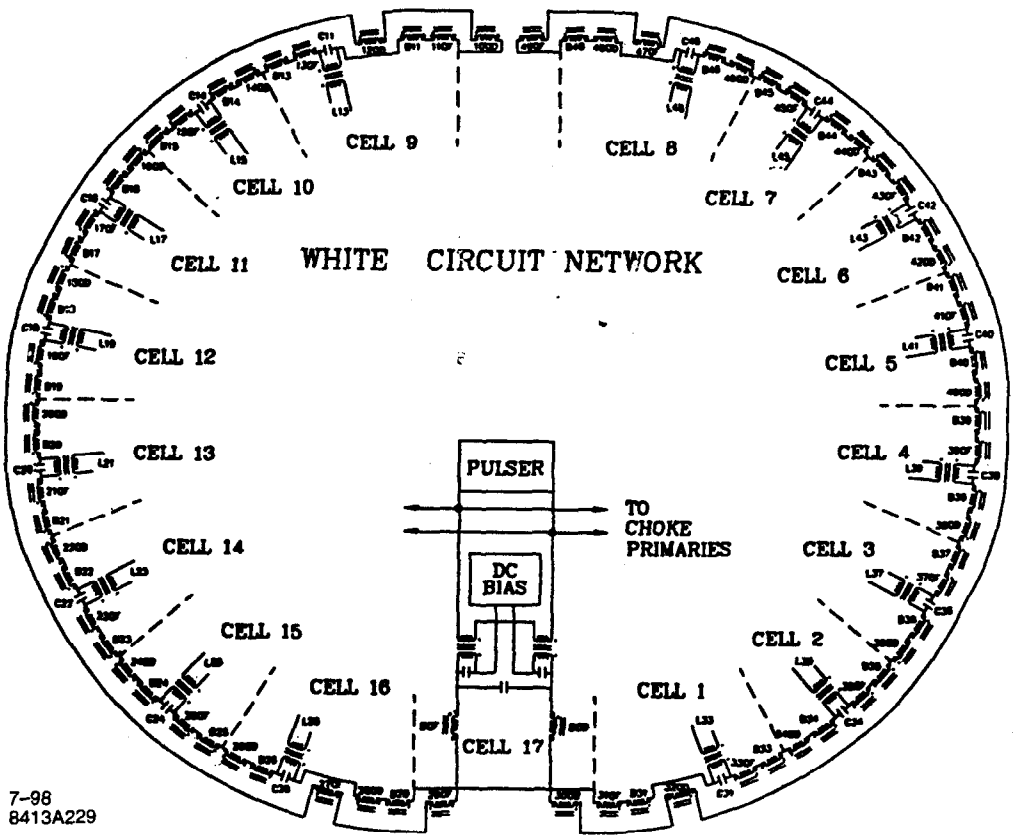

Figure 5.1 10 Hz White circuit for the SSRL Booster.

The cell choke serves three functions: 1) it provides inductance for the 10 Hz system; 2) it provides a DC path for the biased current in the string; and 3) it acts as a transformer to couple the AC power to the White circuit. The DC bias-current is fed from the DC power supply into the string of magnets and chokes connected in series.

To compensate for manufacturing differences between the dipoles and quadrupoles, a supply trim also drives each quadrupole family. To keep the induced voltage on this trim supply close to zero, the trim currents also are driven through a voltage-bucking transformer.

The AC power for the White circuit is generated in a pulser network (Figure 5.2), which periodically discharges a capacitor through the cell chokes during the negative part of the 10 Hz cycle. The pulse capacitor is charged through a charging choke from a power supply. The pulse capacitance and the inductance of the pulse choke determine the charging pulse waveform. Table 5.1 gives the White circuit component specifications.

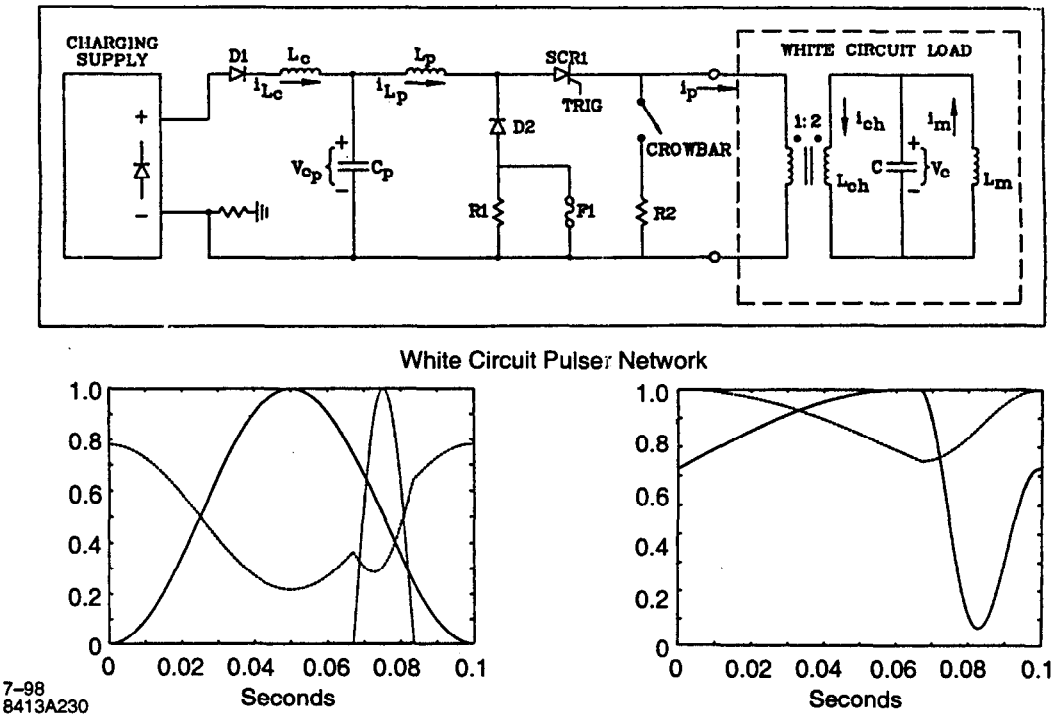

Figure 5.2 Pulser network for the booster White circuit.

Table 5.1 3 GeV White circuit component specifications.

Component	Quantity	Value	Rating	DC/AC Power (kW) at 3 GeV
Dipole	32	21.1 mH	630 A pk/380 A rms	2.4/2.9
QF	20	1.0 mH	630 A pk/380 A rms	.46/.43
QD	20	0.8 mH	630 A pk/380 A rms	.40/.36
Bucking Choke	2	20.0 mH	630 A pk/380 A rms	3.9/5.0
Cell Choke	17	80.0 mH	500 A pk/345 A rms	7.8/4.1
Cell Capacitor	16	8.9 mF	640 V rms	0.0/0.5
Cell 17 C_0	1	5.8 mF	2 kV pk	0.0/1.0
Cell 17 $C_{x,y}$	2	6.3 mF	320 V rms	0.0/0.2
Charging Choke	1	250 mH	273 A pk/210 A rms	0.0/5.0
Pulse Choke	1	2.0 mH	4 kA pk/1.2 kA rms	0.0/10.0
Pulse Capacitor	1	14.2 mF	2 kV pk	0.0/2.0
DC Bias Supply	1	735 VDC, 320 ADC	1200 VDC, 400 ADC	235 kW
AC Charging Supply	1	1020 VDC 210 Arms. 273 A pk	1200 VDC, 300 Arms	215 kW

5.2.1.1 DC Bias Supply

A new water-cooled transformer has already been installed to improve cooling in the DC-Bias power supply. The only components that need additional cooling for 3 GeV operation are the

silicon controlled rectifiers (SCRs). A water-cooled heat-sink assembly for the SCRs will be installed. The transformer will also be reconnected to its higher voltage taps for operation at 3 GeV.

5.2.1.2 Pulser Supply

The pulser supply runs cooler than the DC supply, and measurements of the transformer show that its temperature will be acceptable at 3 GeV. The SCRs will be mounted to a water-cooled heat-sink assembly, and the transformer will be reconnected to its higher voltage taps.

5.2.1.3 Quadrupole Tracking Supplies

The quadrupole trim supplies now run at a fraction of their rated output for 2.3 GeV operation, so they are sufficient, without modification, for 3 GeV operation.

5.2.1.4 Chokes

The charging choke in the pulser network filters the charging of the pulse capacitor. At 2.3 GeV, the choke is on the threshold of saturation. It will be rebuilt or replaced with a choke rated for 3 GeV operation.

A new pulse choke rated for 3 GeV operation was installed in 1994 and does not require upgrading.

The cell chokes were designed and tested to remain linear up to 3.5 GeV. However, some welds were not strong enough to accommodate 10 Hz ramping, causing some end laminations to shake loose. The welds have since been reinforced for 2.3 GeV operation. They will receive further mechanical reinforcement to facilitate 3 GeV operation.

The bucking chokes require no modification for 3 GeV operation.

5.2.1.5 Capacitors

All of the White-circuit capacitor banks and power-supply filter capacitors are rated for the voltages and currents necessary for 3 GeV operation. SLAC has a large supply of spare capacitors.

Individual strings of capacitors in each of the larger banks are fused to prevent catastrophic failures within the capacitor banks. These fuses are specifically rated for 3 GeV operation.

5.2.1.6 Cell Interlock

A White-circuit cell-interlock system will be implemented for SPEAR 3 to protect White-circuit components operating at 3 GeV. The interlock will detect the 10 Hz harmonic content of each cell. If a capacitor in a cell capacitor bank fails, the resonant frequency of that cell will change, breaking the 16-fold symmetry of the White circuit–and causing an increased charging current in that cell. When the cell interlock detects that this current has exceeded a given threshold, it shuts down the White circuit. These current-monitoring transformers are already installed.

5.2.1.7 Pulser Firing Circuit

The SCR and the diode used in the pulser-firing circuit are both rated for 3 GeV operation.

5.2.1.8 Corrector Supplies

There are individual corrector supplies and windings for each magnet to correct injection-field errors. Since the injection energy will not change, there is no need to change any of these elements.

5.2.1.9 Cabling

The cabling in the booster is rated for 3 GeV operation. Two short cables will be installed to charge the pulser for 3 GeV operation.

5.2.2 Booster Magnets

The booster magnets, including 32 dipoles, 20 QF quadrupoles and 20 QD quadrupoles, were designed to run at fields corresponding to 5 GeV, so the target operating level of 3 GeV falls well within their capacity.

Although the magnetic properties of the quadrupoles exceed the 3 GeV specifications, the supports for the quadrupole coils must be upgraded for 10 Hz, 3 GeV operation; otherwise, the coils may vibrate loose.

The magnet bussing and cabling is rated for 3 GeV operation, and no changes to these components are necessary.

5.2.3 Ejection Septum Magnet System

The ejection septum magnet will run with increased power for 3 GeV operation.

The ejection septum power supply provides one-half of a 30 Hz sine-wave current pulse through the septum magnet. It uses a DC power supply to charge a capacitor bank, then discharges the capacitor bank through an inductor to produce the desired pulse shape.

The original DC power supply used for 2.3 GeV operation has already been upgraded to meet the 3 GeV requirements. The entire ejection septum system has been tested at 3 GeV with no evidence of distortion, saturation or heating; it requires no reworking for SPEAR 3.

5.2.4 Ejection Kickers

The ejection kickers produce a magnetic pulse that deflects the stored beam into the ejection septum [4]. The kicker energy is stored in delay lines and released into the kicker when a thyratron is pulsed. System components, including the kicker, pulser PFN cables, thyratron, pulse-shaping components, and kicker magnet, were designed and built for 3 GeV operation.

During 3 GeV operation, the kicker's power supply will run at 20 kV, with an average current of 9 mA. Since the supply is a 30 kV, 100 mA unit, it will run well within its rated capacity at 3 GeV.

5.2.5 Booster RF System

The booster RF system [2], which has a single, five-cell, standing-wave, π-mode cavity operating at 358.533 MHz, will be modified to support ramp energies of 3 GeV. The RF system is identical to the model originally developed for PEP-I, and subsequently modified for 358.5 MHz operation on SPEAR 2 [5]. Due to the ramping duty cycle of <25% and minimal beam loading, the power requirements for 3 GeV booster operation are much less than those associated with the 3 GeV storage ring. Nevertheless, the peak power to the booster must be adequate to reach the final 3 GeV energy at the end of the acceleration cycle. Table 5.2 gives booster-beam and RF parameters.

The booster RF cavity matches the SPEAR 2 cavities precisely, except it has a lower power rating (of 125 kW). For the <1 mA beam current, parasitic mode losses are low.

Table 5.2 Booster beam and rf parameters for 3 GeV operation.

Parameter	Value	Remarks
Beam energy	0.1-3.0 GeV	100 ms waveform cycle period
Bending radius	11.8 m	
RF frequency	358.533 MHz	
Revolution frequency	2.241 MHz	
Harmonic number	160	
Parasitic loss	0.4 keV avg	estimated
Synch. rad. loss/turn	600 keV/turn pk	at 3.0 GeV
Total loss per turn	610 keV pk	at 3.0 GeV
Beam loading	approximately 0	0.6 mA beam current
Peak gap voltage	1.2 MV pk	over voltage factor = 2
Peak RF power	60 kW pk	42 kV, 6.7 A at power supply

5.2.5.1 Booster RF Cavity

Table 5.3 summarizes the characteristics of the booster 5-cell RF cavity.

Table 5.3 Booster 5-cell RF cavity specifications

Parameter	3 GeV value	Max rating	Remarks
Frequency	358.533 MHz		
Shunt impedance	26 MΩ		V_g^2/P_{RF} linac ohms
Q value	23000		unloaded
RF power dissipation	40 kW avg 160 kW pk	125 kW avg 500 kW pk	cooling-limited; 0.25 duty factor
Gap Voltage	1.0 MV avg 2.0 MV pk	1.8 MV avg 3.5 MV pk	summed over 5 cells; 0.25 duty factor
Window power	40 kW avg	125 kW avg	90 kW max recommended
Water cooling flow rate	160 gpm	160 gpm	

Because the booster RF cavity is ramped from minimum to peak power with a duty factor of approximately 25%, the peak RF power needed by the cavity is a factor of approximately 3 times higher than the average power, and the peak gap voltage is about twice the average value.

Since automatic feedback control by the two movable tuners achieves the resonance-frequency tuning and inter-cell power balancing, the cell temperatures are monitored, but not interlocked. On the other hand, the 45 gpm LCW flow rate that supplies three parallel cavity-cooling channels (so as to maintain a 30° C cavity temperature) is interlocked so that the klystron is disabled when the flow drops to roughly half of the full rate.

The cavity is processed following each annual shutdown up to the gap voltage of 0.8 MV with 25 kW of steady-state power.

5.2.5.2 RF HV Power System

The low-level RF system provides a few mW of 358.533 MHz control power to a new 25 W solid-state preamplifier that can drive the klystron up to 500 kW. DC power to the klystron is provided by

a high-voltage power supply (HVPS) rated for 47kV and 7 A. After raising the output voltage with transformer tap modifications, this HVPS will be sufficient for 3 GeV booster operation.

The booster RF HVPS operates with a 480 VAC, 3-phase primary power source. The primary delta winding has five hard-wired taps that produce 80-100% of the full 47 kV output at 5% intervals. Table 5.4 shows voltage-current characteristics at various tap settings

Table 5.4 Booster RF HVPS tap changes.

Tap (%)	Voltage (kV)	Current (A)	P_{RF}, max (kW)	Vg, max (MV)	Remarks
80	37.6	5.41	81	1.44	2.35 GeV
85	40.0	5.92	95	1.56	
90	42.3	6.46	109	1.67	3 GeV
95	44.7	7.00	125	1.79	maximum current
100	47.0	(7.56)	(142)	(1.91)	over-current

A SPEAR 3 RF supply voltage of 42.3 kV has been selected to prevent the klystron from experiencing oscillations that impair load stability.

A soft-start circuit is used to reduce transient voltage spikes during the switch-on of the HVPS. The circuit consists of SCR AC line regulators for the HV transformer primary phase voltages (Figure 5.3). The SCRs ramp the HVPS voltage to full value in approximately 1 s.

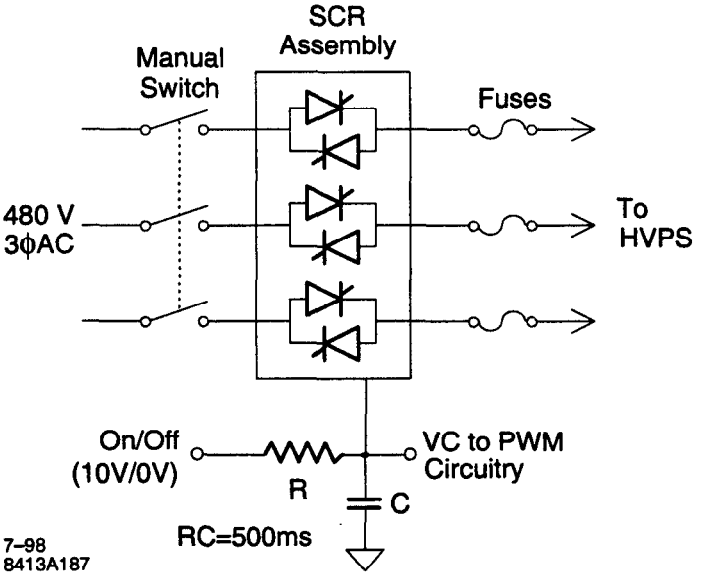

Figure 5.3 SCR soft-start circuit for the booster RF HVPS.

5.2.5.3 Klystrons

The 500 kW CW klystron used for the booster is identical to those designed and manufactured by the SLAC Klystron Department, originally for PEP-I at 352 MHz, and then for SPEAR 2 at 358.5 MHz [6]. Table 5.5 gives the parameters for the three currently active klystrons (two for SPEAR 2, one for the booster, and one spare klystron). [7] As the table shows, maximum possible output power and efficiency vary from tube-to-tube, as defined by the ratio of klystron RF output to input

DC power. In SPEAR 2, the maximum power for RF cavity operation is limited by the window power rating of 250 kW. All the tubes are interchangeable.

Table 5.5 SPEAR klystron specifications.

Parameter	Unit	8S9			10S11			Booster			Spare		
Beam voltage	kV	50	60	65	50	60	65	50	60	63	50	60	65
Beam current	A	8.4	10.9	12.2	8.0	10.4	11.6	8.5	11.0	11.8	8.0	10.4	11.6
Beam power	kW	420	654	793	400	624	754	425	660	743	400	624	754
RF power	kW	228	361	434	228	334	409	210	364	420	182	321	397
Efficiency	%	54.3	55.2	54.7	57.0	53.5	54.2	49.4	55.2	56.5	45.5	51.4	52.7
Gain	dB	45	46	46	45	43	44	42	43	44	44	45	46

The booster RF klystron is identical to the ones now used for SPEAR 2. Figure 5.4 illustrates the booster klystron-ramped output for 2.35 GeV operation on SPEAR 2. Figure 5.2.5.4 discusses this ramping waveform.

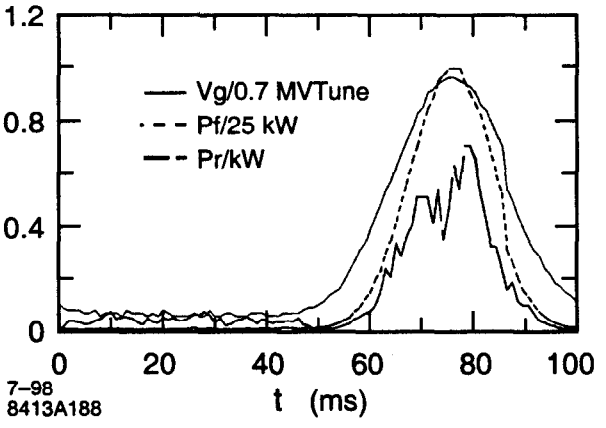

Figure 5.4 Waveforms of the cavity's gap-voltage, the klystron-forward power, and the reflected power from the booster RF cavity as a function of time (2.35 GeV operation). An electron bunch is ejected 5.5 ms prior to the gap-voltage peak.

In the event that one tube fails, it will be replaced with a spare tube and sent to the SLAC Klystron department for repair.

5.2.5.4 RF Control System

The booster-RF control system (Figure 5.6), derived from the PEP-I and SPEAR 2 systems [8], has the following regulating functions:

- **Gap Voltage**

  The gap-voltage amplitudes at each of five cells are detected by probes with a 55 dB coupling coefficient. All five individual amplitudes are summed, and compared to the reference voltage. The error signal controls the RF attenuator in the low-level RF controller.

- **Cavity Phase**

The RF power to the cavity is sampled at the cavity input. Its phase to the cell #3 probe is compared to a reference. This loop drives the two tuners in common mode so that they stay tuned when the cavity temperature changes.

- **Klystron Phase**

  The klystron operating at around 60 kV of beam voltage introduces a phase modulation arising from the high voltage DC power supply ripple. The cell #3 probe signal is compared with the master oscillator signal. The difference controls the RF phase to the klystron.

- **Field Balance**

  While the common mode action of the two tuners enables the system to stay tuned, it also gives rise to a field imbalance between the five cells. The field amplitude at the two last cells (#1 and #5) are sampled and compared. The difference determines the differential movements of the two tuners.

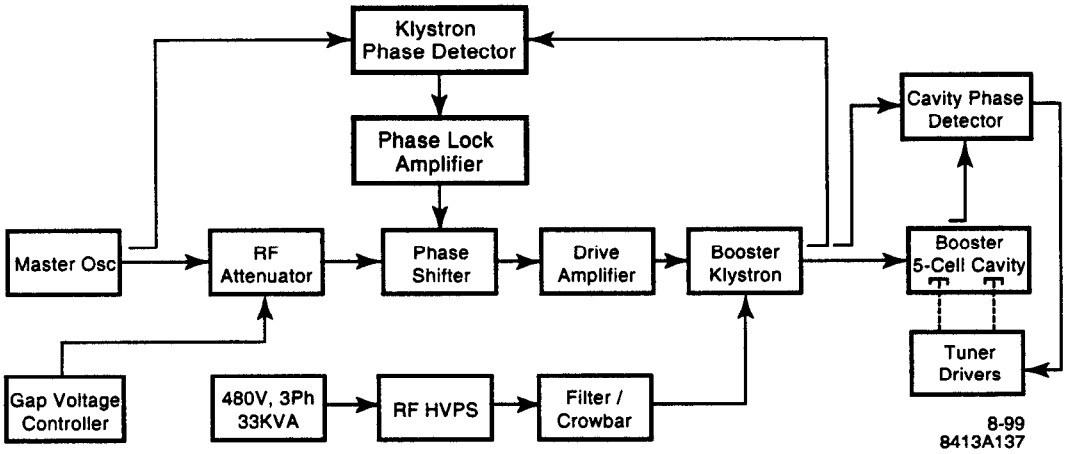

Figure 5.5 Klystron and cavity phase-feedback control.

Other interlock functions protect against excessive reflected power from the cavities (> 2:1), loss of cooling water flow, excessive vacuum pressure, and cavity overvoltage, etc.

The booster's RF control system resembles that of the SPEAR 2 RF, except the cavity's gap voltage is ramped at 10 Hz with a programmable waveform. The 1000-point, 100 ms waveform function (f(t) =eV(t)) is given by

$$f(t) = a\dot{E}(t)T_{rev} + U_0(E(t)) \tag{1}$$

$$\text{where } U_0(E(t)) = E(t)^4 \cdot \frac{88.5}{\rho(m)} \cdot 10^{-6} \tag{2}$$

$$E(t) = E_{DC} - E_{AC}\cos(\omega t + \phi) \tag{3}$$

with a = the operator-controlled scaling factor, $\dot{E}$ (t)= the time derivative of beam energy E, T_{rev} = the booster revolution period, U_0 = the energy loss (per turn, in GeV), ρ = booster dipole bending radius (11.9 m). E_{DC} and E_{AC} represent, respectively, the DC bias and AC amplitude factors of the sinusoidal booster energy ramp, (1.5 GeV each), where $\omega = 2\pi \times 10$ Hz, and ϕ = a phase factor.

Sample-and-hold amplifiers sample system waveforms at specific points in the ramp for use in the regulating and interlock circuitry.

5.3 BTS Transport Line Upgrade

The main dipoles and quadrupoles in the injector side of the BTS transport line are all designed to run at 3 GeV. The final dipoles in the SPEAR side of the line, however, cannot steer the 3 GeV beam and must be replaced. Some BTS correctors will also be replaced to permit 3 GeV operation.

5.3.1 BTS Magnets

The existing dipoles mounted on the injection raft near the spear septum (Figure 5.5) are not strong enough for 3 GeV operation. New 3 GeV dipoles will be built from the cores of two existing dipoles, one from the electron injection raft and the other from the unused positron injection raft. New coils and supports are required.

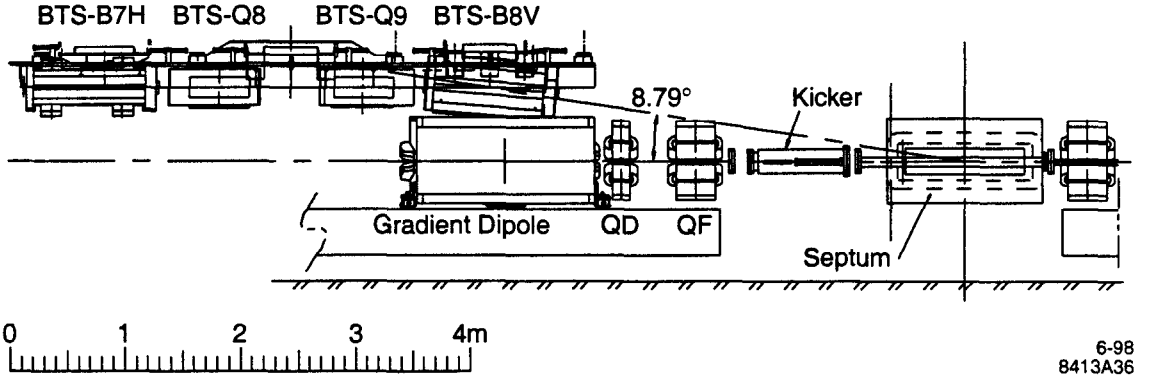

Figure 5.6 BTS injection raft near the SPEAR septum

Six existing correctors for the injector side of the BTS line do not have adequate cooling for 3 GeV operation and will be replaced for SPEAR 3.

5.3.2 BTS Power Supplies

The existing power supplies for the main magnets and correctors in the injector side of the BTS line all operate suitably at 3 GeV.

Power supplies for the B7H and B8V magnets near the SPEAR septum will be replaced. Power supply specifications are shown in Table 4.35.

5.4 Injector Instrumentation and Control

The injector has the standard instrumentation needed for normal operations and diagnostics. Since this instrumentation is independent of energy, no major changes need to be made. The only changes are: 1) to replace the insertable phosphor screens used to monitor beam position in the SPEAR injection raft, and 2) to upgrade the machine protection system with the White circuit cell interlock.

5.4.1 Computer Control System

The injector control system is run on a VMS system, which controls individual CAMAC crates through ethernet connections [6]. No new controls are needed, and no new systems need to be monitored.

5.4.2 Beam Monitoring Systems

The linac has several existing devices for monitoring the beam. Insertable phosphor screens are used to measure beam size and position at various points along the linac. Non-intercepting stripline beam position monitors (BPMs) are used to maintain beam steering from the linac to the booster during injection. Six toroid monitors are used to measure the total current out of the gun, after the chopper, and along the linac.

The booster also has stripline BPMs around the ring. A booster diagnostic sector contains a capacitive pickup current monitor, a stripline monitor, a toroid monitor, and a synchrotron light monitor.

The BTS line also has beam-position monitors, toroids, and insertable screens. The screens in the final injection raft near the SPEAR septum need to be replaced, since the entire raft must be rebuilt for SPEAR 3.

5.4.3 Injector Machine Protection System

The injector has a standard machine-protection system (*Section 4.9.2*) that has worked well to prevent catastrophic machine failures. All of the pulsed power systems have additional protection components to prevent failures during conditions characterized by high peak power, but low average power.

The trip levels on all machine protection systems are set to for triggering the protected system's rated values. They do not need modification for 3 GeV operation. The cell interlock system, which guards against running the White circuit with a cell out-of-resonance (Section 5.2.1.6), stands as the only additional system that must be installed during the upgrade.

References

[1] H. Wiedemann et al., "The 3 GeV Synchrotron Injector for SPEAR," Proc. of the 1991 IEEE Particle Accel. Conf., San Francisco, 2688-2690.

[2] J. N. Weaver et al., "The Linac and Booster RF System of a Dedicated Injector for SPEAR," Proc. of the 1991 IEEE Particle Accel. Conf., San Francisco, 769–771.

[3] R. Hettel, et al., "The 10 Hz Resonant Magnet Power Supply System for the SSRL 3 GeV Injector," Proc. of the 1991 IEEE Particle Accel. Conf., San Francisco, 926–928.

[4] H.-D. Nuhn et al., "The SSRL Injector Kickers", Proc. of the 1991 IEEE Particle Accel. Conf., San Francisco, 973–975.

[5] Allen, M.A., et al., "Design and Operation of the SPEAR II RF System," (SLAC-PUB-1563), presented at the 1975 Particle Accelerator Conference, Washington, D.C., March 12–14, 1975.

[6] Konrad, G.T., "Performance of a High Efficiency High Power UHF Klystron," (SLAC-PUB-1896), presented at the 1977 Particle Accelerator Conference, Chicago, Illinois, March 16–18, 1977.

[7] Fowkes, W.R., "SPEAR Klystron Test Data," Private communication.

[8] Pellegrin, J.-L. and H. Schwarz, "Control Electronics of the PEP RF System," (SLAC-PUB-2664), presented at the 1981 Particle Accelerator Conference, Washington, D.C., March 11–13, 1981.

Accelerator Facilities & Installation 6

The SPEAR 3 upgrade will leave the conventional facilities of the SSRL Accelerator largely unchanged. No new buildings will be necessary, nor will substantial changes be made to the infrastructure of utilities supporting the accelerator and beam lines. However, the ring shielding, cooling water, and electrical systems will undergo modification.

The main installation of SPEAR 3 components will take place near the end of the upgrade project, during an extended shutdown period of approximately six months. Preparatory work and some modifications take place during the normal 2- to 3-month shutdown periods preceding the extended one.

The following sections discuss the accelerator facility modifications within the context of the SPEAR 3 installation plan.

6.1 SPEAR 3 Facilities

As discussed below, SPEAR 3 facility modifications will affect: shielding, LCW, tunnel insulation, as well as the electrical and fire protection utilities.

6.1.1 Tunnel Shielding

SPEAR's concrete shielding consists of 240 wall blocks (24" thick) and 164 roof (12" thick) blocks, with double-thickness roof blocks (24") where the injection line connects to SPEAR. In most instances, the steel corners of the roof blocks are welded to the side blocks; however, some are attached by bolted angles instead of welds. New beam line alcove walls have been poured in locations that provide optimal radiation protection. A typical cross-section of the SPEAR tunnel appears in Figure 6.1.

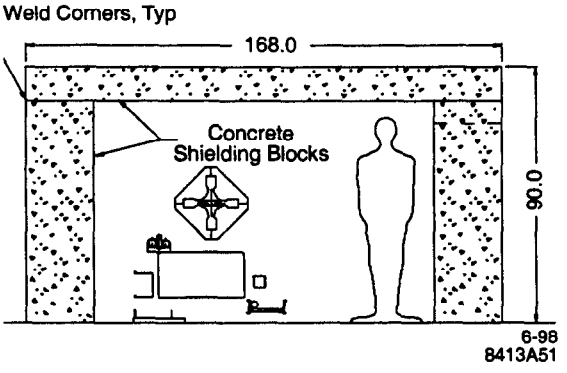

Figure 6.1 A cross-section of the SPEAR tunnel showing wall and roof shielding blocks.

The current shielding of the SPEAR storage ring provides radiological coverage sufficient for current operational parameters. These parameters will change to reflect enhancements to both current (100 mA to 500 mA) and injection energy (2.37 to 3.0 GeV). Preliminary calculations [1] from the SLAC Radiation Physics group indicate that the existing wall-and-roof shielding can be made adequate for SPEAR 3 through 1) the addition of supplementary shielding in appropriate locations, and 2) the integration of a radiation-loss monitor within the Beam Containment System (BCS; Section 4.9.3.3). This takes into account new roof shielding, which will be installed in both the East and West pit areas to reduce sky-shine produced during the injection process.

To enclose (and thermally insulate) the accelerator (Figure 6.2), shielding will be added to the roof and side walls of the East and West long straight sections of SPEAR, which measure 34 ft-wide × 40 ft-long × 7 ft-deep pit areas containing cable and utility channels. Platforms will be poured to support the matching cell-lattice hardware and to provide a base for future insertion devices.

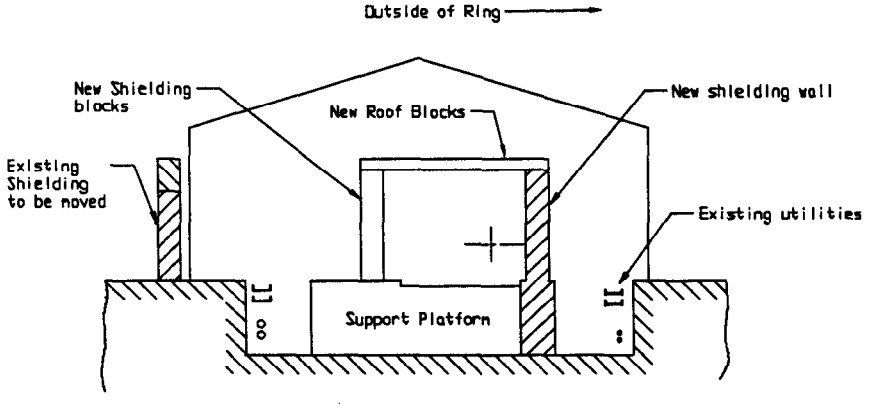

Figure 6.2 New roof shielding for the East & West pit locations.

6.1.2 LCW System

The existing low-conductivity water (LCW) system is sufficient for the new SPEAR 3 magnets, vacuum system, and existing beam lines. However, the addition of new, single-cell RF cavities (along with appropriate circulators and water loads) will raise the total LCW requirement beyond the existing piping capacity. Fortunately, LCW capacity can be increased from 2000 gpm to 3000 gpm through the installation of new connections to the LCW pipes that now supply the injector. RF

load cooling requirements will be met by a stand-alone high-conductivity water (HCW) system (Section 6.1.3).

The LCW system has a supply pressure of 250 psi and a return pressure of 50 psi. The LCW input temperature is 30°C, with a stability of ±0.5°C. New LCW headers will be installed at each girder location to accommodate magnet- and vacuum system connections, as well as to provide a method of isolating the water circuits serving individual components. Table 6.1 shows SSRL's total LCW flow requirements.

Table 6.1 LCW requirements for SPEAR 3 operations at 3.0 GeV and 500 mA. Items with * are stand-alone systems and not counted in the total gpm.

Components	Qty	Total Flow (gpm)
Dipoles	36	238
Quadrupoles	94	150
Sextupoles	72	130
Correctors	72	30
Other magnets	18	54
Straight sections	18	180
SR Absorbers (7x18)	126	360
Vacuum chamber	18	162
Beam Line front ends + 4 future	15	150
RF cavities	4	320
Klystrons	2	240
Circulators	2	20
RF loads (HCW)	4	300*
Water cooled buss	3	15
Power supply building	1	130
Electromagnet Wiggler	2	200
Building 120 + 6 beam lines	6	165
Building 131 + 5 beam lines + 4 future beam lines	9	265
Total		2809

6.1.3 HCW System

A high-conductivity water (HCW) cooling system is needed to absorb power deposited in the loads used for the RF circulators and Magic-Tees (Section 4.5.7). The required flow of 300 gpm will be provided by a stand-alone, HCW, recirculating heat-exchanger system (Section 4.5.7). A rust-inhibitor added to the conventional cooling-tower water increases its conductivity to a level optimal for RF power absorption. Conductivity is continuously monitored and controlled. No special temperature control is required.

6.1.4 Tunnel Environment

The SPEAR ring tunnel is exposed to the weather on all sides, except where buildings have been added to the outside portion of the ring to house beam lines (approximately 60% coverage by buildings). In these areas, the buildings extend to include the outer wall, leaving only the roof exposed to the environment.

Typically, the 24-hour temperature-variation cycle inside the ring lags the outside temperature by approximately 12 hours. Figures 6.3 and 6.4 illustrate that the temperature variation inside the tunnel has been measured at approximately 3°C (29°C to 33°C), while the outside temperature changed by 20°C (8°C to 28°C). During this same time period, the temperature of the iron core of one quadrupole magnet exhibited a temperature range from 32.5°C to 33.5°C. The East and West pit areas, which are not shielded nor insulated, exhibit a temperature variation similar to the outside ambient temperature. Section 6.1.1 describes plans to shield and insulate these two areas.

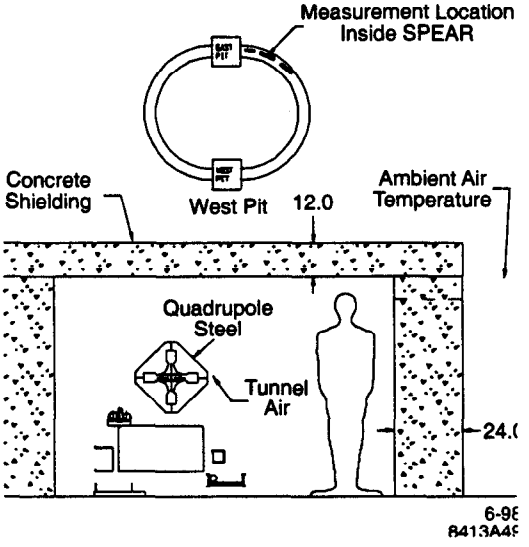

Figure 6.3 The location of temperature thermocouples in the SPEAR tunnel.

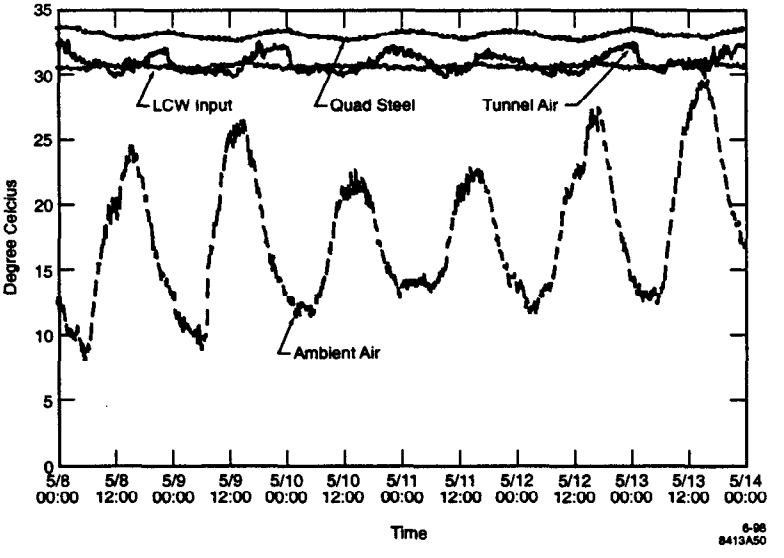

Figure 6.4 Quadrupole, outside ambient air, inside tunnel air, and input LCW temperatures shown over a 5-day period during normal SPEAR operations.

Given the existing shielding structure of SPEAR and its interaction with the environment, a forced air-conditioning system would create more of a thermal gradient than a closed system would [2, Appendix A.3]. The new shielding enclosures for the East and West pits will yield more uniform temperature behavior throughout the ring, by providing thermal insulation–and reducing temperature gradients in the arcs as well. Section 3.4.1.3 addresses the effects of the anticipated ± 1°C diurnal tunnel temperature excursions on beam orbit stability. For the most part, they can be corrected with the Orbit Feedback system (Section 4.7.1). Special reflective white paint will be used to coat the shielding exposed to the sun, so as to reduce heat absorption by the concrete.

6.1.5 Electrical Utilities

The 480V-120V/208V AC power-distribution and lighting systems will be upgraded to comply with NEC standards for clearance and branch-circuit distribution, and to improve their reliability and utility.

The electrical equipment in the East and West pits will be relocated, and their feeders will be replaced by units having ground conductors. New switch panels will distribute power to the magnet girders. General-purpose quad receptacles and three-phase receptacles (similar to current units) will be installed at every girder, and in the shielding alcoves, as needed. Conduit, wiring, boxes, and supports will be surface-routed. Due to water problems, the existing underground raceway system will be abandoned.

Current lighting, which is inadequate for maintenance procedures, will be removed, and a new system will be installed to double the amount of lighting. Light fixtures will be installed on the outside wall and on the inside wall at most alcoves requiring increased light coverage. Fixtures having feeders that cross the ceiling of removable shielding blocks will be easy to remove for maintenance. The PPS lighting system will be reinstalled with its own circuits. The emergency lighting system will be replaced with units at every other girder for greater coverage during a power outage.

6.1.6 Fire Protection System

The Fire Protection system for the SPEAR ring currently incorporates smoke detectors, but no sprinkler system. An improved smoke detection system will be installed in the SPEAR 3 ring. A safety evaluation has determined that a sprinkler system will not be needed inside the ring (Section 7.7).

6.2 Injector Facilities

The SSRL injector shielding has been designed and built for 3.0 GeV operation. Since the injector is now adequately shielded [3], no shielding changes are required.

The LCW system for the injector is separate from SPEAR's LCW system, and is sufficient for 3.0 GeV operation. The injector LCW system has a capacity of 700 gpm, with a supply pressure of 250 psi and a return of approximately 50 psi. The injector facility requires a minimum flow rate of 350 gpm for 3.0 GeV operation and is currently set for 590 gpm, which includes LCW for other test-facility components at the accelerator.

The main LCW pipes supplying the injector have capacity of 2000 gpm, and will be tapped to provide more LCW flow for SPEAR and the beam lines (Section 6.1.2).

6.3 Installation Plan

The major installations for SPEAR 3 will take place during a single downtime lasting approximately 6 months. To accomplish this, all of the hardware will be tested as much as possible and prepared for installation before the downtime commences. A number of subsystems will be installed during preceding 2- to 3-month downtimes as described below. The injector will be converted for 3 GeV operation before the 6-month downtime so that resources can be focused on the major installations.

6.3.1 6-Month Installation Strategy

The 6-month installation strategy relies on minimizing the number of components to be installed, and also restricting them, wherever possible, to the major-magnet, vacuum chamber, and power supply systems. It is important that ancillary activities not interfere during this period, and that all components be preassembled, performance-tested and located in staging areas prior to installation. Completion of all specified work within the allotted time frame will require multiple shifts.

The first major task for the 6-month installation period involves removal of the existing magnets, vacuum chambers, and concrete support girders. The lifting capacity of the removal crane is insufficient to hoist loaded girders. Therefore, the magnets and vacuum chamber must first be removed from girders.

As much as possible, the new SPEAR 3 magnet and vacuum chamber components will be assembled, aligned, wired, and tested on the new steel girders prior to installation. The full, 10 m-long, standard cell girder assembly weighs approximately 58,000 lbs., too much for the lifting crane, so the dipoles, each weighing 14,800 lbs, will be removed after initial alignment and testing. After the girders have been installed and pre-aligned in the tunnel, the dipoles will be remounted on the girders. The fully pre-assembled components for each of the four matching cells will be mounted on three steel stands, each approximately 4 m long.

Electrical connections to the new accelerator components will undergo simplification. Each girder will receive consolidated terminal points, and a new cable plant will be installed before the 6-month installation period begins. Whenever possible, the new cables will be preterminated and kept coiled up in trays external to the tunnel. Water cooling hoses for individual components will be connected to LCW headers on the girder, which, in turn, can be readily connected after installation to the LCW tunnel manifolds.

6.3.2 Prior Downtimes

Tasks that can be accomplished prior to the extended shutdown period include:

- adding radiation shielding in the east and west long straight sections
- relocating the LCW equipment in the east and west pits
- installing AC power and improving lighting
- installing portions of the new cable plant
- pouring concrete pads for matching cell supports
- pouring small concrete pads to facilitate the fourth supports to the new girders
- upgrading the injector for 3 gev operation.

In addition, miscellaneous instrumentation, control, and power supply components can be installed prior to the 6-month period. It may be necessary to increase the prior downtime period from 2 to 3 months, depending on the quantity of work to be done.

6.3.3 Procedures and Tooling

Trained personnel and written installation procedures are key to the success of the 6-month installation effort. Special travelers will be used to ensure all hardware components have been properly inspected and tested before they are moved to the staging area. Personnel will be trained in these procedures and installation techniques.

Special installation tools will be developed and tested on prototype setups to ensure the smooth and safe handling and installation of critical components. Prior to installation within the tunnel, pre-assembled accelerator components will be tested, checked, and verified as ready for installation.

6.3.4 Ring Installation Procedure

At the beginning of the 6-month downtime, accelerator and beam line vacuum chambers will be vented and capped. Many of the vacuum components designated for reuse must be kept in UHV conditions, since they will not be baked out after the downtime. The insertion devices will remain in place. Following the vacuum work, a majority of the roof shielding blocks and some wall blocks will be removed to provide access. Existing magnets, vacuum chambers, LCW lines, cables and other components will be systematically removed from the girders, after which the girders themselves will be removed. Any concrete floor-work for the new girders that hasn't already been completed during prior downtimes must be performed before the new girders are installed. Horizontal and vertical support hardware will be installed onto the standard cell piers, fourth girder support pads, and matching cell pads to prepare for the installation sequence.

Inventories of ring components for SPEAR 2 and SPEAR 3 appear in Tables 6.2 and 6.3, respectively. The following component installation sequence is planned:

- remove the shielding blocks
- install and rough-align the preassembled girders
- install and align the dipoles
- final-align the magnets and vacuum chambers
- install the new straight sections
- replace the shielding blocks
- connect the bellows with the straight sections
- install the beam line front-end components
- complete the magnet-bus and cable connections
- complete I&C and MPS connections

A schedule for the 6-month installation appears in Figure 8.2.

Table 6.2 Inventory of SPEAR 2 components.

Component	Quantity	Total Weight (tons)
Dipoles	36	200
Quadrupoles	54	81
Sextupoles	36	18
Concrete girders	18	126
RF cavities	2	2
Vacuum chambers	18	1
Total		428

Table 6.3 Inventory of SPEAR 3 components.

Component	Quantity	Total Weight (tons)
Dipoles	36	280
Quadrupoles	96	144
Sextupoles	54	54
Standard-Cell girders	14	105
Matching-Cell girders	12	30
RF cavities	4	2
Vacuum chambers	54	27
Total		642

6.3.5 Power Supply Installation

SPEAR 3 power supply system installation during the 6-month downtime in Building 118 entails the following major tasks:

- Removal of the AC distribution system and the old power supplies.
- Removal and replacement of the existing floor in Building 118.
- Installation of the new AC distribution equipment.
- Installation of the new and reused power supplies.
- Modification of the reused raceways and installation of new raceways.
- Modifying the reusable cables/bus (and installing new cable, as well).
- Terminating new and reused cables at the power supply and load ends.

There is more than sufficient room in Building 118 to house all the reused and new power supplies. The planned layout of power supplies in Building 118 is shown in Figure 6.5. Since all the power supplies can be fed from a 480 V distribution system, the 4160 V distribution equipment in Building 118 will be removed.

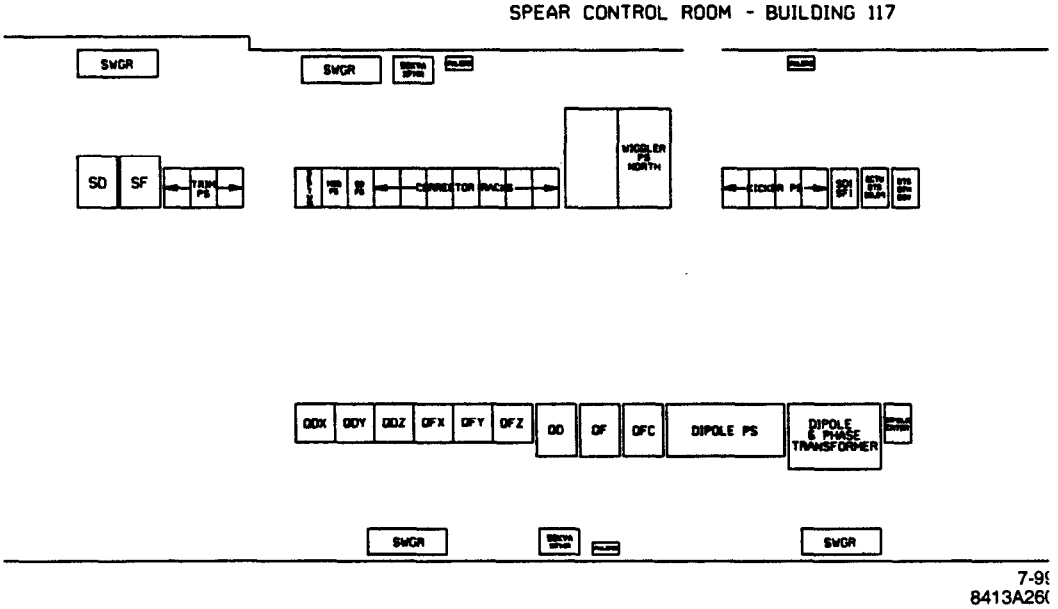

7-9
8413A26

Figure 6.5 Floor plan of the power supply building 118.

6.3.5.1 AC and Old Power Supply Removal

The AC distribution system for the power supplies (and support equipment) is reaching the end of its reliable life, and therefore must be redone. Furthermore, the 4160 V system is no longer required. Other distribution circuits must be reconfigured electrically and physically to meet SPEAR 3 needs. All 4160 V, 480 V, and 208V/120V switchgear, transformers, panel boards, raceways and cable will be removed. To ensure that the system de-energization and removal is achieved in a safe and orderly way, a detailed plan will be drawn up to identify all circuits slated for removal. SLAC's Lock-and-Tag verification procedures [4,5] will be strictly enforced before any circuit is removed. Decommissioning and removal of the existing AC distribution system begins by ensuring that all feeds into Building 118 are locked open.

Many SPEAR power supplies now in Building 118 have either reached the end of their useful lives, or their rating/performance levels do not coincide with SPEAR 3 needs. These power supplies are not slated for reuse. Whether new or reused, all power supply cable must be disconnected, because the floor of Building 118 will be upgraded to facilitate the proper mounting of all power supplies. All power supplies not designated for reuse will be removed. Those power supplies designated for reuse will be properly packaged and placed into storage until the time of reinstallation. The power supply cables can be cut to facilitate removal. Once disconnected, the power supplies themselves can be dismantled or simply removed from their floor anchors and fork-lifted away for storage or salvage.

6.3.5.2 Concrete Floor

All power supplies, whether freestanding or rack-mounted, must be bolted to the floor to preclude their overturning during an earthquake. The floor in Building 118 is part asphalt and part concrete. Since asphalt lacks the necessary strength, and the existing concrete lacks the thickness to conform to SLAC's seismic hold-down requirements, the existing asphalt/concrete floor will be removed prior to power supply installation and replaced with a 5-inch thick concrete floor.

6.3.5.3 AC Distribution Installation

The AC one-line diagram for the power supplies in Building 118 is shown in Figure 6.6. Not shown on this diagram are the downstream branch circuit breakers located in each freestanding power supply (or in the racks where power supplies are mounted). The power is derived from two 200 kVA transformers and circuit breakers (4B-155 and 4B-156), which are located in Substation 507, adjacent to Building 118. All the other equipment shown in Figure 6.6 are located indoors, within Building 118.

AC power for the SPEAR 3 supplies is at the 480 V or 208 V, 3-phase level. Power to operate the power supply controllers (and other controls) is supplied as single-phase 120 V. No higher system voltage is required. Branch AC power for the power supplies is located in 480 V switchgear or in 208V/120V panel boards. Furthermore, the 480 V switchgear is PPS-interlocked, as discussed in Section 4.6.5.3. The switchgear and panel boards are located in visual proximity to the power supplies they serve. Not shown in Figure 6.6 are the downstream-branch circuit breakers located in each freestanding power supply.

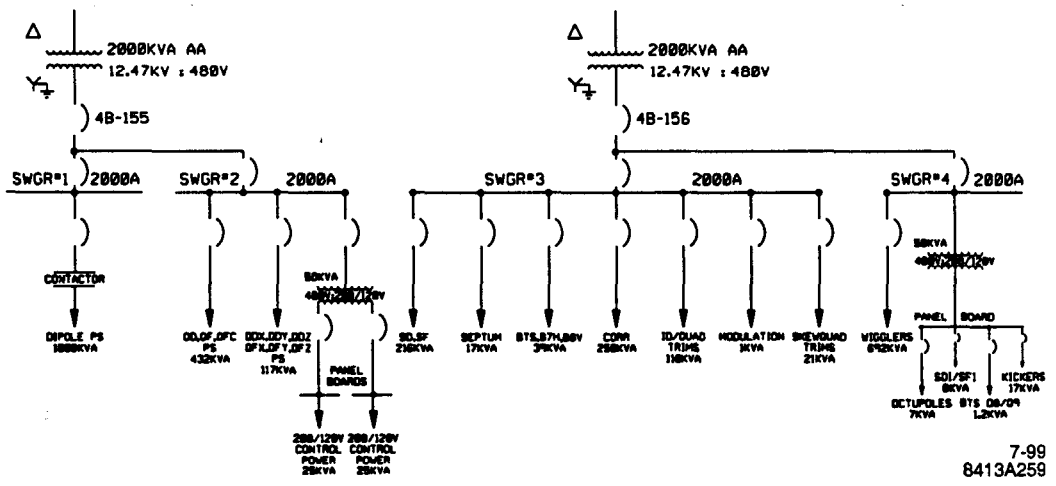

Figure 6.6 AC power one-line diagram for power supply systems in Building 118.

6.3.5.4 Power Supply Installation

Approximately 80 power supplies (together with their racks) must be installed for SPEAR 3. To prevent tipping during an earthquake, freestanding power supplies and racks will be placed into position and anchored to the concrete floor at all four corners. Rack-mounted power supplies will be assembled and wired as much as possible prior to installation in Building 118. Items included in the shop pre-assembly are AC distribution panels, power supply controllers, wiring power strips internal to the rack, convenience outlets, and power supply mounting shelves. If the necessary components are on hand, power supplies will be mounted onto racks before the racks themselves are installed. Otherwise, the power supplies will be mounted on the installed racks. Power supply and distribution layouts will accommodate future expansion and a possible migration from series-connected, magnet-family supplies toward more individual magnet power supplies.

6.3.5.5 Raceway, Bus and Cable Installation

Due to the large amount of equipment that will be installed in SPEAR 3, the raceway and cable plant installation will be complex and labor-intensive. All existing unused cables will be removed. Cable removal will eliminate bad appearances, reduce heat buildup, avert cable tray overfill, and create space for new cables.

Considerable cable documentation is required. Drawings, including layouts, coding sheets, wiring diagrams, etc., will be made for contract bidding and for installation. Some of the needed information will have to be extracted from the field. Block wiring diagrams will be created, and all the new and reused cable plant will be documented in the CAPTAR database [6].

All damaged or corroded cable tray will be replaced. Cable tray systems will be modified, as required, to conform to the new building, power supply, and magnet layouts and positions. There are instances where existing wall-mounted cables will be put into the cable tray. When cable trays carrying high voltages are accessible to personnel, covers will be placed over the trays. The heat loading in the covered trays will be evaluated to ensure that cable temperatures do not exceed the cable insulation ratings.

6.3.6 SPEAR 3 Start-up and Commissioning

After installation is complete, SPEAR 3 start-up will follow practices used after long downtimes. The linac and booster systems will be made operational before SPEAR 3 is turned on. The SSRL

Operations Group will begin a two-shift work schedule during the linac and booster system checkouts, and then go to three shifts per day when the beam is established.tart-up schedules for the SSRL injector and SPEAR 3 after the installation are shown in Tables 6.4 and 6.5, respectively.

Table 6.4 SSRL injector start-up schedule

#	DESCRIPTION	Oct		Nov		Dec		Jan
1	SHIFT SUMMARY							
2	TWO SHIFTS		++++++					
3	THREE SHIFTS			++++++	++++++	++++++	++++++	+++++
4	linac & LTB	++++	++					
5	Prepare BAS for sign-off		+					
6	ACM/BCS checks (no beam)		++	+				
7	Pre-checks		++					
8	Prepare PSs for PPS certification		++					
9	Prepare RF for PPS certification		+++					
10	BCS checks (BSOICs)			+				
11	PPS certification			+++				
12	Finish linac bake-out.			+				
13	Power supply interlink checks			+++				
14	S-band interlink checks			+++				
15	Process linac (beam)				+++			
16	ACM certification (with beam)				+			
17	ACM - scope calibration				+			
18	Beam to booster				+++			
19	BOOSTER & BTS							
20	LCW On & flow checks							
21	Prepare BAS for sign-off		++++	+				
22	Pre-checks		+++	++				
23	BCS checks (BIOSICs)			++				
24	Prepare PSs for PPS certification			+				
25	Prepare RF for PPS certification			+				
26	Heat and smoke detectors test			+				
27	Kicker tests			+				
28	PPS certification			++				
29	RF interlink checks			++				
30	RF hot tests			+				
31	RF processing			++				
32	Power supply checks				+++			
33	Power supply hot tests				+++			
34								
35	Establish beam				+++++			
36	Injector radiation measurements				++			
37	Beam to SPEAR Faraday Cup				++			
38	Beam To SPEAR					+++++		

Table 6.5 SPEAR 3 start-up schedule.

#	DESCRIPTION	Oct		Nov		Dec		Jan
39								
40	spear							
41	Prepare BAS for sign-off	++						
42	LCW On & flow checks	++++++						
43	Beam line pre-run checks	+++++	++++++					
44	MPS checks	+++++	++++++					
45	Beam line PPS checks		++	++++++				
46	SPEAR pre-run checks		++	++++++				
47	Ring lock-up		++					
48	BCS checks (BSOICs)		++					
49	Kicker tests			++++++				
50								
51	Prepare PSs for PPS certification			++++++				
52	Prepare RF for PPS certification			++++++				
53	PPS certification			++	++++			
54	Power supplies PPS certification				++			
55	Global PPS certification				++			
56	New power supply checks				++++++			
57	RF interlink checks				++++++			
58	PS interlink & power tests				++++++			
59	RF processing				++++++			
60	PS polarity checks				++			
61								
63	CONFIGURATION DEVELOPMENT							
64	3 GeV configuration development					++++++	++++++	
65	BLA checks					++		
66	BPM calibration (QMS)						++++++	
67	Prepare beam lines for steering						++++++	
68	Steer beam lines						+++++	
69	Radiation measurements						++++++	
70	Prepare beam lines for users						++++++	++
71	Scrub & Accelerator Physics run						++++	++++++
72	Beam to users							++

References

[1] Vylet, Vashek: Shielding and Radiation Safety Considerations for the SPEAR 3 Upgrade, RP-98-8, June 2, 1998

[2] G. Bowden, internal SSRL note, 1997.

[3] N. Ipe; Radiological Aspects of the SSRL/SLAC 3.0 GeV Injector, internal document, SLAC TN 9111, September 1991.

[4] SLAC Lock-And-Tag Program For The Control Of Hazardous Energy, Document Number SLAC-I-730-OA10Z-001.

[5] Bulletin 50, "Verification of No-Voltage Status in Beam Line Housings."

[6] CAPTAR is the SLAC Cable Plant Tracking Database designed using the commercial Oracle relational database program.

Environment, Safety & Health and Quality Assurance

7

SLAC's management policies and work practices integrate safety and environmental protection at all levels, thus safeguarding workers, the public, and the environment. Following DOE P450.4, Safety Management System Policy, which promotes the Work Smart Standards process, SLAC has developed and implemented an Integrated Safety Management plan (ISM), which builds upon measurable performance metrics as well as SLAC programs already incorporating ISM elements successfully.

The ISM process focuses on 'core functions,' which: 1) define the scope of the work, 2) identify and analyze attendant hazards, 3) develop and implement hazard controls, 4) perform the work under rigorous control, and 4) use feedback from actual work experiences to improve the safety system. Responsibility for achieving and maintaining excellence in this system rests with SLAC's line managers, who implement SLAC ES&H policies for all personnel they supervise.

Existing and mature programs at SLAC ensure the proper management of all project phases, from design and installation to testing and operation. For all new projects and facility modifications, such as the SPEAR 3 upgrade project, the SLAC Safety Overview Committee assigns "citizen committees" to perform safety reviews. Each group possesses special expertise in areas including, but not limited to: radiation safety, electrical safety, earthquake safety, and fire protection.

Operating SPEAR in its present configuration has given us an opportunity to identify the principal hazards and risks associated with electron storage rings. They are: ionizing radiation, electrical safety issues, non-ionizing radiation, seismic safety issues, fire safety (including emergency preparedness), construction activities, hazardous material issues and environmental protection relating to the design, component manufacturing, system installation and operation of the SPEAR 3 facility. Table 7.1 summarizes these hazards and their associated mitigation controls.

The SPEAR 3 upgrade will not generate any hazards that have not already been defined, and the project will not present any significant challenges within the realm of ES&H. All aspects of the upgrade will conform to the applicable Work Smart Standards SLAC has written into its contract with the DOE.

Table 7.1 Hazard identification and mitigation

Item	Hazard	Possible Causes	Mitigating Controls
1	Ionizing radiation exposure, outside accelerator housing. • Prompt radiation	• Personnel error • Interlock failure	• Safety procedures • Design, maintenance and inspection of radiation safety systems • Training
2	Ionizing radiation exposure, inside accelerator housing. • Prompt • Residual • Contamination	• Personnel error • Interlock failure	• Safety procedures • Design, maintenance and inspection of radiation safety systems • Training
3	Fire; inside accelerator housing. • Electrical • Welding/cutting • Smoking • Hot work (soldering)	• Equipment failure • Personnel error	• Sprinklers (Pits) • Smoke detectors • Fire alarms • Exit routes • Training • On-site Fire Department
4	Fire; equipment and control areas. • Electrical • Welding/cutting • Smoking • Hot work (soldering)	• Equipment failure • Personnel error	• Sprinklers (Pits) • Smoke detectors • Fire alarms • Exit routes • Training • On-site Fire Department
5	Electric shock. • High voltage • Low voltage/high current • Exposed 110v	• Personnel error • Equipment failure • Interlock failure	• NEC Compliance • Design, maintenance and inspection of electrical interlock systems. • Procedures (L & T) • Training • PPE
6	Non-ionizing radiation exposure. • RF	• Personnel error • Equipment failure • Interlock error	• Design, maintenance, and inspection of interlock systems. • Procedures • Training
7	Construction activities. • Heavy equipment • Material handling • Slips/trip/falls	• Personnel error • Equipment failure	• Barriers • Procedures • Training • Inspections
8	Seismic hazards.	• Earthquake	• Design, construction, and upgrade of structures (buildings, accelerator housings) and equipment to building and structural codes • Field inspections
9	Exposure to hazardous materials, including: • Cryogens • Solvents • Oils • Welding/cutting fumes	• Personnel error • Equipment failure	• Engineering analysis and inspection of systems using hazardous materials • Procedures • PPE • Training • Ventilation
10	Adverse effects to environment. • Spills • Water discharges to sanitary • and storm drains • Noise • Air emissions (dust, leaks) • Soil contamination	• Construction and installation activities • Equipment failure • Personnel error	• Training • Procedures • Inspections

7.1 Ionizing Radiation

The design and operation of all radiation-producing facilities at SLAC is governed by the ALARA (as low as reasonably achievable) policy. SLAC has always maintained radiation dose limits below the maximum allowed by regulation.

7.1.1 Radiation Shielding

Shielding for SPEAR 3 will conform to the Radiation Safety Systems Technical Basis Document, Chapter 1 Radiological Guidelines for Shielding and Barriers (SLAC-I-720-0A05Z-002). Under normal operation the design criterion will be (i) 1 rem/yr at 30 cm from the shield surface, assuming a 2000 hr working year and an occupancy factor of 1. In addition, as SSRL has non-radiological workers (Users), additional shielding may be required to maintain their annual effective dose equivalent below 0.1 rem/yr taking exposure duration and occupancy factors into account. SLAC internal design criteria also require that under a system failure (ii) the effective dose equivalent shall not exceed 3 rem for a broad beam and 12 rem for a narrow beam, and that under an accident scenario that requires human intervention to turn off the beam (iii), the maximum dose equivalent shall not exceed 25 rem averaged over a one-hour period.

An analysis of the present shielding indicates that potential beam losses from SPEAR 3 during injection could produce high radiation doses in both the forward and lateral directions. While loss of the stored beam either as a "single point loss" or as a "distributed loss" could produce unacceptable cumulative dose values over the course of a normal run of 10 months, localized shielding in the form of shadow masks and/or lateral shielding can mitigate this hazard to acceptable values. Definition of the type and amount of local shielding depends on the final configuration of SPEAR 3, and such definition will have to be done on a case-by-case basis for the beam lines. Installation of an electron beam loss monitor around the circumference of the ring will also provide a diagnostic capability usable to determine where beam losses are taking place. Adding this monitoring package into the beam containment system (BCS) will further help maintain dose levels below the limits allowed at SLAC.

7.1.2 Personnel Protection System

The personnel protection system (PPS) (Section 4.9.3.2) consists of electrical interlocks and mechanical barriers whose primary functions are to prevent entry of personnel into a radiation enclosure when a beam is operating and also to turn the beam off when a security violation is detected. Other PPS functions include: (i) providing interlocks for the orderly searching of an area before a beam is turned on, (ii) allowance for various access states, such as No Access, Controlled Access, or Permitted Access, (iii) provision for emergency shut-off capabilities, (iv) control of the electrical hazards in beam housing areas. As installation of SPEAR 3 will not require a significant change to the present shielding footprint, the PPS will undergo only those upgrades and enhancements necessary to address the new facility and operating conditions (i.e. expansion of the input interface to accommodate new power supplies, access points or other components which the PPS must control). The PPS will remain largely unchanged in terms of its design, function and configuration, and all additions will conform to the Radiation Safety Systems Technical Basis Document, Chapter 2 Personnel Protection Systems (SLAC-I-720-0A05Z-002).

7.1.3 Beam Containment System

The beam containment system (BCS) (Section 4.9.3.3) prevents accelerated beams from diverging from the desired channel, and it detects excessive beam energies or intensity levels that can cause unacceptable radiation levels. Beam containment is usually accomplished by a combination of

passive devices such as collimators, which are designed to absorb errant beams, and active devices such as electronic monitors, which shut off the beam when they detect out-of-tolerance conditions. The BCS currently in SPEAR consists of passive mechanical devices such as slits, collimators, magnets, electron beam stoppers, dumps, photon beam stoppers, and injection beam stoppers, and active electronic devices such as average-current monitors, burn-through monitors, and beam shut-off ion chambers. Additionally, SPEAR 3 will install long ion chambers in the accelerator tunnel, which sense both single point and distributed beam losses.

Long ion chambers (Section 4.9.3.3.1) send a signal that has been calibrated against radiation levels outside the shielding to the BCS electronics, which in turn prevent injection if radiation levels go above a preset limit. The system will also be used as a beam loss diagnostic tool, enabling the accurate location of beam losses and helping operations personnel with steering.

7.1.4 Radiation Safety Training

In accordance with SLAC's Site Access, ES&H Training, and Radiation Dosimetry (SLAC-I-720-0A00Z002), all individuals at SLAC who enter the radiologically-controlled area (RCA) or the accelerator area must be properly trained or escorted by a properly trained individual. Levels of training depend on the area to be accessed and, in some cases, the duration of the individual's stay (Table 7.2).

Table 7.2 Minimum training for unescorted access.

Access Required	Duration of Access	Potential Dose (mrem/yr)	Required Training Level					Dosimeter
			Safety Orientation	EOESH	GERT	RWT I	RWT II	
Accelerator Area, No RCA	<60 days	0	x					
Accelerator Area, No RCA	>60 days	0		x				
Accelerator Area, RCA	Any	<100		x	x			x
Accelerator Area, RCA	Any	>100		x	x	x		x
Accelerator Area, RCA High Radiation Area	Any	Any		x	x	x		x
Accelerator Area, RCA Contamination Area	Any	Any		x	x	x	x	x

7.2 Electrical Safety

By nature, an accelerator facility has subsystems that either produce or use high voltages or high currents. These subsystems can present an electrical hazard to personnel if not managed properly. As SPEAR 3 will operate in a mode similar to the present machine, a strong understanding already exits of the control and work procedures for the electrical subsystems---as well as for entry into the accelerator housing. Primary mitigation of the hazard will occur through the de-energizing of equipment and the effective use of Lock-and-Tag procedures.

Thus, the design, upgrade, installation and operation of electrical equipment will comply with the National Electrical Code, the Code of Federal Regulations, Subpart S Electrical and SLAC's policy on Electrical Safety, SLAC ES&H Manual, Chapter 8 (SLAC-I-720-0A29Z-001-R007). Entry into the accelerator housing will require complete lock-down of all electrical hazards, the application of group lock-out/tag-out hardware, as well as personnel locks, as appropriate. In specific cases, electrical hazards may be mitigated by the selective use of mechanical barriers that have been interlocked to further reduce the risk of exposure to electrical shock. Various levels of electrical

safety training and Lock and Tag training are provided by SLAC for those personnel who may work on or near potential electrical hazards.

Infrequently, it may be necessary to complete work on energized equipment. Such tasks are conducted under very limited and controlled conditions, using qualified employees and requiring the full approval of the appropriate Associate Director.

Special procedures will be developed to permit authorized personnel to occupy areas adjacent to energized magnets. These procedures are called RASK, for "Restricted Access Safety Key." Under these procedures, a special RASK authorization form must be completed to obtain a key that enables (turns on) the electrical power supply for a single magnet, or unique string of magnets to be tested. During this time the emergency-off buttons remain active and will shut off the power supply when pushed.

7.3 Non-Ionizing Radiation

The SPEAR 3 RF system will produce radio frequency radiation in the 476 MHz range, which when not controlled could adversely affect the health of personnel working on or near the system. SPEAR 3 will incorporate safety measures based on the present operation. These include pressurized wave guides and a policy of strict adherence to procedures for installing and testing of the RF system.

Wave guides will be pressurized with a regulated source of instrument air. Since the volumetric supply rate is limited, a leak in the wave guide causes a pressure drop, subsequent actuation of a pressure switch, and finally, shutdown of the storage ring. After the completion of repairs to the wave guide, mandatory testing of the repair for RF leakage will take place.

Pressurization guards mainly against operation of the system plagued by a missing piece of wave guide or an improperly assembled flange joint. Although the most likely cause of RF leakage under operating conditions is that a wave guide joint is loose or undone, it is possible for the system to be gas tight but not RF leak tight. This occurs when flange bolts are not properly tightened and the rubber gasket is not fully compressed. This is avoided by ensuring all bolts are tightened to a predetermined value and by testing for rf leaks after all installation, maintenance and shut-down activities.

7.4 Emergency Preparedness

The U. S. Geological Survey estimates the chance of one or more large earthquakes (magnitude 7 or greater) hitting the San Francisco Bay area in the coming 30 years at about 67 percent. This represents the emergency situation most likely to arise at SLAC.

7.4.1 Seismic Safety

SLAC structures are designed and constructed to reduce major earthquake damage to acceptable levels. As SPEAR 3 is a significant upgrade to an existing facility, the present SPEAR accelerator housing will undergo a technical assessment of it's seismic stability. The SLAC Earthquake Safety Committee will direct this. To ensure and maintain a safe and healthful workplace, the design and installation of experimental equipment for SPEAR 3 will also be reviewed by the SLAC Earthquake Safety Committee, as mandated by the SLAC Safety Program.

7.4.2 Emergency Planning

The design, review, installation, and operation of all experimental equipment at SLAC is done in a manner that minimizes the risk of accident or injury to personnel and property in the event of either

a natural disaster or emergency situation. SLAC's formal emergency planning system as described in the SLAC Emergency Preparedness Plan (SLAC-I-720-70000-105) will help ensure a logical, organized, and efficient site-wide response to any emergency. Facility-specific procedures which supplement the SLAC plan, support a timely initial response, further decreasing the probability of personal injury and limiting potential loss or damage to both property and the environment.

7.5 Construction Safety

During construction operations, oversight of subcontractor activities and safety compliance remains a line-organization responsibility through the University Technical Representative (UTR) or Project Engineer, if a UTR is not assigned to the activity. Detailed activities and job functions are clearly set forth in the SLAC Quality Assurance and Compliance Design Assurance and Construction Inspection Procedure (SLAC-I-770-0A22C-001). Responsibilities include, but are not limited to:

- Apprising subcontractors of SLAC and DOE safety criteria prior to construction.
- Informing subcontractors of the hazards routinely found at SLAC.
- Conducting periodic inspections of subcontractor construction areas to evaluate the quality of the subcontractor's safety compliance program and quality of work.
- Providing information to SLAC Citizen Safety Committees as required or requested.
- Communicating with the subcontractor and resolving safety or quality deficiencies identified by SLAC personnel.
- Receiving subcontractor accident reports and compiling information for reporting to the DOE.

Enforcement of subcontractor requirements is carried out by the SLAC Purchasing Department and may involve with holding payment(s) if applicable codes and standards are not met.

7.6 Hazardous Materials

During the upgrade and operation phases of SPEAR 3, it is anticipated that a minimum amount of hazardous materials will be used. Examples would be paints, epoxies, solvents, oils and lead in the form of shielding etc. There are no current or anticipated activities at SPEAR that would expose workers to levels of contaminants above acceptable levels.

The SLAC Industrial Hygiene Program detailed in the SLAC ES&H Manual addresses potential hazards to workers from the use of hazardous materials. The program identifies how to evaluate workplace hazards at the earliest stages of the project and implement controls to eliminate or mitigate these hazards to an acceptable level.

Site- and facility-specific procedures are also in place for the safe handling, storing, transporting, inspecting and disposing of hazardous materials. These are contained in the SLAC Hazardous Materials Management Handbook (SLAC-I-750-0A06G-001), and the SLAC ES&H Manual, Chapter 4, Hazard Communication (SLAC-I-720-0A29Z-011-R012) which describes minimum standards to maintain for compliance with Code of Federal Regulations (CFR), Part 29, 1910.1200.

The UTR or Project Engineer has added responsibilities with respect to the management of hazardous materials. He or she ensures that subcontractor's personnel are aware of, and in constant compliance with SLAC's written Hazard Communication Plan. This person also keeps affected SLAC personnel informed of hazardous material usage, along with associated hazards and risks.

7.7 Fire Safety

The probability of a fire in SPEAR 3 is expected to be similar to that for present operations, as new ring components will be fabricated primarily from non-flammable materials similar to those used in the current installation. Additionally, combustible materials are kept to a minimum. The most "reasonably foreseeable" incident or event with any substantial consequences would be a fire in the insulating material of the electrical cable plant caused by an overload condition. This differs from the maximum credible fire loss, which assumes proper functioning of the smoke detector system and a normal response from the fire department. In this case, loss would be confined to a single girder, but would include magnets, vacuum chamber and associated cabling. The SLAC ES&H Manual addresses all fire safety issues. Chapter 12, Fire Safety, (SLAC-I-720-0A29Z-001-R007).

Installation of new cables in SPEAR 3 will meet the current SLAC standards for cable insulation and comply with National Electric Code (NEC) standards concerning cable fire resistance. While this reduces the probability of a fire starting, an aspiration type smoke detection system (VESDA) in the accelerator housing and fire breaks in the cable trays will mitigate fire travel. Support buildings for power supplies and electronic equipment are protected by automatic heat-activated wet sprinkler systems and smoke detectors. Fire extinguishers for use by trained personnel are located in all buildings and accelerator housings. The combination of smoke detection systems, sprinklers and on-site fire department (response time ~3 minutes) affords early warning of and timely response to fire or smoke related incidents.

Personnel injury caused by a fire is not expected because all locations within the SPEAR 3 accelerator housing and its support buildings are within 100 feet of an exit. Furthermore, all locations have access to two directions of egress. Multiple entry/exit points also help in keeping property damage to a minimum.

7.8 Environmental Protection

The SPEAR 3 upgrade entails the disassembly of the present magnets and vacuum chambers, replacing the electrical distribution system, minor modifications to the Low Conductivity Water (LCW) system and possibly some limited removal of asphalt and concrete to allow for installation of support piers for stabilizing the concrete girders. Removal of these materials and the subsequent upgrade activities will produce small quantities of hazardous, non-hazardous and radioactive waste that need to be managed through defined channels. Past history indicates that normal operation of the accelerator does not typically produce waste, however, some hardware may have induced radioactivity associated with it from its proximity and time close to the beam. While other components may contain hazardous materials as part of their design, i.e. mineral oil in electrical components, or have radioactive contamination from the LCW system. Core samples of the asphalt, concrete and soil in the accelerator housing show no signs of radioactivity.

All material removed from within the accelerator housing will be surveyed for residual radioactivity or contamination. If none is detected, then items will be salvaged for re-use, recycled as scrap material, or disposed of as non-hazardous waste in an approved off-site landfill. Items that show residual radioactivity or other contamination will be stored on site in the Radioactive Material Storage Yard (RAMSY) for future reuse or ultimate disposal. Any hazardous waste will be disposed of in accordance with SLAC procedures and ultimately to a permitted Treatment, Storage and Disposal Facility, under regulations set forth in the Resource, Conservation and Recovery Act (RCRA).

Component manufacturing and system installation may also produce hazardous wastes, such as solvent used in de-greasing baths or spent cutting fluids etc. These are ongoing operations at SLAC,

where disposal of wastes is routine and in full compliance with SLAC's policies on the management of hazardous materials and waste minimization.

All activities will be managed to prevent adverse impact on ground water and storm water quality, air quality and to minimize any ground disturbing activities.

7.9 Quality Assurance

A Quality Assurance Program Plan (SLAC-I-770-0A17M-001-R001) conforming with DOE Order 5700.6C, Quality Assurance, was established at SLAC to provide laboratory management with guidance and requirements toward achieving quality in pursuit of the laboratory mission. Overall responsibility for the implementation of this program lies with the SLAC Director, while accountability for managing the program at the divisional level rests with the respective Associate Director (AD). For the SPEAR 3 upgrade project, the "Project Leader" has been assigned (via the SSRL Division AD), the responsibility for staffing, documenting, generating Quality Implementing Procedures (QIPs), and implementing the QA program. At the project level this includes developing and maintaining required management systems, or using management systems that are already available.

The QA plan describes SLAC's approach to implementing the ten criteria of DOE Order 5700.6C:

- *Criterion 1*: requires specific Quality Implementing Procedures for all SLAC projects where total project costs exceed $5,000,000.
- *Criterion 2*: as appropriate defines specific requirements and assures adequate qualification and training for individuals connected with the project, including retention of training records.
- *Criterion 3*: defines requirements for management's responsibility with respect to identification, analysis, resolution and follow up of ES&H, technical and compliance issues.
- *Criterion 4*: provides policy for identification of documents (policy, procedures, drawings etc.), records and other specific elements that will have a significant impact on the project and need to be entered into a document control system.
- *Criterion 5*: requires project leaders to define and maintain work processes for R&D efforts that have a significant programmatic impact.
- *Criterion 6*: establishes a responsibility for line management to conduct design reviews and to promote the use of design standards.
- *Criterion 7*: discusses a graded approach to the development of specifications for procurement of items and services based on cost and failure impact.
- *Criterion 8*: established responsibility for the staffing, documenting, and performing of inspection and testing activities related to the project.
- *Criterion 9*: requires participation in the SLAC Institutional Self-Assessment Program.
- *Criterion 10*: provides the authority for the Quality Assurance and Compliance Department to conduct independent assessments of all SLAC facilities and projects as warranted to verify the degree of conformance to QA and ES&H requirements.

Effective use of these criteria will enable the SPEAR 3 project to:

- Incorporate quality and reliability into the facility's design.
- Promote early detection of problems to minimize failure costs and impact on schedule.
- Develop appropriate documentation to support upgrade and operational requirements.
- Establish methods to identify critical systems and to release these systems based on demonstrated performance.

- Define the general requirements for design and readiness reviews for all aspects of the project.
- Assure that personnel are trained before performing critical activities, especially those entailing ES&H consequences.

Cost and Schedule 8

The SPEAR 3 project, as described in the preceding sections, is an upgrade of the existing SPEAR 2 storage ring. The upgrade replaces the SPEAR 2 lattice with a new low emittance lattice involving new magnet elements together with a new vacuum system. A new RF system provides the capability for 500 mA beam current. The SPEAR 3 upgrade is accomplished within the existing radiation shielding enclosure; hence no significant conventional construction is required.

A detailed Work Breakdown Structure (WBS) was developed for the project to insure cost estimate completeness, to facilitate future tracking of costs for all technical subsystems and to insure the proper reporting of all costs and commitments in the accounting process.

The WBS is defined at Level 2 in Section 8.1 and is followed by the associated costs in Section 8.2. Section 8.3 provides a high level overall project schedule together with a more detailed schedule for the final installation period.

8.1 Work Breakdown Structure (WBS)

All efforts and components required for SPEAR 3 are organized by a WBS which provides a definition of the complete project scope and forms the basis for estimated costs needed in the planning, execution, and control of the project. The WBS levels basically follow the following structure:

Level 1:	Total project
Level 2:	Major systems
Level 3:	Subsystems
Level 4:	Subsystem details

Thus WBS Level 1 includes all aspects of the project from initial design through fabrication to final installation of all components. WBS Level 2 provides a definition of SPEAR 3 in terms of ten major systems as follows:

1.1 Magnets and Supports

The existing SPEAR 2 magnets will be removed and replaced by new dipoles, quadrupoles, sextupoles, and correctors designed for the SPEAR 3 lattice. The magnets will be supported and aligned on top of new steel girders. This category also includes magnetic measurements.

1.2 Vacuum System

New copper vacuum chambers will be designed and fabricated according to SPEAR 3 beam aperture requirements with synchrotron light ports that match the position of existing beam lines. Vacuum pumping and beam monitoring systems are included.

1.3 Power Supplies

New power supplies are provided to match the requirements of the new magnets (WBS 1.1). Controller racks and accessories are included as well as the required DC bussing and cabling together and AC power distribution modifications.

1.4 RF System

The RF power will be increased to provide beam currents to 500 mA. The plan involves changing the RF frequency from 358.5 MHz to 476.3 MHz to allow using the RF cavities and components that were designed and fabricated for the PEP-II project.

1.5 Instrumentation and Controls

This area includes modifications and additions to the SPEAR computer control, beam monitoring, lattice diagnostics, and beam protection systems. Associated cable plant requirements for these systems are also included.

1.6 Cable Plant

Cable Plant includes the costs for new cable trays and wire ways, plans for cable removal, and procurements of new power and signal cables required for SPEAR 3 operation.

1.7 Beam Line Front Ends

The beam line front end vacuum system components will be upgraded to accept the increased photon flux density for 500 mA SPEAR 3 operation.

1.8 Facility

The shielding walls of the East and West pits will be modified for the increased SPEAR 3 beam current. Modifications to the LCW and AC power systems are included to match the needs of the new lattice components.

1.9 Installation and Alignment

This category contains all installation and alignment processes for magnets and supports, vacuum, power supplies, RF, instrumentation and controls, injector, beam line front ends, and facilities.

1.10 Management and Accelerator Physics

This area provides support for the overall project including the Project Directorate, Accelerator Physics, Radiation Physics, ES&H, and Administrative Support.

8.2 Project Costs

The SPEAR 3 cost estimate was generated in terms of Engineering Design and Inspection (EDI), Materials and Services (M&S), and Labor at various levels of the WBS described above. Labor categories were selected, representative of the project needs, and are listed in Table 8.1.

Table 8.1 SPEAR 3 labor rates for FY99.

Labor Categories	K$/month
Mechanical Engineer	8.0
Electrical Engineer	8.7
Mechanical or Electrical Designer	6.0
Coordinator	7.0
Physicist	8.0
ES&H professional	7.3
Software Engineer	8.6
Technician	6.0
Administrative Support	5.0
Consultants	9.5
Metrologist/Alignment	8.0
Precision Assembly	10.1
Cleaning/Plating Shop	17.6
Mechanical Fabrication and Welder	12.5
Plant Engineering	11.5
Labor Services	5.6
Carpenter	8.0
Electrician	9.5
Ironworker	7.8
Plumber/Pipefitter	9.6
Riggers	9.0

With the application of the above rates to the ED&I and Labor estimates, the total direct cost for SPEAR 3 (see Table 8.2) is estimated at 36.7 M$(FY99$). Incremental indirect costs for in-house labor and M&S are 5.0 M$, bringing the total costs to 41.8 M$.

Contingency, as applied to this total, was determined by an analysis of each system or subsystem. The contingency will vary depending on the complexity of a particular system and the details of understanding or experience. A risk analysis was made for each of the categories of ED&I, M&S, and Labor. For a particular component, the ED&I was assigned a low risk (10% contingency) if the component design was based on an existing design with recent cost experience. A 25% contingency was assigned to a new design with mini-

mal complexity utilizing straight forward engineering techniques. For a new state-of -the art design, a 50% contingency was applied. A similar analysis was undertaken for M&S and Labor to reflect their uncertainties. As a result, the overall average contingency for the project was estimated at 8.9M$ or 21.3% of the total direct plus indirect costs.

For increases due to escalation, a four year program beginning in FY99 with completion in FY02 was assumed. DoE-projected escalation factors for these years were utilized. This resulted in 2.4 M$ for escalation bringing the total estimated cost to 53.1 M$, as summarized in Table 8.2. Table 8.3 provides the direct costs at WBS Level 3.

Table 8.2 SPEAR 3 Project cost estimate.

WBS	M$
1.1 Magnets and Supports	7.7
1.2 Vacuum System	9.3
1.3 Power Supply System	2.9
1.4 RF System	3.3
1.5 Instrumentation, Control & Protection Systems	2.8
1.6 Cable Plant	1.1
1.7 Beamline Front Ends	1.0
1.8 Facilities	2.0
1.9 Installation & Alignment	3.7
1.A Physics, Management, & Administration	2.9
Total Direct Costs (FY98$)	36.7
Indirects	5.1
Total Direct + Indirect	41.8
Contingency:	8.9
Costs + Contingency (FY98$):	50.7
Escalation	2.4
TOTAL ESTIMATED COSTS (TEC)	**53.1**

Table 8.3 SPEAR 3 cost estimate at WBS Level 3

WBS		k$
1.1	**MAGNETS & SUPPORTS**	**7685**
1.1.1	Dipoles	2093
1.1.2	Quadrupoles	1697
1.1.3	Sextupoles	1221
1.1.4	Correctors	215
1.1.5	Injection Septum	126
1.1.6	Magnetic Measurements	247
1.1.7	Girders and Supports	1161
1.1.8	Girder Preassembly	925
1.2	**VACUUM SYSTEM**	**9276**
1.2.1	Standard Girder Chambers	3483
1.2.2	Matching Girder Chambers	983
1.2.3	Straight Sections & Transitions	1520
1.2.4	Diagnostics & PPS	563
1.2.5	Injection	470
1.2.6	Bellows Modules	681
1.2.7	Girder Chamber Supports	347
1.2.8	Straight Section Supports	357
1.2.9	Pumping & Monitoring	872
1.3	**POWER SUPPLY SYSTEMS**	**2920**
1.3.1	Unipolar DC Supplies	995
1.3.2	Bipolar DC Supplies	350
1.3.3	Pulsed Supplies	221
1.3.4	Controllers	577
1.3.5	Racks & Accessories	127
1.3.6	N/A	-
1.3.7	AC Distribution	594
1.3.8	Facility Refurbishment	56
1.4	**RF SYSTEM**	**3300**
1.4.1	Klystrons	510
1.4.2	Cavities	1801
1.4.3	Waveguides, Circulators & Water Loads	460
1.4.4	Low Level RF & Controls	465
1.4.5	N/A	-

Table 8.3 SPEAR 3 cost estimate at WBS Level 3

WBS		k$
1.4.6	Cooling System	31
1.4.7	Cable & Trays	33
1.5	**I &C, PROTECTION SYSTEMS**	**2790**
1.5.1	Computer Control	816
1.5.2	Beam Monitoring	1018
1.5.3	Lattice Diagnostics	40
1.5.4	Timing System	132
1.5.5	Protection Systems	784
1.6	**CABLE PLANT**	**1140**
1.6.1	Trays & Wireways	386
1.6.2	Cable Removal	49
1.6.3	New Cables	705
1.7	**BEAM LINE FRONT-ENDS**	**967**
1.7.1	Insertion Devices	408
1.7.2	Bend Magnets	559
1.8	**FACILITIES**	**1945**
1.8.1	Shielding	901
1.8.2	LCW Systems	695
1.8.3	N/A	-
1.8.4	Utilities	349
1.9	**INSTALLATION & ALIGNMENT**	**3719**
1.9.1	Magnets & Supports	1553
1.9.2	Vacuum System	328
1.9.3	Power Supplies	346
1.9.4	N/A	-
1.9.5	Instrumentation & Controls	181
1.9.6	Cable Plant	1024
1.9.7	Beam Line Front Ends	234
1.9.8	Facilities	53
1.A	**PHYSICS, MANAGEMENT, & ADMIN.**	**2908**
1.A.1	Accelerator Physics	822
1.A.2	Radiation Physics & ES&H	151
1.A.3	Management & Administration	1935
Total Direct Costs (FY99 k$)		**36650**

8.3 Project Schedule

Funding for the start of SPEAR 3 design efforts (ED&I) was approved June 1, 1999, with authority to proceed with procurements and fabrication granted July 17, 1999.

Major procurements for magnets, vacuum chambers and RF system components will be underway in early FY2000 in order to assure that all technical components and systems are ready for installation prior to the 6-month shutdown scheduled to begin in April 2002. The budget authority required to achieve this schedule is provided in Table 8.4.

The four-year plan for SPEAR 3 component design, fabrication and procurement, assembly and installation is shown in Figure 8.1 for WBS Level 2 systems. The schedule assumes that major procurements, in particular for magnet and vacuum chamber components, can be initiated in early FY2000. This will help to assure that all technical components are available and ready for installation prior to the April 2002 shutdown. The obligational funding profile for this plan is provided below in Table 8.4.

Table 8.4 SPEAR 3 funding profile.

FY	Obligations (M$)
1999	14.0
2000	15.0
2001	14.8
2002	9.3

A summary plan for design, fabrication and installation is provided in Figure 8.1. The installation activities in the fourth quarters of FY2000 and FY2001 include tunnel shielding modifications and electrical system improvements so that the installation efforts in FY2002 will be focused on technical systems. Note that critical decisions CD1, CD2 and CD3 in Figure 8.1 have already been accomplished.

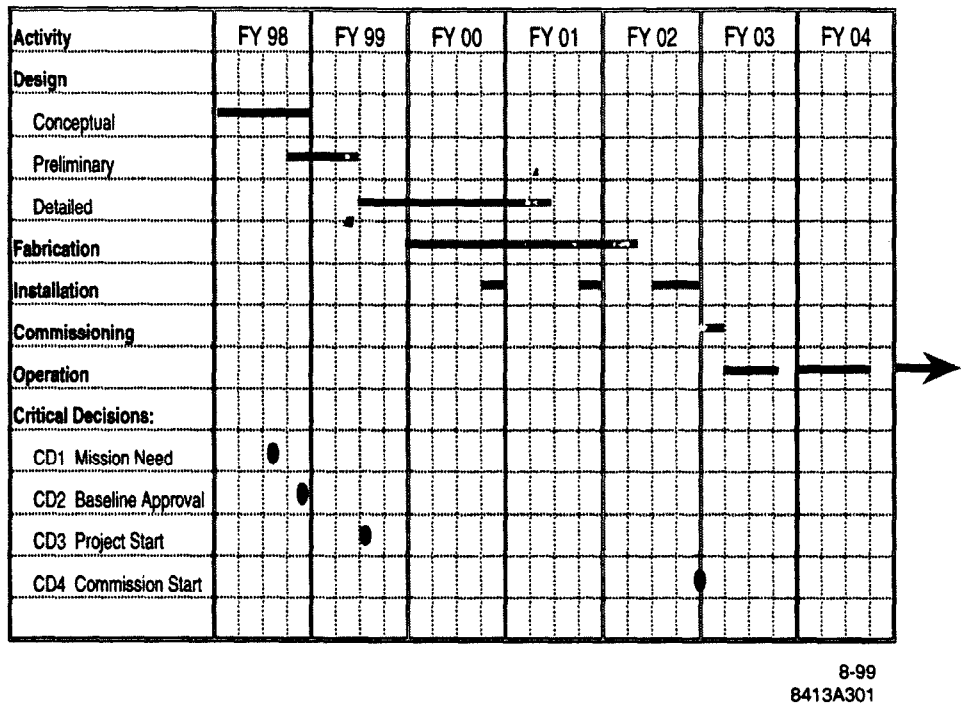

Figure 8.1 SPEAR 3 project summary schedule.

Detailed schedules have been analyzed for each major technical system. The results lead to the overall project obligation and cost profiles shown in Figure 8.2. Although the project start is late in FY99, this plan indicates that 27.4 M$ will be obligated by the end of FY2000, which is close to the budget plan of 29 M$ for FY99 and FY2000 (Table 8.4).

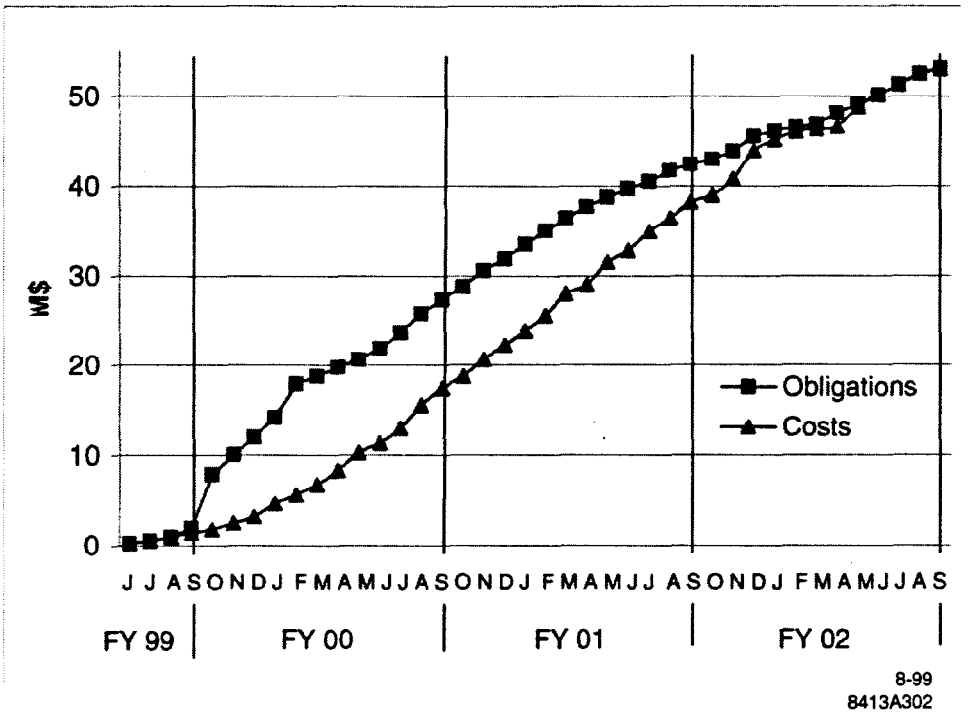

Figure 8.2 SPEAR 3 project obligation and cost profiles.

Details of the 6-month shutdown period for major installation are provided in Figure 8.3. An ambitious but necessary goal is to complete the removal of SPEAR 2 components within the first two months and complete the installation of SPEAR 3 within the next four-month period. The startup period begins in mid-September 2002 and follows the plan used for previous shutdowns. First stored beam in SPEAR 3 is projected for late November 2002, with beam available for users by January 2003.

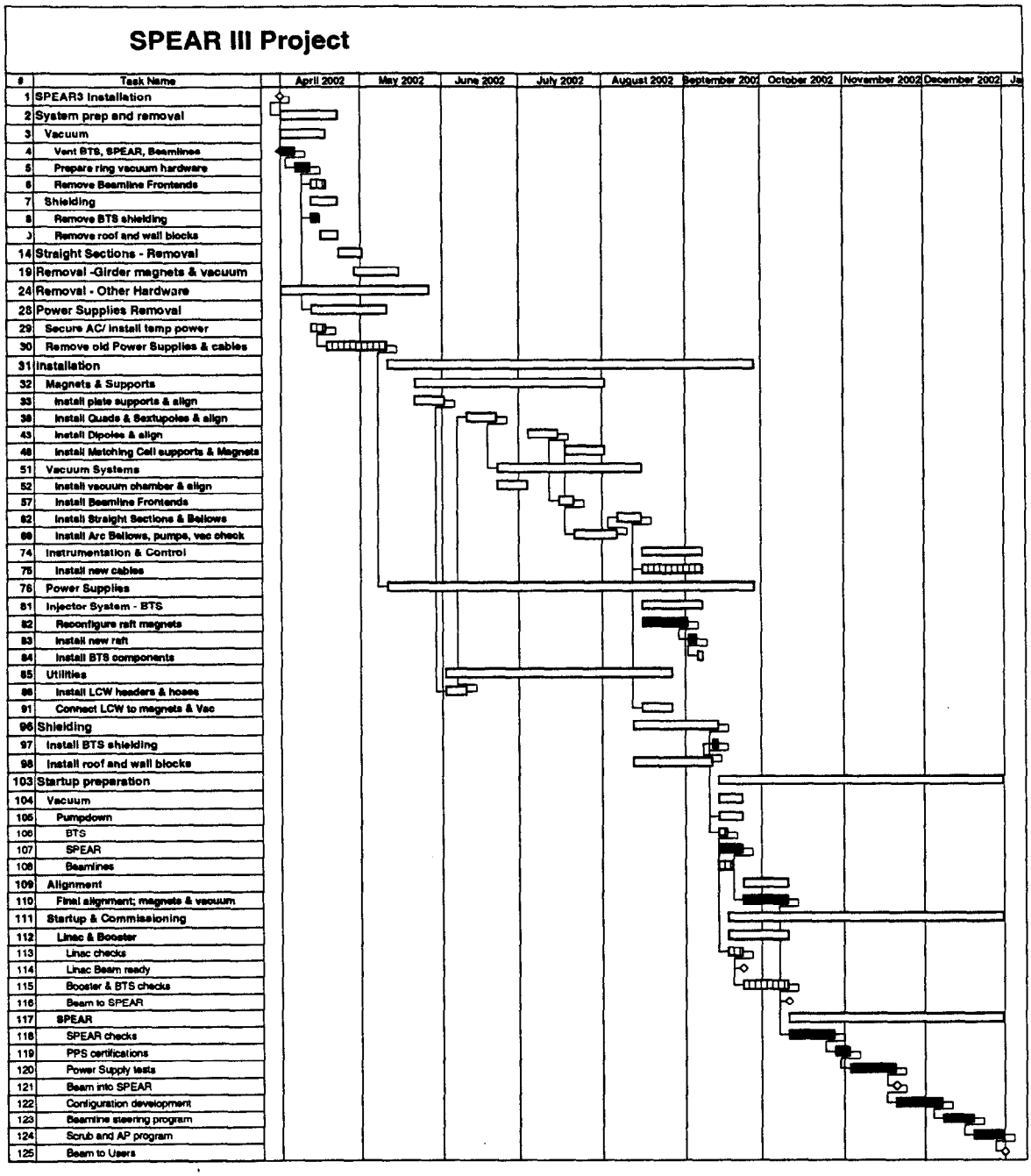

7-98
8413A94

Figure 8.2 6-month SPEAR 3 installation schedule.

SPEAR 3 Design Energy: 3 vs. 3.5 GeV A1

Summary Report from 12/9/97 Meeting

Contents

Attendees: J. Arthur, S. Barrett, R. Boyce, S. Brennan, J. Corbett, M. Cornacchia, M. Dormiani, B. Hedman, R. Hettel, K. Hodgson, P. Kuhn, G. Leblanc, C. Limborg, P. Phizackerley, P. Pianetta, T. Rabedeau, M. Rowen, B. Scott, J. Sebek, D. Shuh, M. Soltis, A. Trauwtwein, H. Winick

1.1 EXECUTIVE SUMMARY

A meeting was held 12/9/97, to review the choice of SPEAR 3 design energy, in the 3 to 3.5 GeV range, in light of recent analyses of storage ring and beam line performance and mechanical design issues that indicate that the original choice of 3.5 GeV might not be optimal. Attendee's included several SSRL staff members and a representative from the SSRL User's Organization.

The design energy defines the lengths of lattice magnets (~ energy E) required to keep peak fields in the yokes safely below saturation levels that introduce excessive high order magnet field components that degrade the dynamic aperture of the lattice. Longer magnets reduce the amount of intervening space available for photon absorbers, correctors, and other vacuum chamber

components. It has been shown elsewhere that storage rings can actually operate acceptably at higher than the design energy (perhaps 10-20% higher), meaning that the 3.5 GeV "safe" lattice presented at the SPEAR 3 Director's Review in November, 1997, might cost more in available space and budget than is warranted unless 3.5 GeV operation is deemed to be a high priority goal for SSRL.

To address this question, the meeting included presentations that introduced the 3 vs. 3.5 GeV design and performance issues (R. Hettel), compared 3 and 3.5 GeV lattice parameters (J. Corbett) and beam dynamics (C. Limborg), showed differences in vacuum and mechanical designs for the two energies (R. Boyce), and compared performances of wiggler and bending magnet beam lines (T. Rabedeau) as well as future undulator beam sources (S. Brennan). **The primary assumption for comparing performance was that the maximum operating current at 3.5 GeV must be reduced by a factor of ~2 from the 3 GeV case so as not to exceed the power density ratings of photon absorbers.** Summaries of these presentations are included in the following report.

Given that storage ring design concepts for either 3 and 3.5 GeV are plausible (although design challenges and associated component costs are less for the 3 GeV-optimized lattice) and that ring performance in both cases is acceptable, the most persuasive arguments for reducing the maximum safe operating level of the magnets from 3.5 GeV to 3 GeV were made in the presentations comparing beam line performance for various source magnets at the two energies. It was shown that the hardening of photon spectrum at 3.5 GeV (critical energy scales as E^2, assuming the same magnet field strength for the two lattices) does not outweigh the assumed reduction of maximum operating current at that energy due to power density limitations (~ $1/E^4$), even for future undulators, until photon energies reach the 11-30 keV range (depending on source magnet and beam line station). Flux, focused flux density, and brightness at 3.5 GeV for photon energies lower than these crossover values, where SSRL occupies a niche in the synchrotron radiation community, would all be reduced due to the lower operating current (by a factor of ~2 for energies below 5 keV). While the natural beam lifetime at 3 GeV is significantly less than at 3.5 GeV due to the Touschek effect, the total top-of-the-fill lifetime at 3 GeV is greater than an acceptable 30 h for currents exceeding ~300 mA; lifetime for high current operation can be increased by using a bunch lengthening cavity and/or by increasing the vertical emittance coupling. It was also shown that the emittance increases as dipole length is reduced (due to the higher magnet field strength and critical photon energy) but that it will remain below 20 nm-rad as long as the dipoles are not shortened by more than ~10-12% of their 3.5 GeV length.

The group consensus at the end of the meeting was that the lattice should be optimized for 3.0 GeV operation while maintaining an emittance at or below 20 nm-rad. Subject to mechanical space and lattice optics constraints, magnet design safety margins will be maximized to provide the possibility of operating above the 3 GeV design energy (on the order of 10% higher), but without a guarantee of reaching 3.5 GeV.

1.2 SUMMARY OF PRESENTATIONS

1.2.1 Introduction

The ring lattice presented at the November '97 SPEAR 3 Director's Review has magnets that operate safely below saturation at 3.5 GeV and is probably capable of operating close to 4 GeV (~10-20% higher energy, based on experiences at the ALS and SRRC where 1.5 GeV lattices have been pushed to ~1.9 GeV operation). Space between magnets is cramped, making it difficult to place photon stops, correctors, BPMs and other vacuum chamber components. The situation would

be relieved if a design energy closer to 3 GeV were chosen, relying on the magnet design safety margin for reaching a higher operating energy if desired.

Other considerations for selecting design energy include differences in beam properties (emittance, dimensions, photon spectrum, stability and lifetime), beam line performance, and lattice geometry for different operational energies.

An additional issue is that the booster synchrotron may not operate reliably at higher than 3 GeV without major upgrades to White Circuit chokes and capacitors. Operating SPEAR at higher than 3 GeV will most likely require energy ramping, precluding the possibility for top-off mode injection without a large investment in upgrading the booster.

The purpose of this meeting was to compare ring and beam line performances and future scientific opportunities at 3 and 3.5 GeV to see if the SPEAR 3 design energy should be lowered towards 3 GeV.

Current scaling assumption for comparing 3 and 3.5 GeV: The principal assumption made for comparing 3 and 3.5 GeV performance is that the operational current at either energy will be limited by the capacities for photon power absorption and power density of some component(s) in the ring. It is assumed that the most likely component(s) to be power-limited will be on a high power insertion device beam lines, rather than on bending magnet lines. The photon power density from an insertion device at a fixed field scales as E^4 (E = beam energy), implying that components rated for I mA at 3 GeV will only be rated for $0.54 \times$ I mA at 3.5 GeV. If in fact the power-limited component were on a bending magnet beam line, the reduction in current at 3.5 GeV would scale as $B(E) \times E^4 = E^5$, where B(E) is the dipole field strength at energy E ($B(E) \sim E$), implying a reduction by a factor of 0.46 times the 3 GeV current. In this report the 0.54 current scaling factor is used for comparing 3 and 3.5 GeV performance.

1.2.2 Accelerator Lattice

The lattice functions for the 3.5 GeV-optimized storage ring Double Bend Achromat (DBA) cell are shown in Figure 1.1. The nominal lattice functions differ slightly for a cell optimized for 3 GeV (Table 1.1). We have determined that the on- and off-momentum dynamic apertures for the 3 and 3.5 GeV lattices do not differ significantly, and that the emittance is raised from 17 nm-rad at 3 GeV to ~20 nm-rad at 3.5 GeV due to an increase in dipole magnet field.

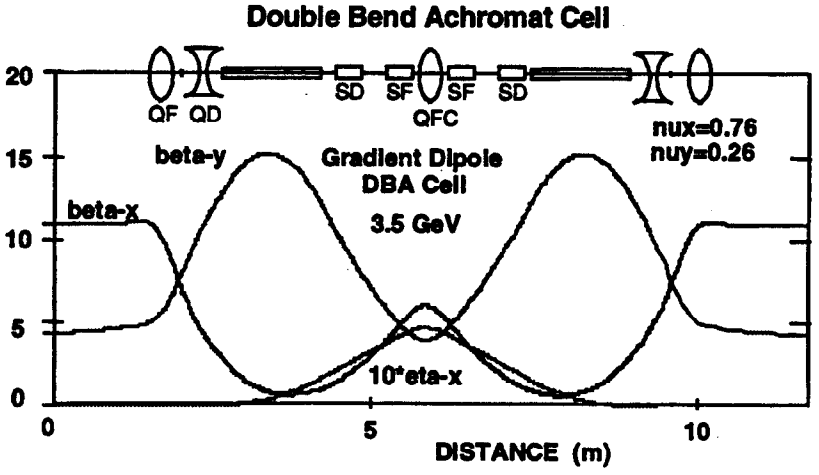

Figure 1.1 DBA cell lattice functions for 3.5 GeV

Integrated magnet field strengths are less for the 3 GeV lattice, meaning that shorter magnets can be used. Dipole lengths have been reduced by 10% from their 1.55 m, 3.5 GeV length, and other magnets have been shortened as well, creating space between magnets for vacuum chamber components and correctors. It is desirable to keep the dipoles as long as reasonably possible to minimize the increase in emittance. Table 1.2 summarizes the resulting beam, lattice and magnet parameters for different dipole magnet configurations at 3 and 3.5 GeV (dipole centers moved closer together, remaining fixed, and moved farther apart than their 3.5 GeV placement on the arc cell girder) and the respective changes in inter-magnet spacing. The effects of changing dipole separation are qualitatively summarized in Table 1.3. Keeping the dipole centers close to their 3.5 GeV locations is likely to yield an optimum for reducing magnet strengths and providing room where needed between magnets. Having shorter dipole magnets reduces the ring path length, which must be compensated by moving the lattice outward in the East and West interaction regions.

Table 1.2 Parameters for 3.5 GeV lattice and 3.0 GeV lattices having different dipole locations (Figure 1.2). Quadrupole and sextupole values are normalized strength/effective length (m).

	Review Lattice	Bends Out	Bends Out	Bends In	Bends Center
Energy (GeV)	3.5	3.5	3.0	3.0	3.0
Emittance (nm-rad)	16.6	16.6	19.3	20.0	18.9
Straight Section βx (m)	10.9	10.1	9.5	11.4	10.4
Straight Section βy (m)	4.4	4.35	4.6	4.3	4.5
Straight Section σx (μm)	425	410	430	477	443
Magnet Strength/Length:					
Dipole (T, m)	1.39/1.55	1.39/1.55	1.34/1.28	1.34/1.28	1.34/1.28
Dipole grad (m^{-2})	-.34	-.34	-.34	-.34	-.34
QF (m^{-2}, m)	1.6/.35	1.7/.35	1.9/.32	2.0/.27	2.0/.29
QD (m^{-2}, m)	-0.9/.20	-1.2/.15	-1.6/.15	-1.2/.15	-1.2/.15
QFC (m^{-2}, m)	1.6/.6	1.6/.55	1.9/.44	2.0/.46	2.0/.44
SF (m^{-3}, m)	43/.3	43/.3	27/.25	37/.25	33/.25
SD (m^{-3}, m)	53/.3	46/.25	40/.25	40/.25	46/.25
Interval Length:					
QF-QD (m)	.40	.38	.41	.63	.52
SF-SD (m)	.35	.57	.80	.62	.71
Matching Straight (m)	4.5	4.5	4.5	4.5	4.5
Interaction Straight (m)	8.5	6.7	5.3	9.5	7.4

Table 1.3 Effect of moving dipole center point location on arc girder.

Dipoles IN	Dipoles OUT
higher βx	lower βx
lower βy	higher βy
higher QFC	lower QFC
higher SF/SD	lower SF/SD
shorter SF/SD gap	longer SF/SD gap
lower QF/QD	higher QF/QD

Table 1.3 Effect of moving dipole center point location on arc girder.

Dipoles IN	Dipoles OUT
longer QF/QD gap	shorter QF/QD gap
IR away from wall	IR toward wall
longer IR straight	shorter IR straight
higher peak βx	lower peak βx
beam line alignment in	beam line alignment out

1.2.3 Collective Effects and Lifetime

Longitudinal and transverse multibunch instability damping times, growth times and threshold currents are not significantly different for lattices optimized for 3 and 3.5 GeV operating at 3 GeV (Table 1.4 to Table 1.6). The longitudinal instability current threshold is 2.4 times higher at 3.5 GeV than at 3 GeV for the same rf cavity higher order mode characteristics. However recent calculations show that the beam will be longitudinally stable at 3 GeV up to ~350 mA. The transverse instability thresholds are not much different for the two energies and transverse feedback systems will be needed for both cases.

Table 1.4 Damping times for SPEAR 3 at 3 and 3.5 GeV (~ E^3/ρ, ρ = bend radius). "Long bends" are rated for 3.5 GeV, "short bends" are rated for 3 GeV.

Damping	3 GeV, short bends (absolute/relative)	3 GeV, long bends (absolute/relative)	3.5 GeV, long bends (absolute/relative)
Longitudinal	2.76 ms/0.87	3.15 ms/1.0	1.98 ms/0.63
Horizontal	4.14 ms/0.96	4.33 ms/1.0	2.73 ms/0.63
Vertical	4.96 ms/0.91	5.47 ms/1.0	3.45 ms/0.63

Table 1.5 Relative multibunch instability growth times at 3 and 3.5 GeV "Long bends" are rated for 3.5 GeV, "short bends" are rated for 3 GeV. (Vrf = 3.2 MV/3.7 MV for 3/3.5 GeV)

	3 GeV, short bends	3 GeV, long bends	3.5 GeV, long bends
Longitudinal	0.95	1.0	0.7
Transverse	1.2	1.0	1.3

Table 1.6 Relative multibunch instability threshold currents at 3 and 3.5 GeV. "Long bends" rated for 3.5 GeV, "short bends" for 3 GeV. (Vrf = 3.2 MV/3.7 MV for 3/3.5 GeV)

	3 GeV, short bends	3 GeV, long bends	3.5 GeV, long bends
Longitudinal	1.2	1.0	2.4
Transverse	0.9	1.0	1.2

Table 1.7 compares the lifetime at 3 GeV for a current I with that at 3.5 GeV and 0.54 x I so as to maintain a constant photon power density. The rf gap voltage is set to provide a 3% rf bucket size (3.2 MV at 3 GeV, 3.7 MV at 3.5 GeV). The present rf system will only support up to ~300 mA at 3 GeV and 60 mA at 3.5 GeV; the higher current cases in Table 1.7 will require an rf system upgrade.

The natural lifetime at 3 GeV, with 200 mA filled in 140 out of a possible 280 rf buckets, is ~49 h, resulting from a 75 h gas scattering lifetime and a 145 h Touschek lifetime. The gas scattering lifetimes in Table 1.7 are computed from very conservative values of CO-equivalent pressure, and are dominated bremsstahlung gas scattering effect (Figure 1.2). The gas scattering lifetime has a weak dependency on energy. Gas pressures in Table 1.7 have been scaled for different currents.

Table 1.7 Beam lifetimes at 3 and 3.5 GeV for currents yielding equal power densities. All cases assume 140 bunches filled. Horizontal-vertical coupling is 1%.

3 GeV current (mA)	Pressure CO-eq (nTorr)	Touschek life(h)	Gasscat life(h)	Tot life (h)	Curr at 24h (mA)	3.5 GeV current (mA)	Pressure CO-eq (nTorr)	Tous-chek life(h)	Gas scat life(h)	Tot life (h)	Curr at 24h (mA)
200	0.6	145	75	49	150	108	0.32	318	141	97	88
370	1.1	83	41	27	220	200	0.6	172	76	52	130
500	1.5	58	30	20	240	270	0.81	127	56	39	175

Touschek lifetime scales like E^4 when assuming constant momentum acceptance, and is clearly better at 3.5 GeV. The 3 GeV Touschek lifetime is acceptable at 200 mA, but clearly deteriorates as beam current is increased. To first order, the Touschek lifetime is inversely proportional to electron bunch density and can be improved by reducing that density by increasing the number of bunches for a given current, increasing the horizontal-vertical emittance coupling, and increasing the bunch length with a harmonic rf cavity. For example a factor of 2 increase in Touschek lifetime can be gained either by doubling the bunch length or by increasing the coupling to 4% (which increases vertical beam size by a factor of 2). Increasing the number of bunches for a given current has the added benefit of reducing higher order mode heating in the vacuum chamber ($\sim I_{bunch}^2$), but the gain in lifetime is partially counteracted by a reduction in wakefield-induced bunch lengthening for the lower bunch current. A lower bunch current also reduces the head-tail damping of transverse multibunch instabilities, an effect that is greater for a higher bunch current. It is therefore likely that a bunch lengthening cavity is the best way to gain a Touschek lifetime for high current operation at 3 GeV that is comparable to 3.5 GeV operation.

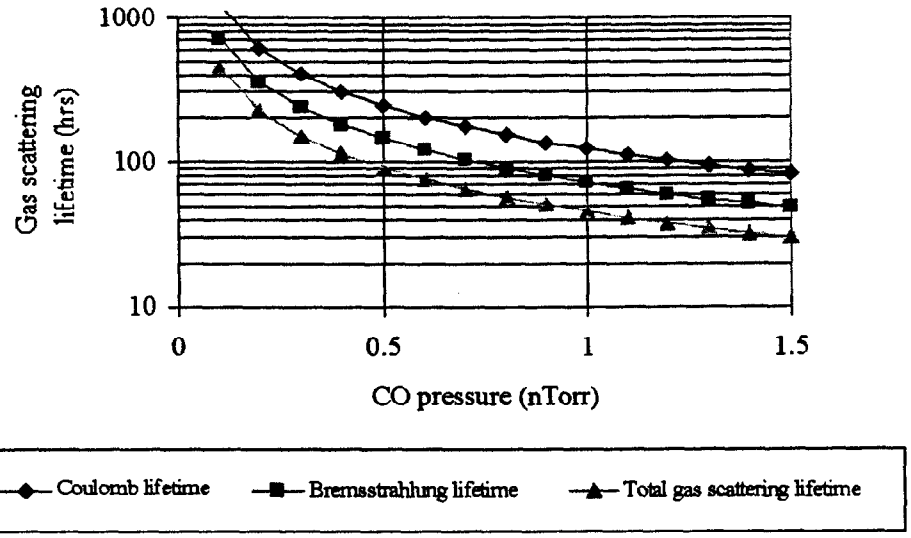

Figure 1.2 Gas scattering lifetime as function of ring pressure.

1.2.4 Accelerator Mechanical Design Issues

Space is more limited in the 3.5 GeV lattice for the placement of photon stops, ion pumps, BPMs and correctors, and other girder vacuum chamber components (Table 1.8), especially between and after the downstream QF-QD quadrupole doublet and the upstream SF-SD sextupole pair. The mechanical design task is easier for the 3 GeV lattice because magnets can be made shorter to

provide more space. The minimum separation of the QF-QD doublet magnets will be determined by the design of the discrete horizontal/vertical corrector magnet that will be located in the intervening space.

In the 3.5 GeV design, the photon beam strikes a cooled vacuum chamber wall in the area of the downstream QF magnet (Figure 1.3), raising ring pressure in the vicinity of the beam. A lattice with magnets shorter than the 3.5 GeV versions may provide enough space between the downstream QF and the insertion device chambers to locate a discrete photon stop further from the beam.

Repositioning the dipole magnets to optimize the 3 GeV lattice design will require a small change in the amount that dipole beam lines must be realigned compared with the.5 GeV case.

Table 1.8 Vacuum chamber components located between magnets.

Space	Components	Space	Components
ID-QF	ID, bellows, BPM, flanges, mask, supports, IP	QFC-SF	coil space
QF-QD	IP, absorber, corrector, support	SF-SD	absorber, IP, corr, bellows, flanges, support
QD-B	BPM, coil space, support	SD-B	BPM, coil space, support
B-SD	absorber, IP, support	B-QD	coil space, support
SD-SF	absorber, IP, corr, bellows, flanges, support	QD-QF	IP, absorbers, corrector, support
SF-QFC	BPM, coil space, ID exit flange	QF-ID	ID, bellows, BPM, flanges, mask, supports, IP

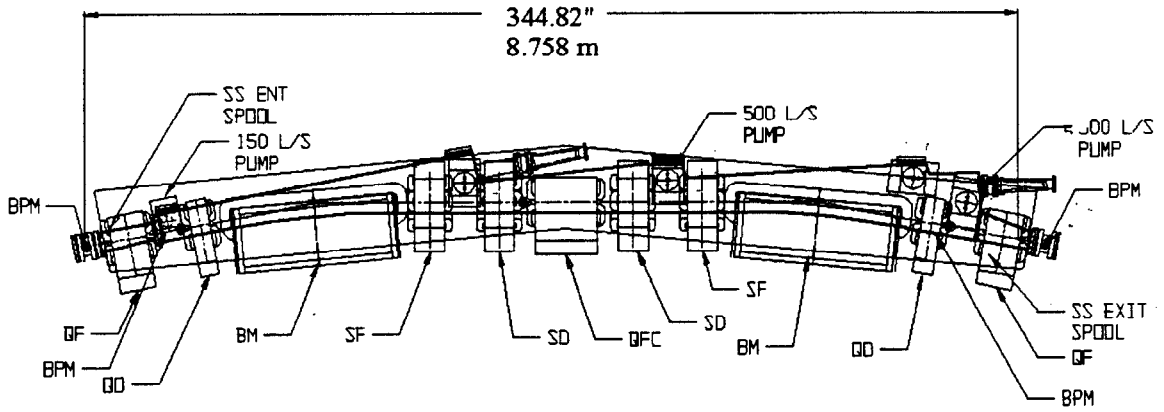

Figure 1.3 Arc girder vacuum chamber. Beam strikes cooled chamber wall in the area of the right hand QF magnet.

1.2.5 Wiggler and Bending Magnet Beam Line Performance

Principal factors governing beam line performance include:

1. Critical energy (~BE^2) at 3.5 GeV is 1.36 times higher for wigglers and 1.59 times higher for bending magnets than at 3 GeV.
2. The beam source size ($\sigma_x\sigma_y$ ~ emittance ~ E^2) at 3.5 GeV is 1.36 times higher than at 3 GeV.
3. Power density from IDs ($dP/d\Omega \sim BE^4I$), rather than from bending magnets, is assumed to be the determining parameter for photon absorber design. To maintain a constant power

density, the operating current at 3.5 GeV must be reduced to 0.54 times the current at 3 GeV as discussed in section 1; this normalization is used to compare beam line performances.

4. The horizontal fan width for wigglers is reduced at 3.5 GeV (~1/E), affecting wiggler side station beams.
5. Photon flux is relevant figure of merit for unfocused beam lines and most ID side stations; focused flux density (intensity) is figure of merit for focused beam lines.

Given the current scaling assumption discussed above, bend magnet and wiggler flux and focused flux densities at low photon energies are a factor of ~2 greater for SPEAR operating at 3.0 GeV than for 3.5 GeV operation. As the photon energy increases, the 3.0 GeV performance edge shrinks and then vanishes between ~15-30 keV depending on the beam line station. Figures 4-7 show comparative performances of representative low critical energy sources which would benefit the most from 3.5 GeV operation. The crossover point where 3.5 GeV performance exceeds that for 3 GeV moves to higher photon energy with higher critical field. (e.g. BLs 4, 7, 9, 10 and 11).

Insertion device radiation fans become more narrow as the ring operating energy increases (Figure 1.8). Consequently, wiggler side stations situated near the edge of radiation fans suffer beam loss and increased sensitivity to horizontal orbit related beam noise. On some side stations, the beam noise susceptibility can be reduced by reducing the fan acceptance; however, this solution is less effective on stations employing toroidal optics (e.g., beam line 9-3).

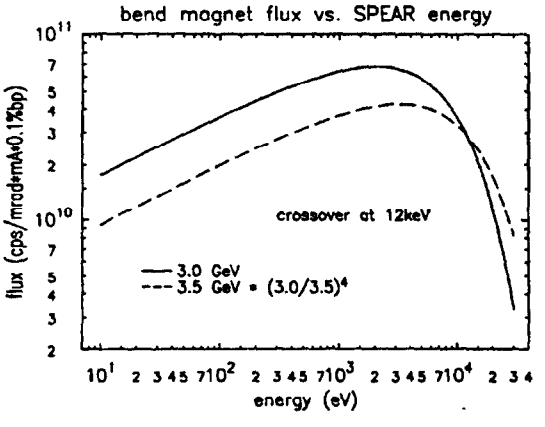

Figure 1.4 Bend magnet flux for SPEAR 3 and 3.5 GeV.

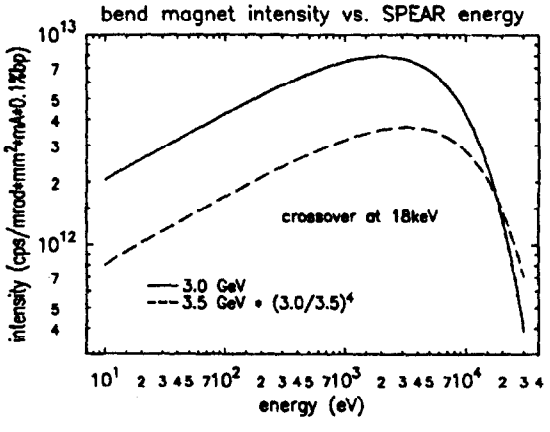

Figure 1.5 Bend magnet focused flux density for SPEAR 3 at 3 and 3.5 GeV

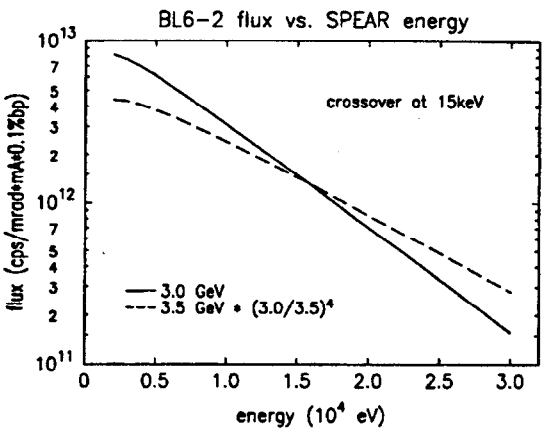

Figure 1.6 BL 6-2 wiggler flux for SPEAR 3 at 3 and 3.5 GeV.

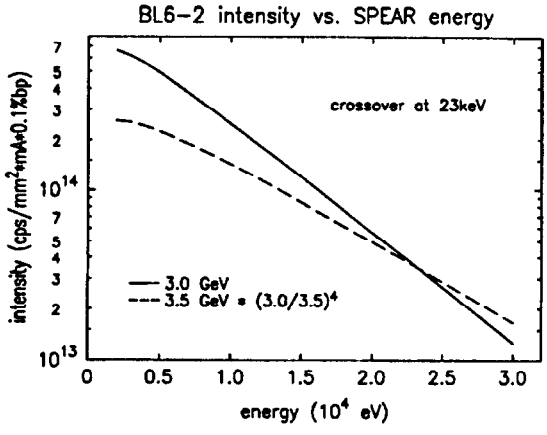

Figure 1.7 BL 6-2 wiggler focused flux density for SPEAR 3 at 3 and 3.5 GeV.

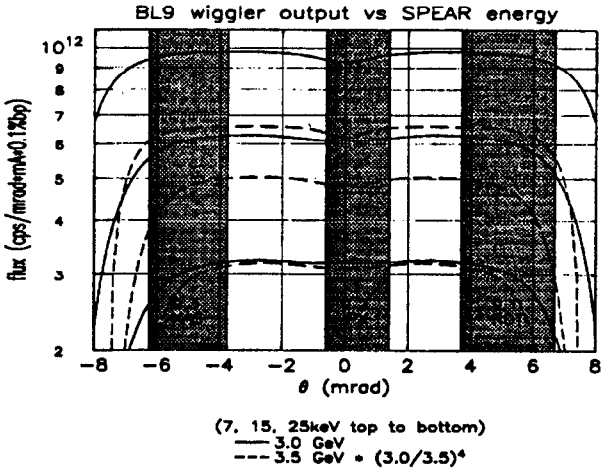

Figure 1.8 BL 6-2 wiggler flux vs. angular acceptance for SPEAR 3 at 3 and 3.5 GeV.

1.2.6 Future Undulator Performance

The brightness of the ~1.5 keV fundamental of a 2 m APS type A undulator (0.9 T, 3.3 cm period - not optimized for SPEAR 3) is 3 x 10^{18} at 3 GeV and 200 mA, a factor of ~2 greater than at 3.5 GeV with a current scaled to 110 mA (Figure 1.9). Brightness at 3 GeV exceeds that for 3.5 GeV up to ~11 keV (the 13th harmonic at 3 GeV, the 7th harmonic at 3.5 GeV). The 7th harmonic is likely to be the highest usable harmonic from a practical undulator, indicating that the actual 3/3.5 GeV crossover point in photon energy is somewhat lower than 11 keV.

Comparative performances of a 4m APS type A device at 3 and 3.5 GeV are depicted in Figure 1.10. Again 3 GeV brightness exceeds that at 3.5 GeV and reduced current out to ~11 keV. The brightness of the ~1.5 keV fundamental is >7 x 10^{18} at 3 GeV, 200 mA. This general trend of improved performance in the fundamental and first several harmonics also describes the comparative brightness at 3 GeV and 3.5 GeV, with reduced current, of a future small gap, in-vacuum, short period undulator.

For comparison, the published curves for APS undulators show a brightness in the mid-10^{18} down to ~ 2 keV. The ALS has several undulators for the energy region below 1 keV that have brightness close to the 10^{18} range. However, there is a gap in the 1-2 keV energy range which is not effectively covered by either source at present.

It is clear from these comparisons that undulators on SPEAR 3 provide world class brightness in the 1-4 keV range and significantly less than world class performance in the hard x-ray regime. This suggests that the marginal improvements in hard x-ray brightness associated with raising the SPEAR operating energy to 3.5 GeV but running at reduced current are not warranted in light of the reduced performance of the existing bend magnet, insertion device, and potential 1-4 keV undulator beam lines in comparison to their 3.0 GeV performance. However, it is also recognized that a user of high energy photons (of order 20-30 keV depending on beam line) would benefit from 3.5 GeV SPEAR operation. mai

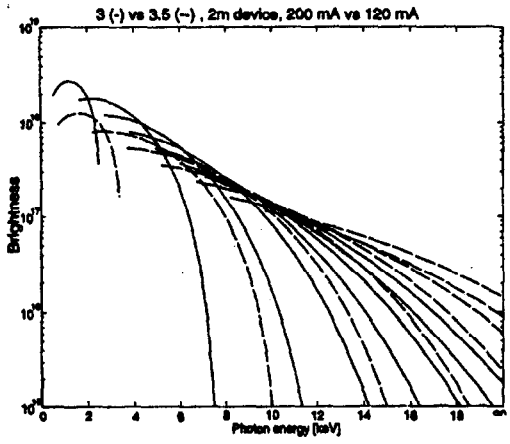

Figure 1.9 Brightness of 2 m Undulator A (from APS) on SPEAR 3 at 3 (—) and 3.5 (---) GeV.

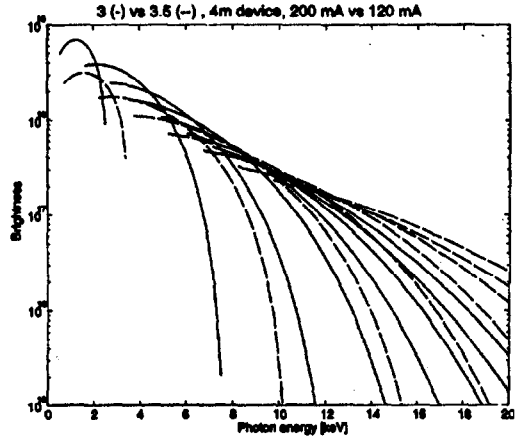

Figure 1.10 Brightness of 2 m Undulator A (from APS) on SPEAR 3 at 3 (*f*) and 3.5 (---) GeV.

1.2.7 Conclusions

Assuming that the SPEAR 3 current is limited by insertion device or bend magnet radiated power density, the performance of existing beam lines of this type, together with that of future undulators, is better at 3 GeV than at 3.5 GeV for photon energies up to the 11-30 keV range, depending on source magnet and experimental station.

The performance of storage ring lattices optimized for 3 and 3.5 GeV appear to be almost identical except that the emittance will increase if dipole magnets are shortened from their 3.5 GeV lengths to take advantage of a lower design energy. The emittance may exceed 20 nm-rad if the dipoles are shortened by much more than ~10% of their 1.55 m, 3.5 GeV length.

While beam lifetime and stability is intrinsically better at 3.5 GeV, they are adequate at 3 GeV if proper measures are taken. In particular, the Touschek lifetime at 3 GeV can be raised by increasing the horizontal-vertical emittance coupling and/or the electron bunch length using an active rf cavity. The increase in Touschek lifetime gained by filling more beam buckets for a given total current is uncertain because bunch length decreases with lower bunch current, offsetting the intended reduction in bunch electron density.

The mechanical design of vacuum chamber components, corrector magnets, and radiation masks is simplified, and related costs reduced accordingly, by having shorter magnets, optimized for 3 GeV, and more space between magnets. Higher energy operation (of order 10% higher) will be possible with magnets designed to operate safely at 3 GeV.

In conclusion, the group consensus is that the SSRL scientific niche of flux-limited experiments at energies below approximately 20 keV and brightness limited experiments in the 1-4 keV energy range is best served by optimizing the SPEAR 3 lattice for 3.0 GeV operation while maintaining an emittance at or below 20 nm-rad. In interest of the possible benefit to users of high energy photons (above 20 or 30 keV), magnet design safety margins will be maximized, subject to mechanical space and lattice optics constraints, to provide the possibility of operating above the 3 GeV design energy (of order 10% higher).

Alignment A2

1.1 SPEAR3 Alignment Proposal

This chapter will describe procedures and methods which, carried out in a professional manor, will yield the aligned position of all Spear III components within their position tolerances. Major geodetic principles governing the survey and alignment measurement space are briefly revisited and their relationship to a lattice coordinate system shown. The chapter then continues with a discussion of the activities involved in the step by step sequence from initial lay-out to final alignment

1.1 SPEAR3 Surveying Reference Frame

Horizontal position differences between the projection of points on the geoid or a best fitting local ellipsoid and those on a local tangential plane are not significant for a network the size of Spear III. Hence, it is not necessary to project original observations like angles and distances into the local planar system to arrive at planar rectangular coordinates.

However, in the vertical plane, the curvature of the earth needs to be considered (figure f11_a). Since leveling is done with respect to gravity, the reference surface is the geoid. Table 1 shows the projection errors as a function of the distance from the coordinate system's origin. Notice that for distances as short as 20 m the deviation between plane and sphere is already 0.03 mm (table t11_a).

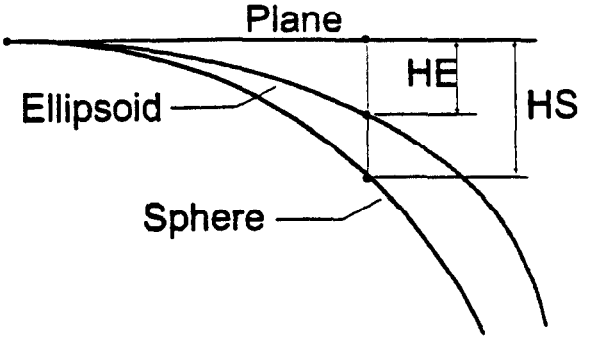

1.2 Network Design Philosophy

The global alignment tolerance and advances in surveying make it possible to consider foregoing the traditional design of a two tiered network hierarchy. Omitting a primary network not only removes many constraints for component placement since much fewer lines of sight need to be maintained, but also presents a significant reduction in alignment costs.

Omitting the global structural support of a "surface network" however increases the requirements for the tunnel network. It would be difficult to meet these requirements by traditional forced centered "2+1-D" triangulation and trilateration techniques. However, a 3-D "free stationing" approach does not require forced centered instrument set-ups, thus eliminating the need for the set-up hardware and their systematic error contribution. Removable heavy duty metal tripods, translation stages, CERN sockets and optical plummets are not needed (fig. f111_a and f111_b). The network design still must consider other systematic error effects, especially lateral refraction . Another important consideration is the target reference system. The design of such becomes much easier with free stationing since we are dealing only with targets and not with instruments. Accordingly, it

is proposed to use a design which is now widely used in high precision metrology. This approach is centered around a 1,5" sphere. Different targets can be incorporated into the sphere in such a way that the position of the target is invariant to any rotational position of the sphere. At SLAC, designs have been developed to incorporate into the sphere theodolite targets (fig. f111_c), photogrammetric reflective targets as well as glass and air corner cubes (fig. f111_d). Receptacles for the spheres, which are usually referred to as "nests" or "cups", have been designed to accommodate different functions. Designs are available at SLAC for cups tack-welded onto magnets, for mounting cups on wall brackets and for a "centered" removable mounting into tooling ball bushings (fig. f111_e).

Alignment Proposal A2

This chapter will describe procedures and methods which, carried out in a professional manor, will yield the aligned position of all Spear III components within their position tolerances. Major geodetic principles governing the survey and alignment measurement space are briefly revisited and their relationship to a lattice coordinate system shown. The chapter then continues with a discussion of the activities involved in the step by step sequence from initial lay-out to final alignment. [1]

2.1 Spear III Surveying Reference Frame

Horizontal position differences between the projection of points on the geoid [2] or a best fitting local ellipsoid and those on a local tangential plane are not significant for a network the size of Spear III. Hence, it is not necessary to project original observations like angles and distances into the local planar system to arrive at planar rectangular coordinates.

However, in the vertical plane, the curvature of the earth needs to be considered (Figure 2.12). Since leveling is done with respect to gravity, the reference surface is the geoid. Table 1 shows the projection errors as a function of the distance from the coordinate system's origin. Notice that for distances as short as 20 m the deviation between plane and sphere is already 0.03 mm (Table 2.12).

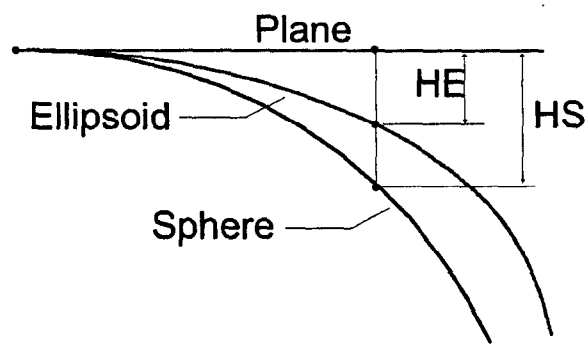

Figure 2.12 Effect of earth curvature

Table 2.12 Curvature Correction

Distance r [m]	Sphere H_S [m]	Ellipsoid H_E [m]
20	0.00003	0.00003
50	0.00020	0.00016
100	0.00078	0.00063
1000	0.07846	0.06257

2.1.1 Network Design Philosophy

The global alignment tolerance and advances in surveying make it possible to consider foregoing the traditional design of a two tiered network hierarchy. Omitting a primary network not only removes many constraints for component placement since much fewer lines of sight need to be maintained, but also presents a significant reduction in alignment costs.

Omitting the global structural support of a "surface network" however increases the requirements for the tunnel network. It would be difficult to meet these requirements by traditional forced centered [4] "2+1-D" triangulation and trilateration techniques [4]. However, a 3-D "free stationing" [5] approach does not require forced centered instrument set-ups, thus eliminating the need for the set-up hardware and their systematic error contribution. Removable heavy duty metal tripods, translation stages, CERN sockets and optical plummets are not needed ((Figure 2.12 and Figure 2.14). The network design still must consider other systematic error effects, especially lateral refraction [6]. Another important consideration is the target reference system. The design of such becomes much easier with free stationing since we are dealing only with targets and not with instruments. Accordingly, it is proposed to use a design which is now widely used in high precision metrology. This approach is centered around a 1,5" [7] sphere. Different targets can be incorporated into the sphere in such a way that the position of the target is invariant to any rotational position of the sphere. At SLAC, designs have been developed to incorporate into the sphere theodolite targets (Figure 2.15), photogrammetric reflective targets as well as glass and air corner cubes (Figure 2.16) . Receptacles for the spheres, which are usually referred to as "nests" or "cups", have been designed to accommodate different functions. Designs are available at SLAC for cups tack-welded onto magnets, for mounting cups on wall brackets and for a "centered" removable mounting into tooling ball bushings (Figure 2.16).

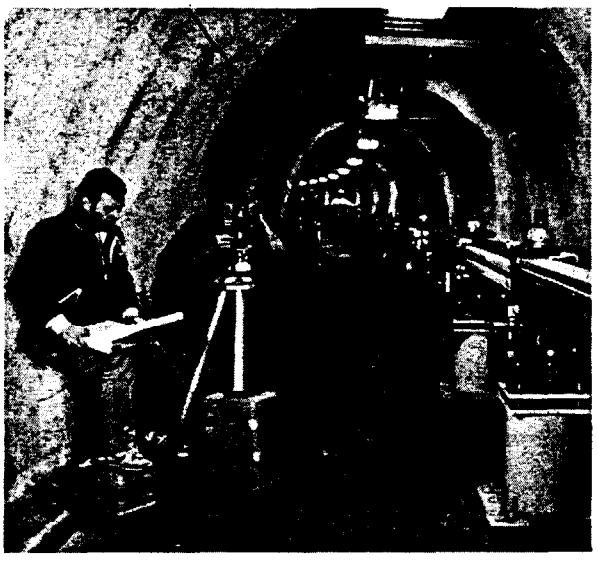

Figure 2.13 Forced Centered Set-up at SLAC

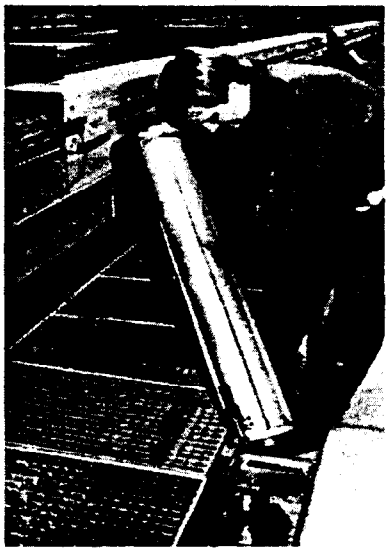

Figure 2.14 DESY HERA set-up

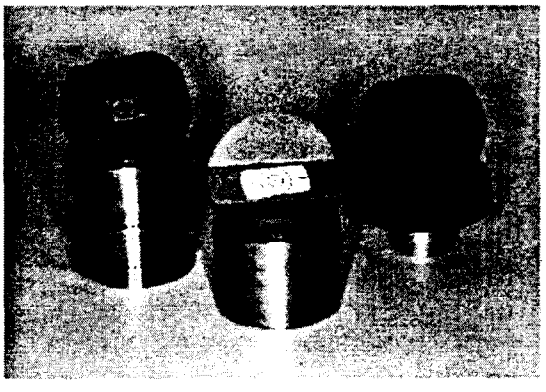

Figure 2.15 Sphere mounted theodolite target

Figure 2.16 Sphere mounted glass and air reflectors

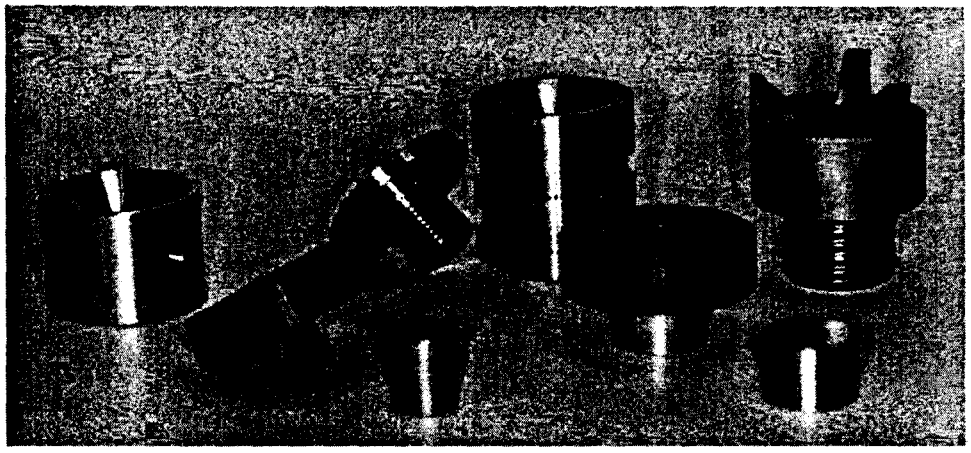

Figure 2.17 Sphere receptacles: floor, component, and wall bracket fixed mount versions, removablecentered version

2.1.2 Network Lay-Out

The SPEAR III global network consists of four part parts: the injector network, the booster network, the storage ring network and the beam line networks.

2.1.2.1 *Injector and Booster Networks*

Both the injector and booster networks already exist in the SSRL facility and are sufficient for use in SPEAR III. Additional observations and accesses will be required to tie these networks to the storage ring network.

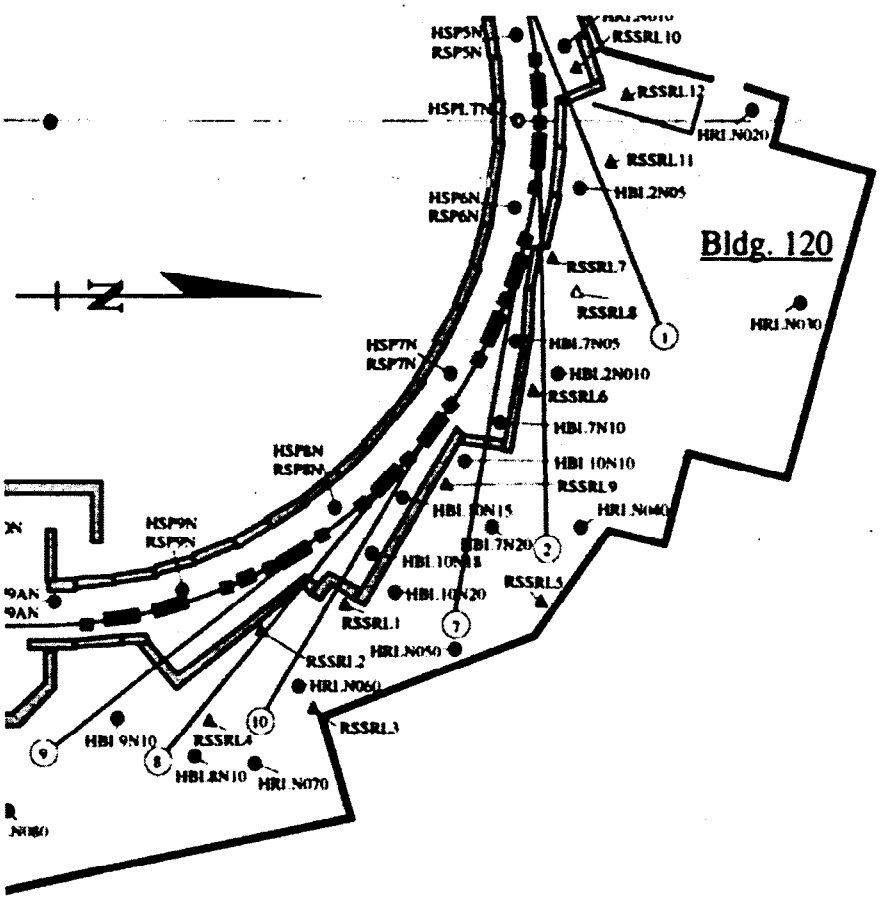

Figure 2.18 North arc of SPEAR ring.

2.1.2.2 *Storage Ring Network*

The storage ring network's overall geometry is dictated by the machine lay-out and the fact, that the free stationing method requires a greater number of reference points. The geometry should also permit observing each target point from at least three different stations. The reference points can be of two different hierarchical classes. The second order points, or tie points, mainly serve to connect the orientation of free stationed instruments, while the first order points additionally provide the long term global orientation; they are the equivalent to traditional traverse points or monuments. The tie points are not required to have long term stability, but must be stable long enough to allow the positioning of components within that region. The existing storage ring network will be utilized as the first order points and second order densification will be required between these. The stability of the current network is shown in Table 2.15 by the horizontal displacements obtained between the 95 and 97 resurveys of the primary network. Studies are ongoing as to whether the concrete shielding block walls will give the required short term stability to be used as tie points or whether additional complex floor monuments will be required. The above sketch (Figure 2.18) shows a typical section of the lay-out.

Table 2.15 Horizontal displacements in primary network between 95 and 97.

Station	Dx (mm)	Dy (mm)	Total (mm)	Semi-major (mm)	Semi-minor (mm)	Az major (gons)	To Ellipse (mm)
SP1N	-0.15	0.06	0.16*	0.41	0.3	41	0.31
SP2N	0	0.11	0.11	0.41	0.32	55	0.35
SP3N	-0.18	-0.29	0.34*	0.4	0.33	55	0.4
SP4N	-0.23	0.12	0.26*	0.38	0.34	49	0.34
SP5N	-0.09	0.08	0.12	0.35	0.34	32	0.34
SP6N	0.35	-0.34	0.49**	0.37	0.33	374	0.36
SP7N	0.13	-0.24	0.28*	0.39	0.3	362	0.39
SP8N	-0.06	-0.11	0.12*	0.37	0.28	357	0.29
SP9N	-0.06	0.02	0.06	0.35	0.28	362	0.32
SP9AN	-0.03	0.02	0.04	0.36	0.27	354	0.35
HSP1N	-0.5	0.05	0.5**	0.35	0.3	308	0.35
SP1S	0.01	-0.06	0.06	0.46	0.32	375	0.44
SP2S	-0.31	-0.04	0.31*	0.45	0.36	361	0.37
SP3S	0.06	0.08	0.1	0.46	0.4	386	0.42
SP5S	0.35	-0.51	0.61**	0.46	0.39	2	0.43
SP6S	0.35	-0.22	0.41**	0.45	0.38	3	0.4
SP8S	-0.18	-0.06	0.2*	0.43	0.36	25	0.39
SP9S	-0.18	-0.44	0.48**	0.43	0.33	33	0.43
SP9AS	-0.17	-0.33	0.37*	0.47	0.3	16	0.46
SP10S	0.57	1.68	1.78**	0.45	0.32	18	0.45
HSPSE	2.23	1.85	2.89**	0.44	0.35	359	0.35
HSP0N	-0.39	0.25	0.47**	0.37	0.32	85	0.34

* Disp beyond the standard error ellipse
** Disp beyond the 95% error ellipse

2.1.2.3 Beam Line Network

The beam line network serves as a reference for the installation of photon chambers and experiments. The initial integration into the storage ring network has been accomplished by measurements using lines of sight through the openings in the shielding wall sections around the beam lines. Re-surveys will require opening some of these windows. Along a beam line, floor-marks and 3D monuments make up the principle structure of the network. Narrowly spaced beam lines will be treated as one single beam line as far as the control network is concerned. Where the separation between beam lines becomes wider, tie points will be added. Figure 2.18 displays a section of the current northeast arc beamline networks with respect to the storage ring network. If deemed necessary, additional measurements of absolute horizontal orientation (azimuths) between the storage ring and the experiment beamlines can be performed using a gyrotheodolite (Figure 2.20). The gyrotheodolite is capable of measuring absolute azimuths to an accuracy of 2-3 seconds of arc.

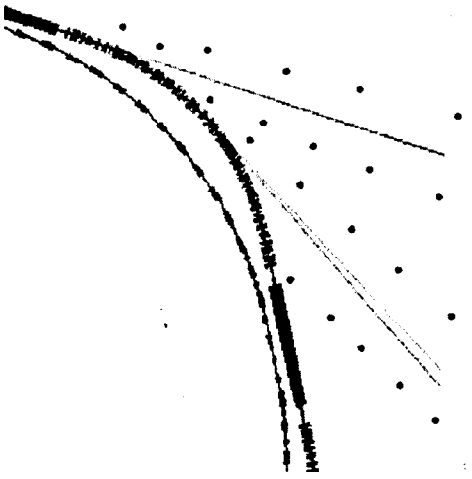

Figure 2.19 Beam line network incl. synchrotron, injector network

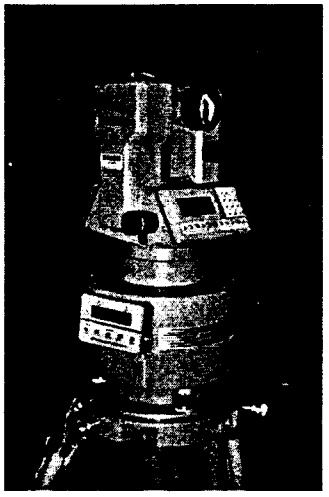

Figure 2.20 DMT Gyrotheodolite

2.1.3 Alignment Coordinate System

The alignment coordinate system currently used for SPEAR will be maintained and is a Cartesian right-handed system. The origin is placed at the center of the ring to reduce the size of the necessary curvature corrections (above). There will be no monument at the center, it is purely a virtual point. The Y-axis assumes the direction of the gravity vector at the center but with opposite sign, the other axes orientations are defined in symmetry to the machine. The Z-axis is perpendicular to the Y-axis, parallel to the tangent at the midpoint of the arc sections, and is positive towards the east pit. The X-axis is defined such that it completes the definition of the right handed orthogonal system. False offsets are applied to all three coordinates to make the distinction between machine and geodetic coordinates.

2.1.4 Network Survey

The most efficient instrumentation for the network observations would be a laser tracker (Figure 2.21) or a servo motor driven total station theodolite (i.e. Leica TDA5000, Figure 2.22). Currently the SLAC Metrology Group possesses each of these instrument types and for reliability both will be utilized in the network measurements. The theodolite has integrated motorized horizontal and vertical drives, is equipped with automatic target centering, is superior in angular accuracy to a laser tracker, but falls a little short in comparison with the tracker's distance resolution. However, Leica has announced the TDA6000, which for all intensive purposes is a TDA5000 with significantly improved distance measurement capability. While the TDA5000 is a borderline alternative, if the TDA6000 is available it will obliterate the need for laser trackers in the static measurements.

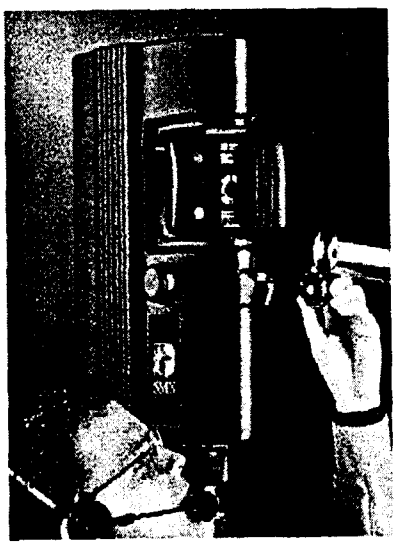

Figure 2.21 SMX Tracker 4500

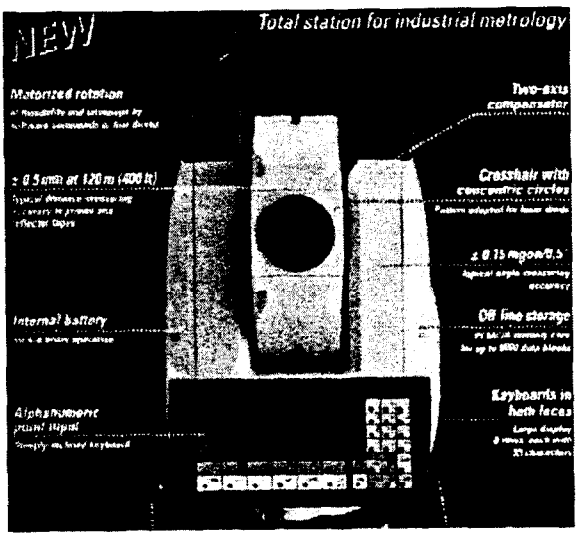

Figure 2.22 Total Station TDA5000

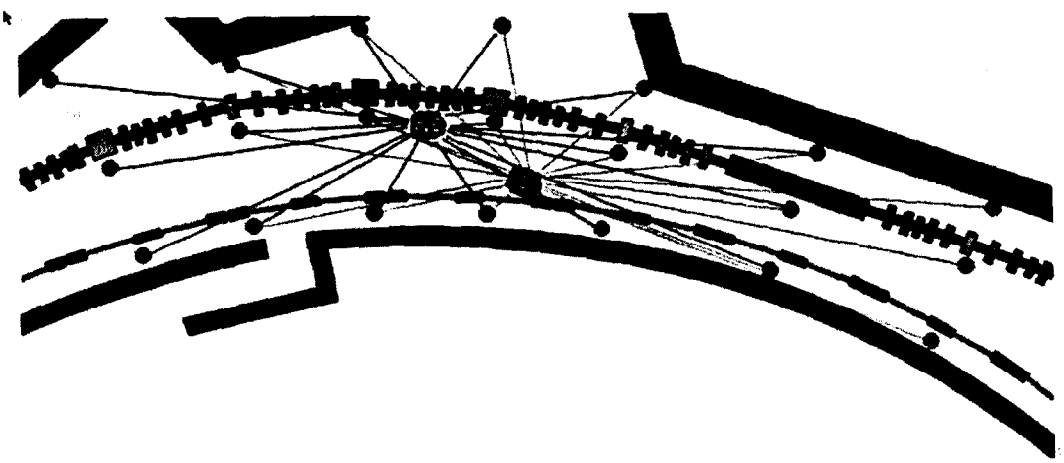

Figure 2.23 TC2002/TDM5000 observation plan schematic

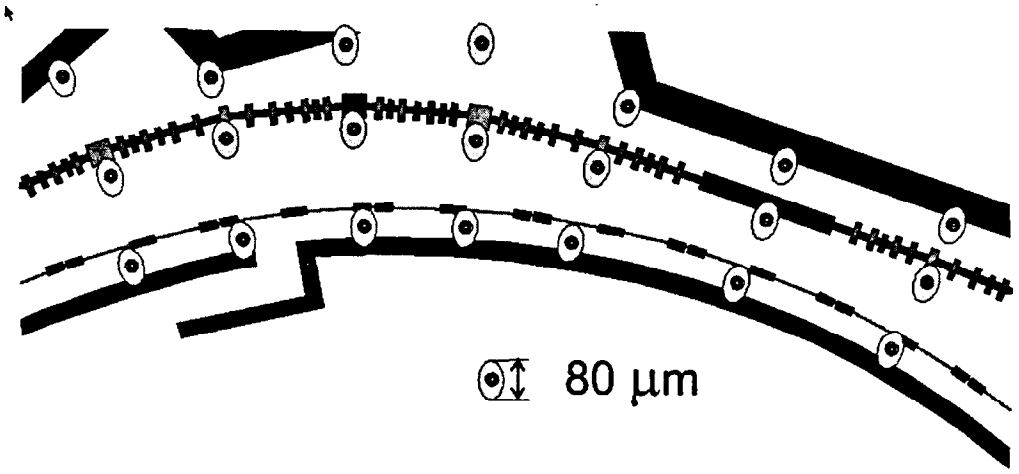

Figure 2.24 Error ellipses for section of tunnel net

The total station will be placed close to the intersection of the diagonals of each reference point quadrilateral (Figure 2.23). From there, four points in a forward direction and four points in backward direction will be measured. The measurement procedure will include three sets of direction measurements to the same eight points in both front and reverse positions plus one set of distances in both positions. If more observations are necessary to strengthen the determination, one could first offset the tracker/total station laterally by about 0.5 m and then repeat the same measurement procedure with an offset in the other lateral direction. The procedure in the other network parts follows an equivalent strategy. To strengthen the elevation determination, all reference points should be observed with a standard high precision double-run level procedure. A Leica NA3000 digital level in combination with 2 m invar rods will be utilized for these measurements. Figure 2.23 previews the anticipated position uncertainties for a small section. A detailed analysis of the network geometry, network densification, the observation plan and the required observation accuracies are being carried out.

2.1.5 Data Analysis and Data-Flow

To reduce the data from the measurements as described above requires special software. This type of analysis software is based on the photogrammetric bundle approach. Since a photogrammetric sensor is arbitrarily oriented in space, not only its translational parameters but also its rotational orientation parameters must be treated as unknowns and become part of the solution. With traditional trilateration/triangulation based analysis software however, pitch and roll are supposed to be oriented to gravity, and yaw is expressed as a function of translations. Additionally, the traditional software assumes that the instrument is set-up centered on a point to which sufficient measurements have been taken. This analysis approach does not work well with free-stationing, and doesn't work at all with the current laser trackers in the Metrology Department's toolbox, since they cannot be oriented directly to gravity.

To reduce errors stemming from transcription of data, the data-flow should be automated. The suggested instruments support direct connection to field computers. The fully automated data-flow should extend from field computers through data analysis to data storage.

Measurements with any type instrument will be guided by software based on rigid procedures running on field data logging computers. The software will also pre-analyze the measurements and will try to determine and flag possible outliers before the measurement set-up is broken down. This

method combined with an automated data-flow will greatly reduce errors and improve measurement consistency and reliability.

The above methodologies and procedures for network measurement and data processing have been adopted at SLAC to meet other alignment projects criteria. Therefore, the software required to perform the data flow, check data validity, and data analysis tasks has already been developed and field verified.

2.2 SPEAR III Lay-out Description Reference Frame

2.2.1 Lattice Coordinate System

The SPEAR III lattice is designed in a right handed beam following coordinate system, where the positive y-axis is perpendicular to the design plane, the z-axis is pointing in the beam direction and perpendicular to the y-axis, and the x-axis is perpendicular to both the y and z-axes.

2.2.2 Tolerance Lists

The relative and absolute positioning tolerances σx, σy, σz of dipoles, quadrupoles and sextupoles are not included here. They are fully described in another section of this report.

2.2.3 Relationship between Coordinate Systems

The relationship between the surveying and the lattice coordinate systems is given by the building design and machine lay-out parameters. The result is a transformation matrix (rotations and translations).

2.3 Fiducializing SPEAR III Magnets

The required alignment tolerances dictate that the components be fiducialized to increase the precision of the alignment. Tangible references must be placed on the components that are compatible with the in tunnel alignment methodology.

2.3.1 Traditional Fiducialization

The correct fiducialization of magnets is as important as their correct alignment since an error in either task will effect the particles' trajectory and cannot be distinguished from each other. Fiducialization can be accomplished either through opto-mechanical and opto-electrical measurements or by using fixtures, which reference to a magnet's reference features. Detailed descriptions can be found in the literature. [8]

The Metrology Department at SLAC currently utilizes a system of bushings tack welded on the components as fiducials. These fiducials accept the wide variety of targets that are used for the component alignment. A minimum of four fiducials on each component are required. They must be located so that optical lines of sight from the in tunnel alignment instrumentation are possible. In addition, maximum spatial separation between fiducials is required to strengthen the geometry for setting the rotational degrees of freedom.

2.3.2 Fiducialization of BPMs

Knowledge about the relative position of sextupoles and BPMs is one of the key factors in the correction scheme for the synchrotron's closed orbit. Similar bushings as used above can again be

used to fiducialize the BPMs. In addition, the beam-based-alignment scheme envisioned will allow the determination of any BPM offsets

2.4 SPEAR III Absolute Positioning

Common to all parts of the machine, free-stationed TDA5000/6000s or laser trackers, oriented to at least four neighboring points, are used for the absolute positioning measurements. The tracking capabilities of these instruments will significantly facilitate the control of any alignment operation (moving components into position).

2.4.1 Synchrotron Absolute Positioning

The concrete girders currently being used in the SPEAR tunnel will remain in place and be reused for SPEAR III. This of course means that there will not be a chance for any prealignment phase outside of the tunnel environment. All components must be aligned once installed upon the concrete girders.

2.4.1.1 Fine Alignment of Girders into SLS Coordinate System

In this step the components will be moved to their nominal positions under the control of a laser tracker/total station/level combination. The "free stationing" approach will be used with the instrument's location being determined by sighting all visible monuments. The component's position is signaled by computing the location of reference targets inserted in the fiducial bushings. By comparing the designed position with the actual position, required adjustments are computed. After the component is adjusted another measurement sequence is performed until the computed adjustments are negligible.

2.4.1.2 *Quality Control Survey*

Once the above step is completed in at least one arc, the critical component positions will be mapped. If the positional residuals exceed the tolerance, a second iteration can be jump started by using the quality control map to quantify the position corrections, which need to be applied. Should a second iteration be necessitated, a new quality control survey is required after completion of the alignment process.

2.5 Smoothing for the SPEAR III

2.5.1 Synchrotron

The absolute positioning for the SPEAR III is quite different from that of large size accelerators. The relative alignment of components on girders is guaranteed by the high quality of the primary network. Beamline extraction points are located at specific locations along the arcs, which dictates that the "as built" SPEAR ring match with these locations. Therefore, the final positions of the arc components must be obtained from the absolute alignment of the machine. However, "smoothing" could occur at the ends of the arcs and into the straight sections where there are no experiment beamline extraction points.

2.6 Instrument Calibration

The survey and alignment instrumentation needs to be maintained and the calibration regularly checked to control systematic errors. Fortunately, the Metrology Department has its own calibration facilities which allows for frequent calibration with rapid turn around. Included in the

facility is an interferometric bench, which gives the ability to maintain a scale standard for all of the various linear measuring devices used.

References

[1] For more information see also: Ruland, R.: Magnet Support and Alignment, in: H. Winick, Editor, Synchrotron Radiation Sources - A Primer, pp. 274 - 304.

[2] The Geoid is the reference surface described by gravity; it is the equipotential surface at mean sea level that is everywhere normal to the gravity vector. Although it is a more regular figure than the earth's surface, it is still irregular due to local mass anomalies that cause departures of up to 150m from the reference ellipsoid. As a result, the geoid is nonsymmetric and its mathematical description nonparametric, rendering it unsuitable as a reference surface for calculations. It is, however, the surface on which most survey measurements are made as the majority of survey instruments is set-up with respect to gravity.
The reference ellipsoid is the regular figure that most closely approximates the shape of the earth, and is therefore widely used in astronomy and geodesy to model the earth. Being a regular mathematical figure, it is the surface on which calculations can be made.

[3] Forced centering refers to a specific instrument mount. This type of mounting system, whether vendor specific or independent, allows the exchange of instruments on a station without loosing the measurement point, i.e. all instruments are by mechanical „force" set up in exactly the same position. However, experience has shown that even the best of these forced centering system have a s of about 50-100 μm. Unfortunately, the forced centering system contributed error is not random. Since a whole set of measurements is usually completed from a slightly offset position, this error behaves mostly systematically. No efficient method is known to determine the offset vector. This error, vertical refraction, and lateral refraction are the biggest contributors to the systematic error budget in surveying engineering.

[4] 2+1 -D refers to the fact that because of mechanical problems in the forced-centering hardware, three-dimensional networks were usually split into separate horizontal (2-D) and vertical (1-D) networks. Both networks were established, measured and analyzed separately.

[5] Rather than setting up the instrument over a known point, the instrument's position is flexible and chosen only following considerations of geometry, line of sight and convenience. To determine the instrument position, at least three points, whose coordinates are already known or are part of a network solution, need to be included in the measurements.

[6] Lateral refraction is caused by horizontal stationary temperature gradients. In a tunnel environment, the tunnel wall is often warmer than the air. This creates vertical stable temperature layers with gradients of only a few hundredth of a degree Celsius per meter. If one runs a traverse close to a tunnel wall on one side only, the systematic accumulation of the effect can be significant. E.g. during the construction of the channel tunnel, a control measurement using gyro theodolites revealed that after about 4 km they had already veered about 0,5 m off the design trajectory.

[7] The " character indicates inches; 1 in = 2.54 cm, hence the diameter of the 1,5" sphere is equivalent to 3.81 cm.

[8] Ruland, R., Setting Reference Targets, in Proceedings of the CERN Accelerator School on "Magnetic Measurements and Alignment," Capri, 1997, in print.

Diurnal Heat Transfer Through Concrete A3

G. Bowden
NLC ME Note 14-98
5/12/98

NLC ME NOTE		
TITLE: Diurnal Heat Transfer Through Concrete		
No. 14-98 Rev 0	*DATE:* 12 May 1998	*AUTHOR:* G.Bowden

Introduction

Temperature stability in accelerator housings is important for the alignment of accelerator structures and beam line magnets. It also is important for the stability of the accelerator's RF drive and all electronic instrumentation used to control the machine. Housings buried underground for radiation shielding reasons benefit from the large insulation and heat capacity of the surrounding earth. Sometimes housings are built on the surface where they are exposed to daily weather. One such example is the synchrotron light source at SPEAR. In 1969, largely for economic reasons, this machine was built on the research yard parking lot next to End Station A at SLAC. The tunnel housing is formed from concrete shielding blocks, 2 ft thick on the sides and 1 ft thick on the roof. Each day, the exterior of the tunnel is exposed to heating and cooling. All three modes of heat transfer are at work. On the outside of the housing, solar radiation is absorbed. The heated surface reradiates to the sky both during the day and at night. Convective heat transfer heats or cools the surface depending on the ambient temperature. Heat moves by conduction through the shielding walls. What are the relative magnitudes of these effects and how do they vary with the wall thickness and the optical properties of the concrete surface? This note estimates these influences on the temperature stability of the tunnel.

Heat Transfer Model

The model ignores many details. Solar heating is very uneven. East walls are heated in the morning. South walls and roofs are heated at mid day. West walls are heated in the evening. This differential aspect of the heating is probably a big multiplyer of thermal misalignment which often depends more on temperature differentials than on changes of the mean temperature. Direct air exchange between the housing and the outside is ignored. Air exchange has been a major contribution to temperature variation in the past at FFTB and elsewhere. Temperature variation is reduced by sealing the tunnel from outside air. The model only considers flat horizontal concrete slabs which form the roof of the housing. Convection, conduction and radiation are considered but evaporation is ignored. The most stable accelerator operating periods occur during extended periods of cloudy rainy weather. Radiation is then minimal. Ambient temperature is nearly constant and damp air has increased thermal conductivity.

The present model is a one dimensional diffusion of heat through a horizontally infinite slab of concrete. The boundary conditions at the top surface consists of three heat fluxes:

Solar radiation

Figure 1 below shows solar power at the earth's surface at various times of day over the year.

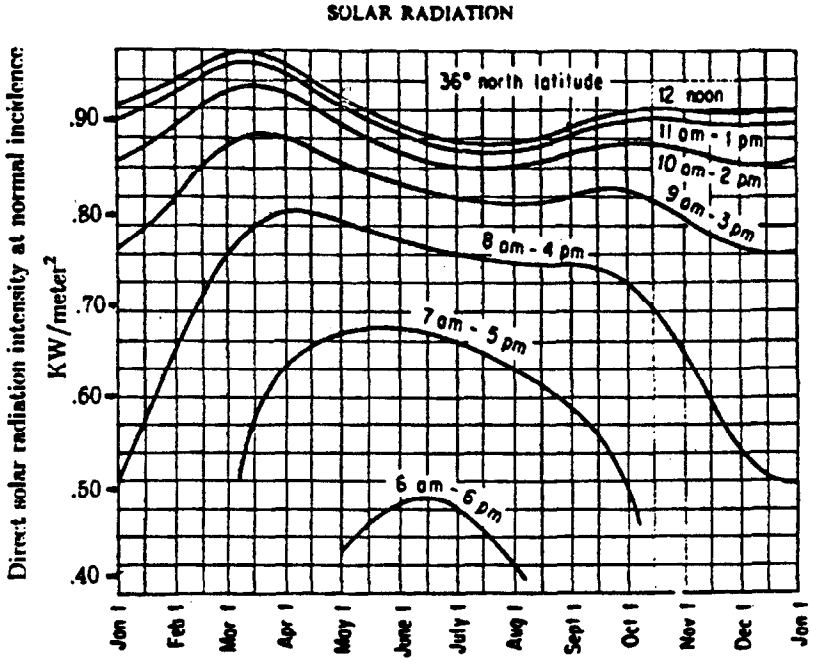

fig.1 Direct Solar intensity at 36° north latitude

This energy flux is through an area normal to the sun's rays at the surface of the earth for latitude 36° north. The solar constant at the edge of the earth's atmosphere is 1.4 KW/m^2. This varies about 7% throughout the year due to variation of the earth/sun distance. A shallow minimum in radiation occurs at the time of mid summer in the northern hemisphere. Much solar energy is absorbed in the atmosphere and at noon in June only about 8.8 KW/m^2 reaches the earth's surface. For horizontal surfaces,this intensity is is further reduced by the cosine of the sun's rays to the vertical:

$$\cos(\theta) = \cos(l)\cos((\frac{15^\circ}{hr})h) + \sin(l)\sin(d) \qquad (1)$$

Here l is latitude = 37° , h is in hours measured from noon, local time. The sun's declination d from the equatorial plane = 23.5° at the summer solstice.

Black body radiation to and from the sky

Radiation emission and absorption depends on both the energy spectrum of the radiation and on the surface properties of the material. For opaque materials, incoming radiation is divided into reflected and absorbed: $\rho + \alpha = 1$. Reflectivity of some surfaces is plotted below in figure 2 for the sun's radiation spectrum. The present model takes the solar absorptance of concrete to be $\alpha_s = 1 - .28 = .72$

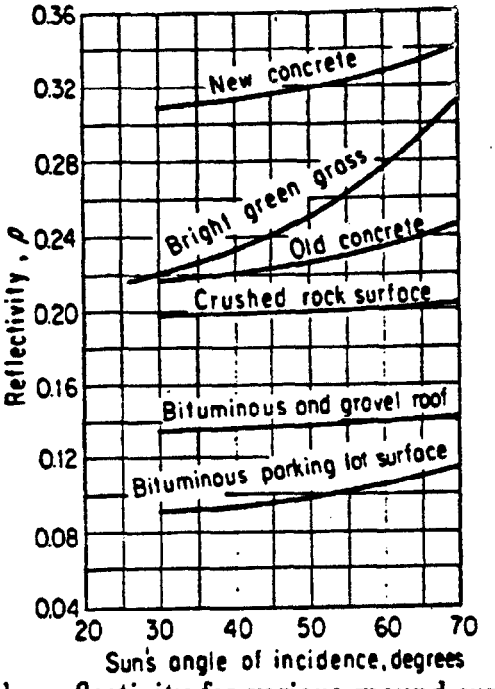

fig.2 Solar reflectivity for various ground surfaces

The effective black body temperature of outer space is 4°K. As seen from the surface of the earth, the sky temperature is much warmer but it can still be significantly cooler than the ambient air temperature. The emissivity T_{sky}/T_{amb} of the clear sky over North America appears to follow equation (2) everywhere to within about 1%. Surprisingly, the sky appears warmest at night. During the day, as a surface is heated by the sun, it will also radiate heat to a cooler sky. This is especially true in dry desert climates with little water vapor in the air. Measured in $°K$, the sky's effective blackbody temperature is related to the absolute ambient air temperature T_{amb} (°K) for dew point temperature T_{dp} (°C) by:

$$T_{sky} = T_{amb}\left[0.711 + 0.0056\,T_{dp} + 0.000073\,T_{dp}^2 + 0.013\cos(15t)\right]^{\frac{1}{4}} \qquad (2)$$

$$\text{For } T_{dp} = 10\ °\text{C}, \begin{cases} T_{amb} = 293°\text{K}\ (20\ °\text{C}), & T_{sky}(\text{midnight}) = 276\ °\text{K}\ (3°\text{C}) \\ T_{amb} = 310\ °\text{K}\ (40°\text{K}), & T_{sky}(\text{noon}) = 289.6\ °\text{K}\ (16.6°\text{C}) \end{cases}$$

T_{dp} is the dewpoint temperature and t is the hour measured from midnight. On a mild night (20°)C, the black body sky temperature is nearly freezing. Radiative cooling can cause frost when the ambient air is still above freezing. While concrete's absorptance of solar radiation is taken as $\alpha_s = .72$, it reemits as a black body at a much lower temperature than the sun surface's. Emissivity for radiative cooling of concrete at 300°K, $\epsilon = .85$ is found from Table 1 below.

EMISSIVITY AND ABSORPTIVITY VALUES FOR VARIOUS SURFACES

Surface	Emissivity or Absorptivity		Absorptivity for Solar Radiation
	50–100 F	1000 F	
A small hole in a large box, sphere, furnace, or enclosure	0.97 to 0.99	0.97 to 0.99	0.97 to 0.99
Black non-metallic surfaces such as asphalt, carbon, slate, paint, paper	0.90 to 0.98	0.90 to 0.98	0.85 to 0.98
Red brick and tile, concrete and stone, rusty steel and iron, dark paints (red, brown, green, etc.)	0.85 to 0.95	0.75 to 0.90	0.65 to 0.80
Yellow and buff brick and stone, firebrick, fire clay	0.85 to 0.95	0.70 to 0.85	0.50 to 0.70
White or light-cream brick, tile, paint or paper, plaster, whitewash	0.85 to 0.95	0.60 to 0.75	0.30 to 0.50
Window glass	0.90 to 0.95	.....	.....
Bright aluminum paint; gilt or bronze paint	0.40 to 0.60	.....	0.30 to 0.50
Dull brass, copper, or aluminum; galvanized steel; polished iron	0.20 to 0.30	0.30 to 0.50	0.40 to 0.65
Polished brass, copper, monel metal	0.02 to 0.05	0.05 to 0.15	0.30 to 0.50
Highly polished aluminum, tin plate, nickel, chromium	0.02 to 0.04	0.05 to 0.10	0.10 to 0.40

Table 1 Black body and solar radiation properties of some surfaces

The model assumes that concrete reradiates heat to the sky as a black body:

$$I = \epsilon\sigma(T_{surf}^4 - T_{sky}^4) \quad \mathrm{KW/m^2} \tag{3}$$

Here temperatures are °K =° C + 273,
$\epsilon = .85, \quad \sigma = .56687 \times 10^{-10} \quad KW/(m^2\ {}^\circ K^4)$.

Convection from a horizontal surface

Heat transfer by free convection depends sensitively on boundary conditions. Some simple geometries have been measured and parameterizations found that are reasonably accurate over a wide range of conditions. For horizontal surfaces, heat transfer depends on whether the surface is a floor or a ceiling. For the present model I ignor that distinction and use a relation found in the LBL Mechanical

Engineering Information Manual, 1988:

$$Q = .002(T_{surf} - T_{air})^{1.25} \quad \mathrm{KW/m^2} \tag{4}$$

Here temperatures are in °C. This relation comes from W.M. Brobeck, 5-30-46. Around room temperature it gives values comparable to modern parameterizations found in *Handbook of Heat Transfer Fundamentals* , editors Rohsenow, Hartnett & Ganić.

Heat Conduction

Heat conduction through the concrete roof block is described by the one dimensional diffusion equation:

$$\frac{\partial T}{\partial t} = \alpha \frac{\partial^2 T}{\partial x^2} \tag{5}$$

Here diffusivity $\alpha \equiv \frac{k}{\rho C_p} = 3.16 \times 10^{-3}$ meters^2/hr for concrete. The prescribed boundary conditions assumed are the outside air temperature and solar intensity. They are shown below in figure 3 for a hot day at the end of June. The equations of heat transfer are then solved for the temperature of the inside-housing concrete surface holding the inside-housing air temperature constant.

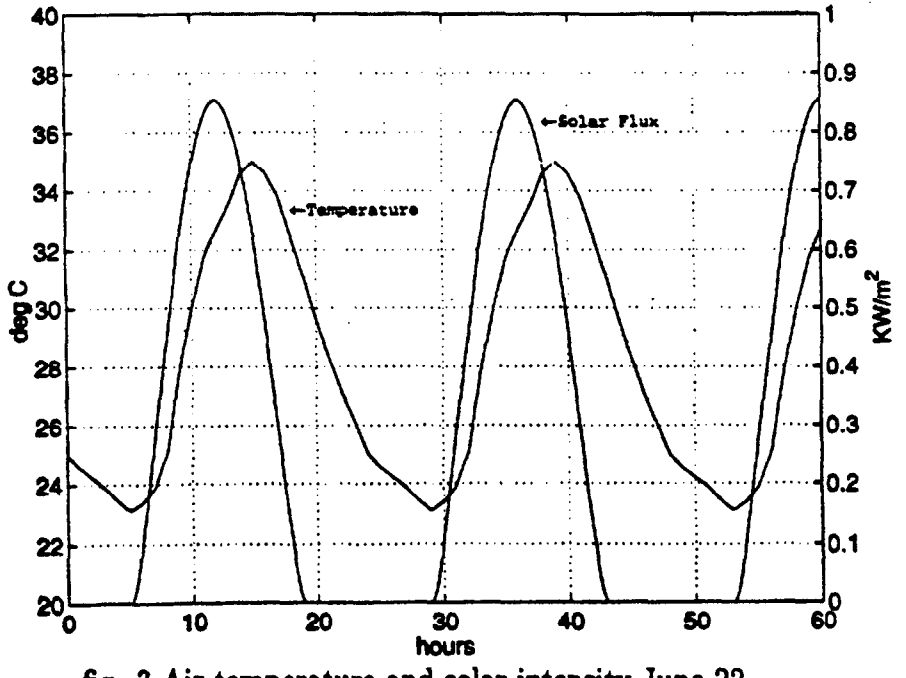

fig. 3 Air temperature and solar intensity June 22

A simple closed form analytic solution to the diffusion equation exists for an infinite

half space driven by a sinusoidal temperature variation at the surface:

$$\frac{\Delta T(x,t)}{T_{ave}} = \cos\left(\sqrt{\frac{\pi}{\alpha\tau_0}}x - 2\pi\frac{t}{\tau_0}\right)e^{-\sqrt{\frac{\pi}{\alpha\tau_0}}x} \tag{6}$$

Here τ_0 is the period of sinusoidal temperature oscilation (hrs).

The present conduction problem has a finite thickness rather than infinite. The surface temperature is not prescribed. It depends on several heat transfer processes which in turn depend on surface temperature as sketched below in figure 4.

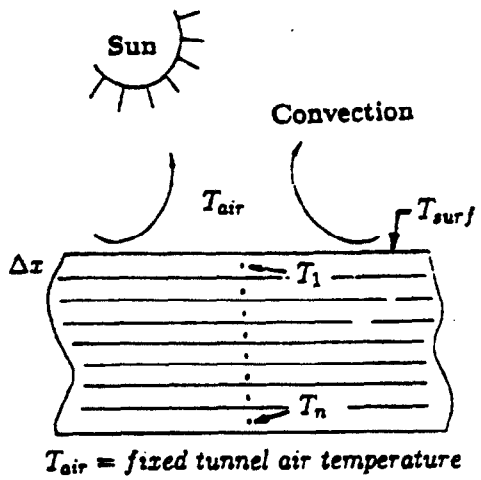

fig.4 Model for diurnal heating of concrete wall

To solve this partial differential equation, a finite difference approximation was used. The concrete roof is divided into 10 slabs. Slab temperature changes were calculated for each slab's inflow/outflow energy balance and its heat capacity. In this way the evolution of slab temperatures was tracked over time. Heat flux at the external surfaces of the concrete roof depends on those surface temperatures. These were approximated by the making a linear extrapolation of the end slab temperatures out $\Delta x/2$ to the surface. With T_{surf} given, net surface heat flux due to solar radiation, convection and blackbody cooling can be estimated at each time step. The temperature change over one time step Δt for slab n is:

$$T_n' - T_n \simeq \frac{\alpha\Delta t}{\Delta x^2}(T_{n+1} - 2T_n + T_{n-1}) \tag{7}$$

For the iteration to be stable this time step must be kept shorter than $\Delta t < \left(\frac{\Delta x^2}{2\alpha}\right)$. Calculations were done with $\Delta t = \left(\frac{\Delta x^2}{3\alpha}\right)$. The propagation of the diurnal

temperature wave into the concrete roof is plotted below in figure 5. The wave is strongly attenuated as it penetrates into the concrete and its relative phase lags further behind, the deeper it goes. Figure 6 summerizes the surface temperature oscillations and heat fluxes for the case of concrete walls 1 ft thick and 2 ft thick for the first 60 hours.

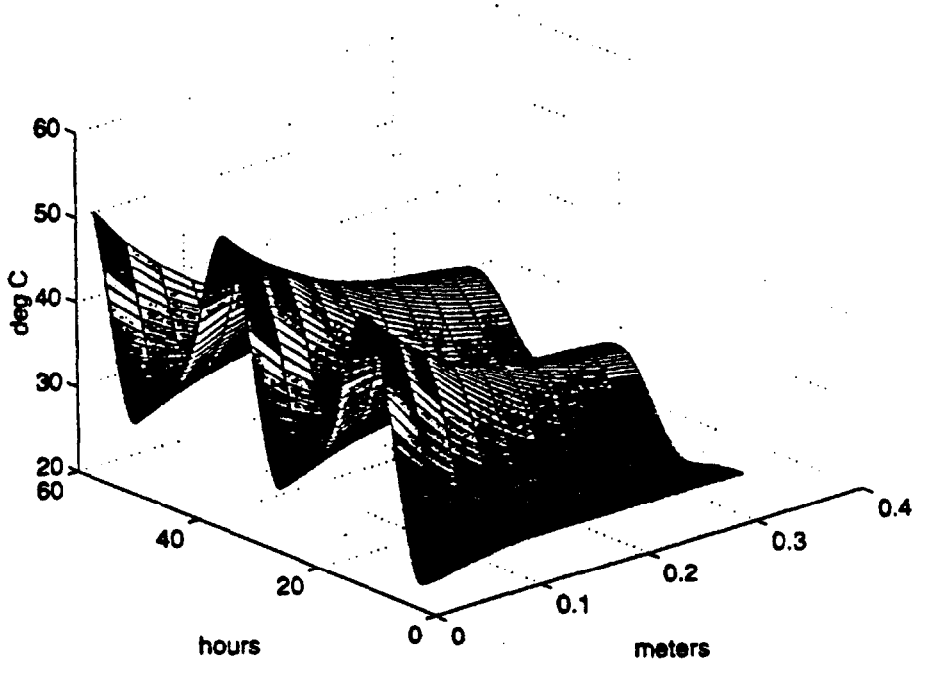

fig.5 Diffusion of diurnal temperature into 1 ft thick concrete roof

Figure 6 on the following page summerizes the surface temperature oscillations and heat fluxes of the case of concrete walls 1 ft thick and 2 ft thick for the first 60 hours.

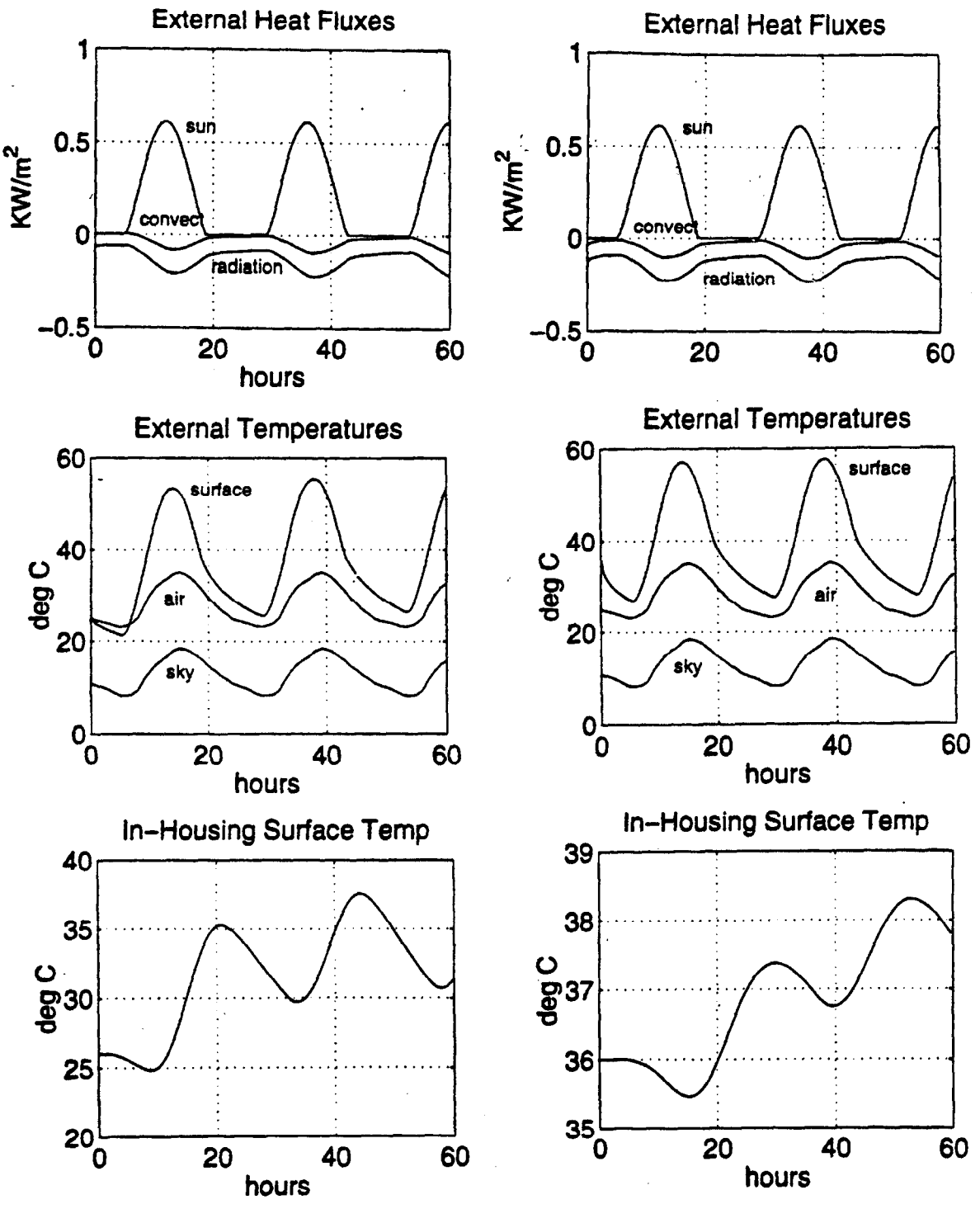

fig.6 Concrete surface temperatures and heat flux
left column 1 ft thick concrete, right column, 2 ft thick concrete.

Observations

Temperature variation on the concrete surface inside the housing is about 6°C full amplitude for 1 ft thickness and drops to about 1.5°C for 2 ft of concrete. Solar power intercepted by a horizontal surface near noon is about 0.6 KW/m^2 which heats the surface to 55°C (131°F). Heat loss by radiation continues around the clock. Once a steady state cycle is reached, convection and radiation balance most of the solar input over the the 24 hour cycle. The rest is carried away in the storage ring's cooling water on such hot days. Because the model's initial assignment of uniform temperature to the concrete was not equal to the steady state final average, the concrete's transient response is visible in the first 60 hours of the simulation. It appears that 2 to 3 days are necessary for the wall to reach steady state diurnal oscillation.

Improvements

Two approaches to reducing the temperature variations inside the housing have been suggested. The simplest is just a coat of white paint. White paint can have a solar absorptance $\alpha_s(\mathrm{ZnO}) \simeq 0.20$ compared to the solar absorptance of bare concrete $\alpha_s(\mathrm{concrete}) \simeq 0.72$. White paint could cut the solar power by a factor of 3.

> [Surprisingly, white paint can still be fairly black at the 8-13 μm infrared wave lengths associated with 300°K black body radiation. Because the atmosphere is quite transparent in this wave length band, heat is easily expelled to outer space. Radiative cooling surfaces have been developed over the last 20 years to exploit this. Isolated from convection and conduction, surfaces could theoretically cool to 50°C below ambient. 15° C has been reached in practice.]

For temperature stability, radiative cooling does not help. Only isolation from the diurnal changes will improve temperature stability. A second suggestion is to build a secondary shade roof over the concrete housing. This is equivalent to shutting off both the direct solar radiation and cutting off the path of reradiation to the sky. Figure 7 shows both a 1 ft thick concrete roof with white paint (left column) and with a shade roof (right column). White paint could cut inside surface temperature excursions from 6°C to 2.5°. A full shade roof might further reduce the diurnal changes down to 1.5°C.

A final approach is insulation. By itself, low thermal conductivity does not reduce the transient response if the material with low thermal conductivity also has low heat capacity. What is needed is a material with both low thermal conductivity and a large capacity to store heat. There is only one material property in the diffusion equation: the diffusivity $\alpha_s \equiv \frac{k}{\rho C_p}$ From this standpoint, loose earth is about 10 times better than concrete and almost as good as granulated cork!

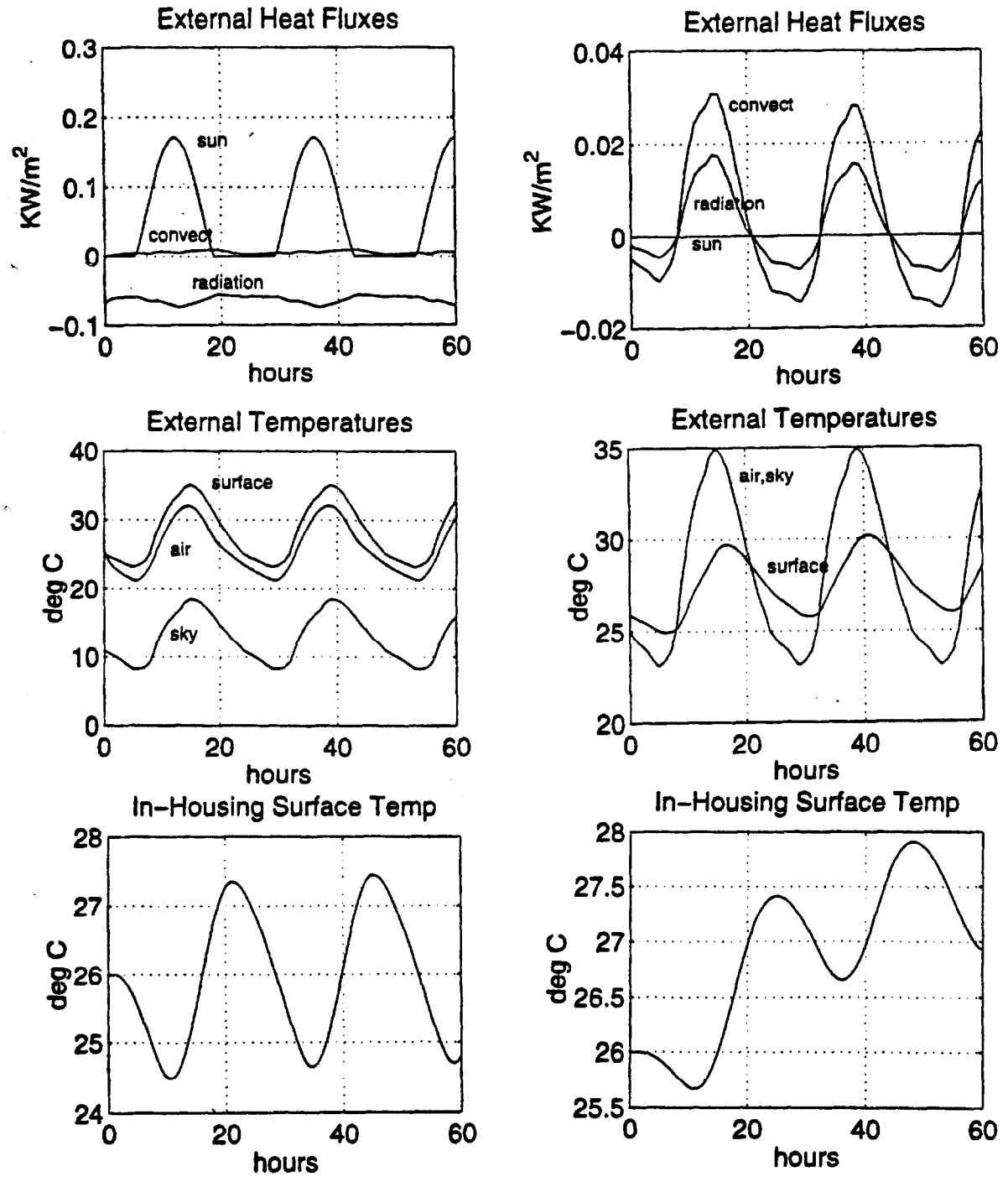

fig.7 left column: white paint, $\alpha_s = 0.2$ right columm: sun shade

Sources

Solar & material data comes from *Thermal Enviornmental Engineering* ,J.L.Threlkeld, 1962.

Black body sky temperature comes from: Technical Note, 'Emissivity of clear skies', P.Berdahl & M. Martin,*Solar Energy* Vol.32, No. 5 p.663-664, 1984.

Modern solar materials are reviewed in *Advances in Solar Energy*, vol.5, 1990., chapter 2, 'Advances in Solar Optical Materials', Carl M. Lampert.

Additional thermal engineering data can be found in *Space Technology*, NASA SP-66, vol. II, Spacecraft Mechanical Engineering, J.L. Adams, 1965.

APPENDIX A.4. Transverse Multibunch Feedback Systems

Transverse coupled bunch oscillations are driven by the excessive resistive wall impedance and chamber HOM strength. In SPEAR 3, these estimated impedances are not high enough to excite transverse instabilities for currents up to 500 mA, especially in the presence of head-tail damping (Section 3.6.2.2). On the other hand, should these instabilities arise in the future due to vacuum chamber modifications or altered operating parameters, their amplitude must be damped to less than 10% of the beam size using horizontal and/or vertical Transverse Feedback Systems. A diagram of a bunch-by-bunch Transverse Feedback System, based on the design developed for the Advanced Light Source and PEP-II [1] is shown in Figure A.4-1.

The transverse dampers, one for each plane, are low-noise, wide bandwidth systems implemented primarily with analog technology. Two 4-electrode detectors, separated in betatron phase in the ring, serve both the horizontal and vertical feedback systems.

The detectors and kickers will be stripline structures. Each detector is a conventional 4-electrode stripline optimized for maximum sensitivity at $3f_{rf}$, where f_{rf} = 476.337 MHz, the SPEAR 3 accelerating frequency. This length is 1/4 of the $3f_{rf}$ wavelength, or 52 mm. Striplines are superior to buttons in this respect, as they have two free dimensional parameters (buttons have one), so the impedance function can be tailored to the application. The detectors shall be carefully manufactured to minimize electrical center offset, and to provide a smooth transition for the signal currents and passing beam current. The electrodes will subtend angles that equalize the image currents in the elliptical geometry, and the downstream ends will be shorted to the chamber. The upstream end is cantilevered, and connects to a vacuum feedthrough through a tapering shim-stock transition, which also allows flexibility. The electrode impedance will be 50 Ω in the even mode.

Beam signals from each detector are processed by separate receivers, to produce horizontal and vertical error signals. The receivers operate on the beam moment ($I_b\Delta x$), which is detected at $3f_{RF}$ (1429 MHz) and demodulated to baseband. Moment signals from each detector are then weighted and combined to produce a signal equivalent to that that would be detected at a location 90° in betatron phase from the kicker.

A second processing stage includes filtering and fast gating functions to enhance the system's flexibility. The filter is a two-tap analog correlator, which is used to remove the constant component of the error signal, produced by the closed-orbit position of the beam. The filter thereby improves the dynamic range of the system. The gating function allows the system to be entirely disabled, or allows individual bunches to be un-damped or anti-damped.

The power amplifiers are Class-A 120 W commercially available units, one amplifier for each electrode. The amplifiers feed the kickers contra-directionally to the entering beam. At low frequency where the kicker directivity is high, little beam power is directed back toward the amplifiers. At higher frequencies the directivity is lowered by poorer transition impedances within the kicker, so the kicker sends this power back toward the amplifiers. High power low-pass filters are used to protect the amplifiers.

The transverse kickers havea 2-electrode stripline design, with each electrode behaving as a 50 Ω transmission line when the pair is driven differentially. The maximum electrode length is 1/2 the

accelerating rf wavelength, or 0.315 m for 476.337 MHz. The electrode cross sections are approximately half ellipses and are positioned to maintain beam stay clear. The transverse shunt impedance is maximized by adjusting the electrode coverage angle, the electrode separation, and the electrode length. Longer electrodes provide a greater maximum shunt impedance. However, the electrodes cannot be longer than the filling time plus the bunch flight time, in order to assure that each bunch is acted on independently. The kickers will produce a maximum impedance of ~10 kΩ, and operate in the DC - $f_{RF}/2$ band.

Heating of the kicker electrodes will result from three sources of electrical loss in the structure. At 150 W (saturated) maximum input to each electrode, approximately 1.7 W is lost in each vacuum feedthrough. This loss is dominated by the presence of the Ni/Mo/Mn brazing system. For a 316 type Stainless Steel electrode, ohmic losses in the electrode are 9 W. This loss can be reduced to 1.2 W by copper plating the strip. A third source is beam HOM heating, estimated at 36 W for stainless steel, and 5 W for copper. While copper electrodes produce less heating, the emissivity of copper is low. For either material, the electrodes reach an equilibrium temperature of >200°C using worst case analysis. This can be reduced to ~ 100°C by building a uniformly heavy, black copper oxide, plasma deposited coating on a copper or copper plated electrode. The rise can be further reduced by limiting the input power to 100 W, near the linear limit of the power amplifiers.

One position detector and one kicker may be located in the 17S18 straight section, and the second component pair in the 10S11 straight section where the requirements of betatron phase advance is met.

References

[1] W. Barry et al., "Design of the ALS Transverse Coupled-bunch Feedback System", Proceedings of the IEEE 1993 Particle Accelerator Conference, 2109-2111.

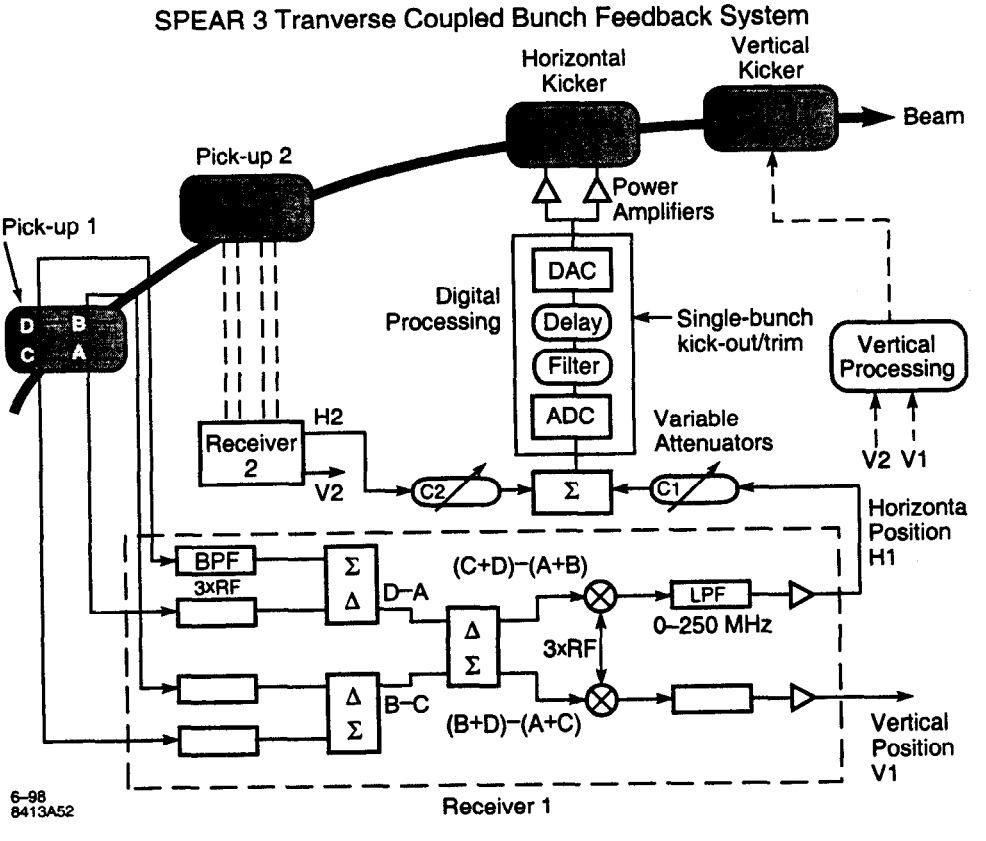

(Figure A.4-1) Transverse Coupled Bunch Feedback system (ALS).

Shielding & Radiation Safety A5

V. Vylet, A. Fasso

DRAFT

Radiation Physics Note RP-98-8
June 2, 1998

SHIELDING AND RADIATION SAFETY CONSIDERATIONS FOR THE SPEAR-3 UPGRADE

Vašhek Vylet and Alberto Fassò

INTRODUCTION

The purpose of this note is to address certain general aspects of shielding and radiation protection related to the SPEAR-3 upgrade. This document concentrates on aspects related to the SPEAR ring enclosure and adjacent areas, without considering individual beamlines. Each beamline constitutes a special case that will have to be assessed at a later stage. Several upgrade scenarios of the storage ring were discussed in the recent past. For the sake of this report we selected the one where the maximum stored current is increased from 100 to 500 mA, and the energy of the injected beam is increased from 2.35 to 3.0 GeV, while the injection current (I_{av} = 0.65 nA) will remain the same.

The beam loss pattern in the SPEAR ring is for the most part unknown. The amount of beam losses and their distribution were based on estimates from reference [1]. Since the new badging policy was introduced at SLAC in January 1988, a dense system of area monitors was put in place. Results of these area monitors could provide valuable information for projections regarding the SPEAR-3 upgrade. We anticipate that when the TLD readings from these monitors become available in the near future, this document might be amended and the current version should be therefore considered as a DRAFT.

SHIELDING CALCULATIONS

A. Method

The beam loss in the SPEAR ring can occur in a large variety of configurations. Our calculations were done for three generic configurations described below. In all cases it was assumed that both the forward and lateral shielding consist of 2 feet of concrete, which corresponds to the current ring and alcove walls in SPEAR. The effect of local shielding was also examined in some cases, more to get a feeling of its effect rather than to solve a particular problem. Specific design of local shielding and shadow masks (shadowing the beam line penetrations through alcove walls) will have to be done case by case, depending on the final layout of beam line components and expected or measured losses.

Calculations for very simple geometries were performed with the SHIELD11 code, while the more complicated cases were simulated using the FLUKA Monte Carlo particle transport code. In FLUKA the photon dose was determined using energy deposition in tissue and the neutron dose equivalent was derived from calculated neutron spectra using fluence-to-dose equivalent conversion factors.

1. Thick target

These calculation were done using the SHIELD11 code, which provides fast results and is well suited for this purpose. For lateral shielding calculations two iron targets were considered, differing in radial thickness: one with 2" and one with 12" in radius. The length was 12" in each case. The larger of the two represents adequately a massive component such as a magnet. The smaller might simulate a less substantive component, or a magnet being hit way off center.

2. Thin target (C-magnet)

The new SPEAR-3 magnets will have a "C" shape, i.e. a narrow opening toward the outer side of the ring. In comparison with the current ring this means removing an important part of local shielding, since the massive magnets shadow rays both in the forward and lateral directions. It is an unfortunate necessity of the design that the magnet opening is on the side of the synchrotron light beam lines, i.e. towards the more occupied side of the ring. One of possible beam loss scenarios in this setup would be a beam striking the beam pipe wall under a glancing angle, in the opening of a C-magnet. This situation was simulated with the FLUKA code, where a 1.12 m long C-dipole was tilted by an angle of 2.44° with respect to the lateral wall and the alcove in the forward direction. The electron beam strikes the 1-cm aluminum beam pipe wall under the 2.44° angle, with the beam loss point being at 70 cm from the lateral wall and 15 m from the alcove wall forward. The angle and distances were approximately derived from the beam line curvature and layout in the vicinity of the BL-9 alcove.

3. RF-cavity

In the current SPEAR ring the two RF cavities have the smallest apertures of all devices and are therefore likely locations of beam loss. Their internal structure is rather complicated and use of SHIELD11 would not be adequate. The FLUKA code was used to simulate a RF cavity, followed by three magnets downstream. In this case the electron beam strikes the cavity at the edge of the entrance aperture. Photon and neutron dose equivalent was evaluated behind a 2 feet thick lateral concrete wall. Cylindrical geometry was used to increase the scoring efficiency, which did not allow for an accurate representation of the C-magnets. However, calculations with the same setup, but with the downstream magnets completely removed, yielded an almost identical lateral dose profile as the original case, proving that the influence of these magnets is inconsequential in this case.

4. Local shielding

Both FLUKA and SHIELD11 results for lateral shielding indicate that a 5-cm thick local shield made of iron would reduce the total dose rate by approximately a factor of two. This comparison is based on the C-dipole case in FLUKA and the 2" target radius in

SHIELD11. SHIELD11 further indicates a factor of 3 reduction by 2" of lead and a factor of 4 by 1 ft of concrete. The effect of local shielding for the thin target forward case is discussed further below.

B. Results

1. Injection losses

Calculations with SHIELD11 and FLUKA codes provide "source terms", i.e. dose per incident particle or dose rate per kWh. Estimates of dose rates and cumulative doses behind shielding were based on beam parameters and beam loss scenarios listed in references 1 and 2. These estimates are presented in worksheet 1 below. The Injection Loss Fraction (ILF) of 0.25 reflects the expected injection efficiency after the upgrade, while the current injection efficiency[1] is ILF=0.40. This worksheet contains an implicit assumption that dose to personnel behind SPEAR shielding results exclusively from beam losses during injection. Estimates from stored beam losses are presented further below.

Column A in the worksheet shows dose rates in case all of the injected beam is lost at one point. This represents the worst mis-steering case. Since part of the losses always occur near the injection septum in the BTS line, it is unlikely that this full power could be lost further downstream in the ring.
The B column shows dose rates for the scenario where beam capture in the ring proceeds as planned, but all the "normal" losses again occur at one singular point, perhaps due to orbit or device misalignement. Such a loss might not be noticed by the operators, unless it causes a trip of a protection device.
Under normal conditions it is assumed that 75% of the expected injection losses will occur at singular points due to low apertures of beam line devices and the remaining 25% will be evenly lost around the storage ring. In column C we have assumed that these singular losses will be evenly distributed among four devices, and the figures in this column represent expected dose rates in the vicinity of one such device.

Since values in column C correspond to normal and average conditions, they were used to calculate cumulative dose equivalent over the running period of 10 months per year (1 month startup, 9 months operation). These cumulative values are presented in the last column entitled DE/y and were calculated using injection times from reference [2]. However, a fraction of the injection time, while the beam is on the BTS screens, was substracted, since it has no effect on occupied areas near the beamlines. The BTS injection point is a very low occupancy area and has additional two feet of lateral concrete shielding.

It is clear that a number of assumptions in the spreadsheet are somewhat arbitrary, such as the fact that expected losses will be divided among four beam line devices, and/or that the dose behind the shielding was accumulated for the same four devices. The current SPEAR ring has no diagnostic devices to monitor the distribution of beam losses. In the

absence of this information, Worksheet 1 provides a range of possible values to be considered.

		Injection Losses A	B	C	
Injection Loss	I	6.50E-10	1.63E-10	3.05E-11	nA
Fraction	P	1.95E+00	4.88E-01	9.14E-02	W
0.25	Q/h	1.46E+13	3.66E+12	6.86E+11	e/h

	Inj. time /y [h][1]
Commissioning	14.0
Normal running	72.4
Machine phys.	24.0
Total	110.4
Adj. Total	110.4

[1] Beam time on BTS screens excluded

A ... total injected beam
B ... normal losses (total * loss fraction), but all at one point
C ... 75% of normal losses distributed among four singular devices

Source		src term mrem/e	Lateral dose rate [mrem/h] A	B	C	DE/y [mrem]
thin target	n	9.09E-13	19.8	4.9	0.9	102
	γ	4.44E-13	6.5	1.6	0.3	
RF cavity	n	3.30E-13	7.2	1.8	0.3	37
	γ	1.60E-13	2.3	0.6	0.1	
thick target 1[2]	n	2.52E-12	95.4	23.8	4.5	494
	γ	4.00E-12	58.5	14.6	2.7	
thick target 2[3]	n	4.01E-13	6.6	1.6	0.3	34
	γ	4.72E-14	0.7	0.2	0.0	

[2] Iron, R=2', L=12'
[3] Iron, R=12', L=12'

bold = total (n+γ), grey = gamma

Source		src term mrem/e	Forward dose rate [mrem/h] A	B	C	DE/y [mrem]
thin target	n	7.44E-11	3423338	855835	160469	17719263
	γ	2.34E-07	3422250	855563	160418	
thick target 1	n	4.03E-14	4.0	1.0	0.19	21
	γ	2.31E-13	3.4	0.8	0.16	

Worksheet 1: Expected dose rates behind lateral and forward shielding, assuming average injection beam loss of 25%. The "Adjusted total" injection time reflects different injection time needed if the loss fraction is different from 25%.

Regardless of any assumptions, however, it is clear that the forward dose rates from the thin target are extremely high: over 160 rem/h for the normal loss scenario. These very high values undoubtedly result from the fact that a large part of the high energy particles escape from the thin target and the electromagnetic shower fully develops in the concrete shielding. Very similar results were previously found by R. Nelson [3] using the EGS-4 code. The high dose rates result almost exclusively from photons. Preliminary results from FLUKA calculations indicate that a lateral 5 cm thick iron plate close to the C-magnet opening will reduce forward dose rates by at least four (possibly 6) orders of magnitude. An accurate representation of the geometry in the forward case, while

preserving a reasonable scoring efficiency, is challenging. However, this geometry might be represented by the thick target 1 in SHIELD11, which indicates a reduction by almost six orders of magnitude (8.0E+5).

2. Stored beam losses
Using source terms from the above worksheets, it can be shown that an instant loss of 500 mA (2.44E+12 electrons) of stored beam at one singular point would result in a dose of 0.6 to 14 mrem, depending on type of target. However, losses of the stored beam are usually spatially distributed around the whole storage ring, so the resulting dose rates will be extremely low. Furthermore, most of these losses are evenly distributed over a period of 24 h.

Over a period of a year, it is expected that about 1.211E+15 electrons will be stored in the SPEAR-3 ring, all of which will be ultimately lost. Another 1.01E+14 electrons/year will be evenly lost around the ring during injection. Currently, about half of the stored current is lost evenly around the ring over a period of 24 h, while the other half is dumped into the ST-1 stopper each day before a new injection. Assuming that this distribution also holds for SPEAR-3, about 7.07E+14 electrons/year will be lost evenly around the ring, and 6.06E+14 electrons/year will end in ST-1.

BEAM CONTAINMENT

Currently there are no beam containment or diagnostic devices permitting to measure and/or limit the extent of local beam losses. The only loss indicator is the (lack of) beam capture rate in the ring, with no information where the beam is being lost. For the SPEAR-3 upgrade, we propose to use LIONs (Long IONization chambers) to mitigate potential radiation safety problems. A LION consist of a coaxial cable that can be deployed over a considerable length along the beamline. It can be used to measure radiation levels inside the enclosure and, from differential timing of the signal at its ends, to determine the location of the beam loss. Incorporating these devices in the storage ring would help to:

1. Limit localized beam losses during injection
2. Serve as diagnostic tool to operators, enabling better beam steering
3. Identify trouble points that could be locally shielded
4. Keep an account of total electron losses over the year, making sure that the "loss budget" is not exceeded.

It is easy to see that items 2 and 3 above would help to reduce the cumulative dose behind shielding and related quantities. However, the purpose of this system could be defeated if operators solve problems with high beam losses by lowering the injection current. Although this would reduce instantaneous loss rates below the BCS trip level, proportionally longer injection times would be needed, ultimately resulting in higher cumulative doses outside the shielding. For this reason we feel that keeping a "loss budget" (item 4) would be useful, since the cumulative dose behind shielding, boundary

dose, ozone production and component and air activation all depend on total electron losses.

PERSONNEL PROTECTION SYSTEM

The current PPS, consisting of access interlocks, search-reset interlocks and Beam Shutoff Ionization Chambers, will remain in place and will be adequate for the upgrade.

OZONE PRODUCTION
AIR ACTIVATION
BOUNDARY DOSE

The three concerns above were treated in separate documents, added to this text as APPENDIX I through III. The SPEAR-3 upgrade does not represent a problem in any of these areas.

DISCUSSION

One of the major questions to be answered is whether the current SPEAR shielding and safety systems are sufficient for the SPEAR-3 upgrade. The design criteria applied to SLAC facilities impose the following limits:

- Cumulative dose of 1 rem/y outside shielding. This means a potential dose to a person, i.e. occupational factors should be applied.
- Cumulative dose of 3 rem per event in the maximum credible accident case
- Dose rates below 25 rem/h in the maximum credible accident case, if the termination of this case is not limited by some physical constraints and depends only on the human factor
- Cumulative dose to personnel limited to 100 mrem/y in areas occupied by non-radiation workers, which is the case of the beamline areas all around SPEAR

Results of area monitors (before 1998) in the occupied areas around beamlines are mostly well below 100 mrem/y. In a few instances results above 100 mrem/y were registered, such as 186 mrem near BL-9 and 140 mrem near BL-5. In both cases the monitors were tucked in rarely accessed areas, the corners of the respective alcoves. Furthermore, the algorithm used to evaluate the neutron component was likely too conservative.

Nevertheless, the upgrade may increase the cumulative dose behind shielding by about a factor of four. This is the result of a five-fold increase in stored current (and therefore potential losses), somewhat mitigated by a lower injection loss fraction, 0.25 instead of 0.4. Since dose behind lateral shielding scales roughly with beam power, the increase in energy from 2.35 to 3.0 GeV increases the corresponding source terms. The final result is therefore 500/100 * 0.25/0.4 * 3.0/2.35 = 3.99.

The highest cumulative dose from normal injection losses in worsheet 1 is 500 mrem/y from the thick target scenario. The impact of this value on personnel exposure is limited by the fact that most injections occur around 5 am in the morning. Furthermore, this value is based on an assumption that beam is always being lost at a particular device. In such a case the recent dense area monitoring and the planned deployment of LIONs should help to identify such devices and local shielding could be applied. In particular, the accuracy of the source term will be soon verified from data of an area monitor placed behind the shielding in the vicinity of the ST-1 stopper, since the cumulative beam loss in this area is well known.

Provided that local shielding is applied along the C-magnets and around identified high-loss points, we believe that the current shielding of the SPEAR ring will be adequate. Implementation of BCS devices such as LIONs should help to limit personnel exposure within prescribed limits.

If all the BCS devices fail in the SPEAR injector, a maximum credible injection beam of 45 W could be obtained[4]. Since dose rates in column A of worksheet 1 correspond to a loss of a 2 W beam, instantaneous dose rates in this accident scenario would be higher by a factor of 22.5. The highest dose rate, 2.1 rem/h for the thick target, is well below the prescribed limit of 25 rem/h. If such a beam were to burn through the steel beam pipe and hit the shielding wall, or burn through a shadow mask and transit through the beamline port in the alcove, extremely high dose rates should be expected. However, the loss of vacuum in the ring would shut off the beam within seconds[5], which should limit the integrated dose below 3 rem. Of course, Beam Shutoff Ionization Chambers and the planned BCS devices in SPEAR constitute the first line of defense against such accidents. It should be noted that these accident scenarios are applicable for the current operations, without the benefit of BCS devices.

The above analysis reflects a conservative approach to planned SPEAR operations. The fact that the beam will be injected at 3 GeV might enable to refill the storage ring once a day to its capacity without dumping the remaining stored beam. This will substantially reduce the number of electrons lost per year and all the related quantities discussed above and in the Appendices I – III. In addition, during the first few years after the upgrade the ring will be filled only to 200 mA. This period will allow to gather data from area monitoring and beam loss budget, allowing time for remediaton of potential problems in the higher regime.

REFERENCES

1. J. Corbett et al., "Electron Beam Loss Estimates for SPEAR 3", October 2, 1997
2. E. Guerra: the above memo condensed in spreadsheet form
3. R. Nelson, personal communication
4. J. Corbett: "Beam Power in BTS", note from 8/2/95.
5. R. Boyce, personnal comunication

Appendix I

Radiation Physics Note RP-98-6
February 20, 1998

OZONE PRODUCTION IN SPEAR ENCLOSURE

Vashek Vylet

INTRODUCTION

The purpose of this note is to estimate ozone concentrations in the SPEAR enclosure resulting from normal operation after the SPEAR 3 upgrade. The present calculations were done using the following assumptions:

Average injection current	0.65 nA (4.1E+9 e⁻/sec) [1]
Injection losses	40% [1]
Effective capture rate in SPEAR	30 mA/min [1]
Maximum stored beam	500 mA
Orbit time	0.78E-6 s

Under normal operation ozone will be generated by

1. injection losses
2. total loss of stored beam (intentional or not)
3. normal gradual loss of stored beam.

Since option 3 is a milder case of 2, only the first two scenarios will be considered here. Ozone production can be estimated using simple approximate methods such as those described by Swanson [2]. Since such methods usually lead to crude and mostly overly conservative estimates, simulations using Monte Carlo transport codes are preferable. Ozone concentrations in the SSRL booster synchrotron were previously estimated by Ipe and Nelson [3] using the EGS4 code. Assuming a point loss on a steel beam pipe in the middle of a 133 m long tunnel (3 m wide and 2.5 m high), they determined that an energy fraction of 0.021 of the lost electron beam was transmitted to the air volume. The same value was used in the present work.

The radiolytic yield (G-value) of ozone is believed to vary between 7.4 to 10.3 ozone molecules per 100 eV deposited in air, depending on instantaneous dose rate [2]. A value of G = 10 is assumed in the estimates below. It was further assumed that free ozone will decompose with a half-life T_d of 50 minutes [2], and that the SPEAR enclosure is not ventilated. During access of personnel inside SPEAR enclosure it is necessary that ozone concentrations do not exceed the Threshold Limit Value (TLV) of 10^{-7}, or 0.1 ppm.

INJECTION LOSSES

It can be deduced from the above that an injection to a 500 mA stored beam will last on average 17 minutes, during which time electrons will be lost at a rate of 9.84E+10 e⁻/min. The energy deposition rate will be

0.021 x 9.84E+10 e⁻/min x 3.0E+9 eV/ e⁻ = 6.2E+18 eV/min

leading to an ozone production rate of

6.2E+18 eV/min x 10 molec./100 eV = 6.2E+17 molecules/min.

It is assumed that these ozone molecules will be promptly mixed and homogeneously distributed within the air volume V = 70,333 cubic feet (approximately 2.0E+9 cm^3) contained in the SPEAR enclosure [4]. Ozone concentration at time t from the start of injection, assuming zero ozone at the beginning, can be described as follows

$$C(t) = K \cdot P \frac{T_d}{V}\left(1 - e^{-\frac{\ln(2)\,t}{T_d}}\right)$$

where C(t) is in ppm, K is a constant converting ozone molecules/cm^3 to ppm[5], P is ozone production rate in molecules/minute, T_d is the decomposition half-life and V is the enclosure volume in cm^3.

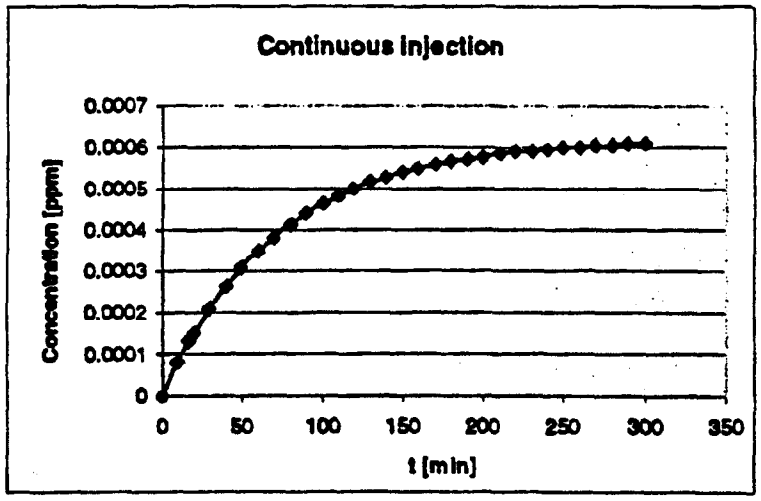

The above figure shows ozone concentration as a function of injection time. After 17 minutes, expected average injection time, ozone concentration will equal 1.3E-4 ppm, almost three orders of magnitude below TLV. Even if injection were to continue indefinitely, the saturation concentration of only 6.2E-4 ppm would be reached.

[5] K = 1E+6/n, where n = 6.02E+23/2400 cm^{-3}, the number of air molecules per cubic cm.

STORED BEAM LOSS

The number of orbiting electrons in the SPEAR ring, assuming a stored beam of 500 mA, is

$$0.5\ A \times (1.6E\text{-}19\ As/e^-)^{-1} \times 0.78E\text{-}6\ s = 2.44E{+}12\ e^-.$$

Total loss of this beam will generate 1.54E+19 ozone molecules, resulting in a concentration of 3.06E-4 ppm. In practice, it is fair to assume that a beam loss, whether intentional or accidental, will be followed by an injection. Typically, at the end of a shift only a fraction of the 500 mA stored beam will remain, so a total loss of 500 mA immediately followed by injection represents the worst case. Evolution of ozone concentration during such a scenario, with an injection time of 17 minutes, is represented in the figure below. The maximum concentration reached at t = 17 min is 3.72E-4 ppm.

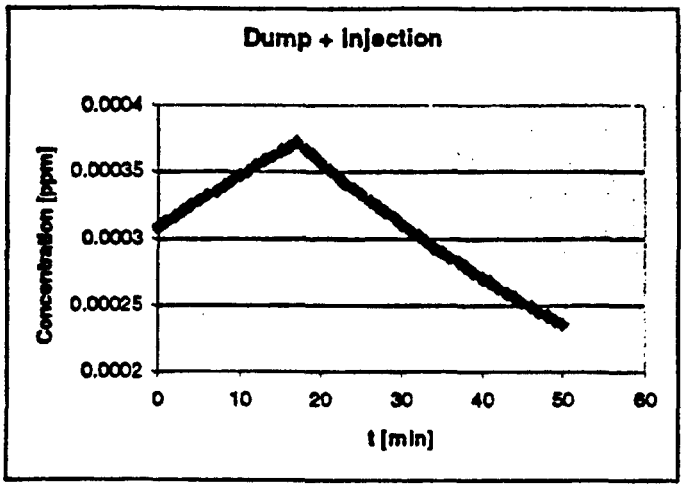

DISCUSSION

The estimated ozone concentrations for typical beam loss scenarios in SPEAR 3 are far below TLV and, barring other constraints, would not prevent immediate access or personnel to the enclosure after ceasing operations. It could be argued that the thin wall of the beampipe (0.3 mm) assumed in EGS4 calculations by Ipe and Nelson does not constitute an optimum target, and a different configuration could yield a higher fraction of energy deposition in air. While this might be true to a certain extent, all other assumptions in their model are conservative:

- the length of the tunnel, 133 m, enables very long particle tracks in the air, which can not be achieved in the circular SPEAR tunnel. The longest tracks one can project there would be about 30 m in the alcove area, and only on one side of the beamline, neglecting the presence of beamline components.
- the density of beamline components in the SPEAR ring is such, that these will shadow the most forward-directed rays, those that would have the longest passage

through air. This will substantially decrease the average path length of charged particles through air and thereby the ozone yield.
- a large fraction of the injected beam is likely to be lost in thick targets, such as the massive magnets or rf cavities. EGS4 calculations [5] show that for a thick target, where the electromagnetic shower is fully contained, the energy carried by escaping particles can be reduced by two orders of magnitude in comparison with a thin target.

One scenario, consisting of a full 0.65nA injection beam continuously sent into the Faraday cup in the injection line, was not considered in the above estimates, because this thick target absorbs a substantial fraction of beam energy, similar to the situation modeled in reference [5].

REFERENCES

1. Corbett et al., "Electron Beam Loss Estimates for SPEAR 3", October 2, 1997
2. W. P. Swanson, IAEA Tech. Reports Series No. 188, 1979
3. N. E. Ipe, SLAC-TN-91-11, September 1991
4. R. Boyce, private communication, February 18, 1998.
5. V. Vylet & T. Lavine, NLCTA Note #46.2, December 1995

Appendix 2

SLAC Memorandum

Date: October 10, 1997
Revised: October 14, 1997

To: Mike Grissom

From: Alberto Fassò

Cc: N. Ipe, I. Evans, R. Sit, V. Vylet

Subject: Air activation from SPEAR3 operation

Air activation in the SPEAR complex (Linac, Booster and SPEAR ring) after the planned SPEAR3 upgrade has been estimated.
The five beam loss scenarios described in a memo J. Corbett, E. Guerra and N. Ipe[1], have been taken as a starting point for the calculation. For each of them the following parameters have been established:

- total time that particular loss pattern happens per year (h)
- beam loss power (W)
- average pathlength traversed by high energy bremsstrahlung in air (m)
- air volume in which the induced activity is diluted (cm^3)
- area of the internal surface of the volume above

The five scenarios are the following:

1. Injection into SPEAR:

   time per year 38 h

   beam loss power 5.07×10^{14} electrons $\times$ 3 GeV $\times 1.6 \times 10^{-10}$ J/GeV $= 2.4 \times 10^5$ J in 38 h $\times$ 3600 sec/h $= 136800$ sec $\Longrightarrow$ 1.78 W

   average pathlength 70 ft = 21 m

   air volume $770 \times 6 \times 6$ $ft^3 = 7.8 \times 10^8$ cm^3

   area of the wall surface 1.71×10^7 cm^2

2. Stored beam in SPEAR:

   time per year 23.77 h/day $\times$ 30.5 day/month $\times$ 9 months = 6500 h

   beam loss power 1.16×10^{15} electrons $\times$ 3.5 GeV $\times 1.6 \times 10^{-10}$ J/GeV $= 6.5 \times 10^5$ J in 6500 h $\times$ 3600 sec/h $= 2.34 \times 10^7$ sec $\Longrightarrow$ 0.028 W

   average pathlength 70 ft = 21 m

   air volume $770 \times 6 \times 6$ $ft^3 = 7.8 \times 10^8$ cm^3

   area of the wall surface 1.71×10^7 cm^2

3. Dumping on the Faraday cup in SPEAR:

   time per year 50 h

   beam loss power 7.33×10^{14} electrons $\times 3$ GeV $\times 1.6 \times 10^{-10}$ J/GeV $= 3.5 \times 10^{5}$ J in 50 h $\times$ 3600 sec/h $= 1.8 \times 10^{5}$ sec $\Longrightarrow$ 1.95 W

   average pathlength 70 ft = 21 m

   air volume $770 \times 6 \times 6$ ft^3 $= 7.8 \times 10^{8}$ cm^3

   area of the wall surface 1.71×10^{7} cm^2

4. Dumping on the Faraday cup in the Linac:

   time per year 5503 h

   beam loss power 6.18×10^{17} electrons $\times 0.12$ GeV $\times 1.6 \times 10^{-10}$ J/GeV $= 1.19 \times 10^{7}$ J in 5503 h $\times$ 3600 sec/h $= 1.98 \times 10^{7}$ sec $\Longrightarrow$ 0.6 W

   average pathlength 3 m (see [2])

   air volume 960 ft^3 $= 2.7 \times 10^{7}$ cm^3 (see [2])

   area of the wall surface 6.6×10^{5} cm^2 (see [2])

5. Beam kept in Booster:

   time per year 1526 h

   beam loss power 1.65×10^{17} electrons $\times 3$ GeV $\times 1.6 \times 10^{-10}$ J/GeV $= 7.92 \times 10^{7}$ J in 1526 h $\times$ 3600 sec/h $= 5.5 \times 10^{6}$ sec $\Longrightarrow$ 14.4 W

   average pathlength 10 m (see [2])

   air volume 7.9×10^{8} (see [2])

   area of the wall surface 9.8×10^{6} cm^2 (see [2])

Using the above data, and following the calculation technique described in [2] and [3], the saturation activities of ^{13}N, ^{15}O, ^{11}C and ^{41}Ar, and the corresponding activity concentrations have been calculated. The data are summarized in the following three tables:

Location	*Conditions*	*Hours*	*Watts*	*Path* (m)	*Volume* (cm^3)	A_{sat} ^{13}N (μCi)	*% DAC* ^{13}N	A_{sat} ^{15}O (μCi)	*% DAC* ^{15}O
SPEAR	Injection	38	1.78	21	7.8×10^8	100	3.4	56	1.8
SPEAR	Stored beam	6500	0.028	21	7.8×10^8	1.6	0.053	0.88	0.028
SPEAR	Faraday cup dumping	50	1.95	21	7.8×10^8	115	3.7	61	1.97
Linac	Faraday cup dumping	5503	0.6	3	2.7×10^7	5.0	4.7	2.7	2.5
Booster	Pre/Post injection	1526	14.4	10	7.9×10^8	400	13	220	6.8

Location	*Conditions*	*Hours*	*Watts*	*Path* (m)	*Volume* (cm^3)	A_{sat} ^{11}C (μCi)	*% DAC* ^{11}C
SPEAR	Injection	38	1.78	21	7.8×10^8	22	0.72
SPEAR	Stored beam	6500	0.028	21	7.8×10^8	0.35	0.011
SPEAR	Faraday cup dumping	50	1.95	21	7.8×10^8	25	0.79
Linac	Faraday cup dumping	5503	0.6	3	2.7×10^7	1.1	1.0
Booster	Pre/Post injection	1526	14.4	10	7.9×10^8	86	2.7

Location	*Conditions*	*Hours*	*Watts*	*Surface* (cm^2)	*Volume* (cm^3)	A_{sat} ^{41}Ar (μCi)	*% DAC* ^{41}Ar
SPEAR	Injection	38	1.78	1.71×10^7	7.8×10^8	4.2	0.18
SPEAR	Stored beam	6500	0.028	1.71×10^7	7.8×10^8	0.067	0.0028
SPEAR	Faraday cup dumping	50	1.95	1.71×10^7	7.8×10^8	4.6	0.19
Linac	Faraday cup dumping	5503	0.6	6.6×10^5	2.7×10^7	1.3	1.6
Booster	Pre/Post injection	1526	14.4	9.8×10^6	7.9×10^8	61	2.6

References

[1] J. Corbett, E. Guerra, N. Ipe, "Electron Beam Loss Estimates for SPEAR 3", October 7, 1997

[2] N. Ipe, "Radiological Aspects of the SSRL 3 GeV Injector", SLAC TN 91-11 (1991)

[3] J.C. Liu, X.S. Mao, W.R. Nelson, SLAC Memorandum to J. Seeman, Dec. 12, 1996

Appendix III

SLAC MEMORANDUM

October 20, 1997

TO: Mike Grissom, Roger Sit
FROM: Vashek Vylet
CC: A. Fasso, N. Ipe, R. Boyce, I. Evans
SUBJECT: Skyshine estimates for SPEAR3

This memo is an update on a previous memo on the same subject from October 13, 1997, in which the neutron dose from SPEAR3 operations at the closest boundary was estimated to be 8.4 mrem/y. This result was obtained using the SKYSHINE program written by Ted Jenkins. Due to the specific geometry of SSRL, namely the fact a steep hillside limits the emission solid angle in the direction of the boundary near the Sand Hill Road, it was suspected that this results might be conservative. It was discovered since, that a measurement was done at the peripheral monitoring station in July 1991 and documented in a memo by J. Liu and M. Grissom [1] (copy attached). The purpose of this memo is to estimate the boundary dose for SPEAR3 operations based on the measured values and assumptions specified by J. Corbett et al.[2]. Using tests with the SKYSHINE code, measured source terms were scaled up to allow for energy increase in SPEAR and booster rings.

Unfortunately, exact beam parameters were not recorded during the measurement. However, it is reasonable to assume that these were typical parameters used routinely and resulting in 100 mA of captured beam in SPEAR. The 1526 h/y [2] of booster operation would contribute 0.025 mrem/y to the boundary dose. Assuming that an increase of SPEAR current from 100 to 500 mA will increase 5 times the injection loss term, the 88 h/y of injection to SPEAR or BTS Faraday cup would contribute 0.05 mrem/y to the boundary dose. In a more conservative approach, one could assume that the source term from [1] is actually an hourly average of higher values, i.e. higher instantaneous dose rates. In that case, arbitrarily assuming that we have 304 hours of injection per year, this assumption would lead to 0.18 mrem/y from SPEAR operations. The upper limit of the skyshine estimate for SPEAR and booster combined would be approximately 0.2 mrem/y. This seems to agree with values derived from past recordings of PM-1 [3].

[1] J. C. Liu, M. Grissom: "Boundary Dose from SSRL Injector Operation", SLAC memo to H. Winici, July 1991
[2] J. Corbett, E. Guerra and N. Ipe: "Electron Beam Loss Estimates for SPEAR3", October 7, 1997
[3] Private communication by R. Sit.

SLAC MEMORANDUM July 19, 1991

TO: H. Winick of SSRL

FROM: James C. Liu and M. Grissom

TOPIC: Boundary dose from SSRL Injector Operation

The signal transmission problem of the SLAC peripheral monitoring (PM) system has finally been solved on June 28, 1991. Calibrations of the PM system using both PuBe-238 neutron source and a pulser were also made by OHP after that.

The correlation between the neutron signal of the SLAC PM1 and the SSRL Injector operation during July 9-13, 1991 is shown in the attached figure. The boundary dose rate in PM1 location should be the maxmium due to its closest distance to SSRL. The large 1 cps signal during 9 am July 9 and 8 am July 10 was due to the pulser test. The two small peaks during 3-6 am July 11 and another two peaks during 2-6 am July 12 were due to SPEAR injection.

Using the hourly and daily PM1 data outputs, the net neutron signal due to SPEAR injection was found to be 130 counts per one-hour SPEAR injection. The natural neutron background signal is 4000 counts per day. Assuming the neutron spectrum at SLAC boundary has an average energy of 0.5 MeV, the above signals can be converted to neutron dose equivalent rates. Assuming there is six-hour SPEAR injection per day for 365 day per year, the neutron dose equivalent rate due to SPEAR injection is 0.2 mrem/y and the natural neutron background is 6 mrem/y.

It has also been found that losing the Booster beam around the Booster ring by turning the ejection kicker off has contributed about 18 counts per one-hour Booster operation to PM1. This is a factor of seven reduction to boundary dose rate, compared with SPEAR injection. This result has confirmed that the stand-by mode for Booster is appropriate.

The total boundary neutron dose equivalent increase due to SSRL Injector operation (assuming 6-hr SPEAR injection and 18-hr Booster stand-by per day) will be less than 0.3 mrem/y. The gamma dose equivalent increase at boundary is negligible. The calculated neutron dose equivalent rates from Booster stand-by mode or SPEAR injection using the SKYSHINE program were in the range between 0.1-1.0 mrem/y. Therefore, the anticipated increase from measurement results also agree with the calculational results.

The boundary dose equivalent rate at PM2 from Injector operation is about a factor of 8 lower than that at PM1. In conclusion, the SALC boundary dose increase due to SSRL Injector operation (0.3 mrem/y) is much less than the SLAC boundary dose equivalent limit of 15 mrem/y.

cc: D. Day;T. Troxel
K. Crook;G. Nelson
M. Grissom
N. Ipe